SCUOLA DI DOTTORATO
UNIVERSITÀ DEGLI STUDI DI MILANO-BICOCCA

School of Medicine and Surgery

PhD program in Neuroscience / Cycle XXXV

Curriculum: Experimental Neuroscience

THE *JANUS FACES* OF THE NANOPARTICLES AT THE NEUROVASCULAR UNIT: A DOUBLE-EDGED SWORD IN NEURODEGENERATION

TERRIBILE GIULIA

Registration number: 862779

Tutor: Professor Giulio Alfredo Sancini

Coordinator: Professor Rosa Maria Moresco

ACADEMIC YEAR 2021/2022

TABLE OF CONTENTS

ABSTRACT

In recent years, the concept of neurovascular unit (NVU) has progressively caught on. The NVU comprises multiple types of brain cells, including endothelial cells (ECs), astrocytes, pericytes, neurons and microglia (MG). Each cell type contributes to the maintenance of the transport through the blood–brain barrier (BBB) and brain tissue homeostasis. NVU dysfunctions have been associated with several disorders of the central nervous system (CNS) and neurodegenerative diseases. As a result, demand for therapeutic tools able to modulate the NVU has been increased. We firstly investigated the inner mechanism of action of liposomes (mApoE-PA-LIP) functionalized with a peptide derived from the apolipoprotein-E receptor-binding domain (mApoE) for BBB targeting and with phosphatidic acid (PA) for amyloid-β (Aβ) binding, previously used to promote peptide removal across the BBB and its peripheral clearance in a mouse model of Alzheimer's disease (AD) (Balducci et al., 2014). In light of previous results, we assessed whether mApoE-PA-LIP impacted on intracellular calcium ($[Ca^{2+}]_i$) dynamics in cultured human cerebral microvascular ECs (hCMEC/D3), as an *in vitro* human BBB model, and in cultured astrocytes. The mApoE-PA-LIP pre-treatment increased the ATP-evoked Ca^{2+} waves in both cell types, also under 0 $[Ca^{2+}]_e$ conditions, thus indicating that this increase is mainly due to endogenous Ca^{2+} release and that metabotropic purinergic receptors (P2Y) are mainly involved. Considering that P2Y receptors represent important pharmacological targets to treat cognitive dysfunctions and their neuroprotective effects in neuroinflammatory processes, the enhancement of purinergic signalling provided by mApoE-PA-LIP could counteract Aβ-induced vasoconstriction and reduction in cerebral blood flow (Forcaia et al., 2021). Moreover, we performed electrophysiological recordings from pyramidal neurons in mouse brain slices to assess whether mApoE-PA-LIP can also modulate the neuronal synaptic transmission. Indeed, mApoE-PA-LIP treatment increased spontaneous excitatory postsynaptic currents (sEPSCs) frequency, giving additional support to promote mApoE-PA-LIP as putative therapeutic tool for AD treatment. In recent years, human epidemiological and animal studies put in evidence how the CNS is emerging as an important target for adverse health effects of airborne pollutants (AP) (Costa et al., 2020), demonstrating also that AP-exposure may also induce synaptic plasticity impairment (Hajipour et al., 2020). Thus, taking into account that the inhalation of airborne particulate matter (PM) may contribute to the

neurodegeneration onset and progression, we moved furthermore towards understanding the inner underlying mechanisms. In lights of this evidence, we investigated the direct effect of AP on hCMEC/D3, that are the first interface between blood and brain, and on MG, the main effector of neuroinflammation, using a standard reference material of diesel exhaust particles (DEP), that is one of the main PM contributors. To study the PM impact on purinergic signalling, we compared the ATP effects on untreated primary MG with those incubated with DEP (10 $\mu g/cm^2$ for 24 hours). Our data showed that DEP-activated MG generated much smaller Ca^{2+} signals ATP-induced, revealing a significant suppression of the receptor-evoked Ca^{2+} signals, probably due to an increase in the resting $[Ca^{2+}]_i$ associated with MG activation (Hoffmann et al., 2003) that in our experiments could be confirmed also from the morphological analysis that revealed ameboid MG phenotype. The same results have been obtained in hCMEC/D3, indicating that the direct exposure to DEP causes also ECs activation. The here outlined results relating to the DEP-induced effects on ECs and on MG stated that DEP causes NVU physiology alterations which, adding together, could lead to the lowering of individual threshold to the onset of neurodegeneration.

KEYWORDS: neurovascular unit; neurodegeneration; nanoparticles; nanomedicine; air pollutants.

INTRODUCTION

1. THE NEUROVASCULAR UNIT (NVU)

The neurovascular unit (NVU) (Figure 1) is a relatively recent concept in neuroscience that broadly describes the relationship between brain cells and their blood vessels (Bell et al., 2020).

This concept was formally introduced in 2001 at Stroke Progress Review Group meeting of the National Institute of Neurological Disorders and Stroke to emphasize the close developmental, structural and functional association between brain cells and the microvasculature and their consequent coordinated reaction to injury (Schaeffer and Iadecola, 2021). Each component is intimately and reciprocally linked to each other, establishing an anatomical and functional whole (Fig. 1), which results in a highly efficient system, involved in several functions with the primary aim to preserve the homeostasis of the brain's microenvironment. Among these, there are two processes that display an intimate involvement: the neurovascular coupling (NVC) and the barrier function accomplished through the blood-brain-barrier (BBB) (Bell et al., 2020).

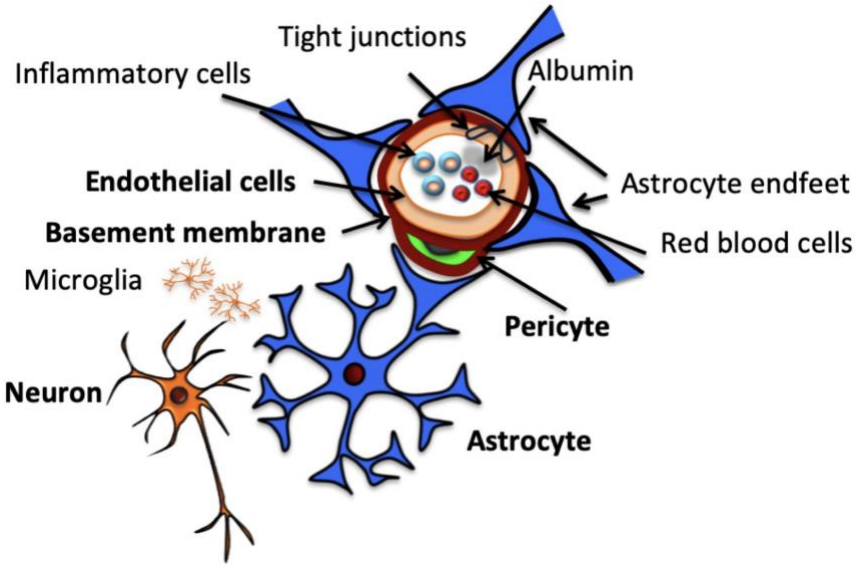

Figure 1. Structure of the neurovascular unit. Schematic representation of NVU structure, including neurons, astrocytes, pericytes, microglial and endothelial cells. Astrocytes surround the vasculature by extending specialized end feet; pericytes sit between astrocytic end feet and endothelial cells, which make up the vascular wall, encased by a continuous basement membrane; endothelial cells are connected by tight junctions, which contribute to BBB function by preventing paracellular diffusion of intraluminal substances, including cells (i.e., inflammatory cells, red blood cells) and proteins (i.e., albumin). Text and figure adapted from (Bell et al., 2020).

1.1 THE MAIN FUNCTIONS OF THE NVU

A) Neurovascular coupling (NVC): cerebral metabolism is supported by the constant supply of oxygen (O_2) and glucose ($C_6H_{12}O_6$); indeed, brain receives one fifth of the cardiac output and its O_2 and $C_6H_{12}O_6$ consumption accounts for approximately 20% of that of total body. O_2 and $C_6H_{12}O_6$ are needed for aerobic metabolism (oxidative phosphorylation) that gives energy for neuronal electrical activity in maintenance of the gradient of ions across the cerebral cell membrane and transmission of electrical impulses; thus, brain functions depend on healthy blood vessels and cardiovascular system.

Both, O_2 and $C_6H_{12}O_6$, are delivered to neurons by cerebral blood flow (CBF) and transport across the BBB. On average, the normal CBF is 54 mL/100 g/min (Lipp, 2014) but it changes proportionally to the energy consumption of each brain region. Thus, flow is higher in regions with higher energy use and lower in regions with lower one, so that flow response can be used to map brain function (functional brain imaging).

Furthermore, brain has a limited intrinsic autonomy due to high energy demand and a lack of energy stores. If CBF is interrupted, brain functions stop in seconds and irreversible damage to neurons occurs in few minutes. Since the CBF regulation is essential to maintain a proper brain function, the mammalian brain has developed a unique mechanism for CBF control known as NVC or also as functional hyperemia (Kisler et al., 2017).

Through this mechanism there is a rapid increase in the rate of CBF and a consequent increased O_2 delivery to brain structures during their activation so that the local blood supply is matched to neuronal demand. Among the vasodilatory factors involved in the CBF regulation there are local metabolites as for example H^+ and K^+, soluble molecules as nitric oxide (NO) and several neurotransmitters, first of all glutamate (Fig. 2) (D'Esposito et al., 2003).

The initial regulation of CBF seems to be mediated trough the glutamate release. Indeed, during increased neuronal activity also the release of synaptic glutamate is increased and it can bind to N-methyl-D-aspartate receptors (NMDA) on near neurons and to metabotropic receptors on their associated astrocytes. This binding causes an increase in the intracellular calcium concentration ($[Ca^{2+}]_i$) either in neuron and astrocytes with the result to stimulate the

release of vasoactive compounds acting on smooth muscle cells or pericytes and vascular endothelial cells to modify vascular tone and intraluminal diameter (McConnell et al., 2017). In astrocytes, this mechanism is mediated by the arachidonic acid (AA) cascade: phospholipase A2 (PLA2), activated by the increase of $[Ca^{2+}]_i$, hydrolyze membrane phospholipids in AA, that in turn acts on vascular walls and, after its conversion in 20-Hydroxyeicosatetraenoic acid (20-HETE), causes vasoconstriction. AA accumulation brings its conversion in prostaglandin and epoxyeicosatrienoic acid (EET) that causes vasodilation. Moreover, an increase of $[Ca^{2+}]_i$ can also causes vasodilation trough the activation of large-conductance calcium-gated potassium channels and the consequent stimulation of K^+ efflux onto vessels. In neurons, NMDA-induced increase of $[Ca^{2+}]_i$ activates neuronal nitric oxide synthase (nNOS) with consequent production of NO, that induces vasodilatation, trough the cGMP pathway on arteriolar smooth muscle cells. Furthermore, there is an activation of PLA2 and a direct modulation of several vasoactive modulators, released from neurons during neural activity, such as acetylcholine, gamma-aminobutyric acid (GABA), neuropeptide Y, somatostatin (McConnell et al., 2017). Along these evidence, the balance of vasoconstrictive and vasodilatory mediators controls the tone of the surrounding vasculature, regulating local CBF and in this process NVU is the fundamental driver providing the basis for linking neurons to cerebral vessels (Bell et al., 2020).

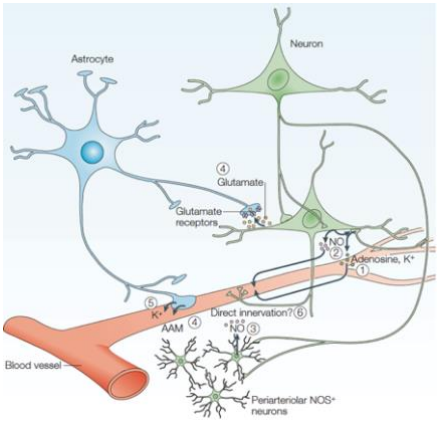

Figure 2. Some of the main mediators of neurovascular coupling. (1) Local metabolites such as K^+, H^+ and adenosine. (2) and (3) Nitric oxide (NO) that act as a retrograde messenger or that it is also locally produced by specialized networks of periarteriolar neurons. (4) Glutamate released from active excitatory synapses can also bind to glutamate receptors on the end feet of astrocytes leading to the formation of vasodilatory arachidonic

acid metabolites. (5) Astrocytes also participate in the re-uptake of K^+ (a potent vasodilator) from nearby active synapses. (6) Smooth muscle cells in the arteriolar wall might also be directly innervated by axon collaterals that control vascular tone. Text and figure adapted from (D'Esposito et al., 2003).

B) Barrier function: the function as a barrier is the second main process in which the NVU is involved. Indeed, the NVU, beyond controlling the CBF, controls the BBB permeability, that is fundamental to maintain the chemical composition of the neuronal "milieu", required for the proper brain function as well as to protect the central nervous system (CNS) from toxins, pathogens, inflammation and injury in general. BBB is a term used to describe the unique properties of the microvasculature of the CNS that is able to tightly regulate the movement of molecules, ions, and cells between the blood and the CNS. This is allowed trough the physical characteristics of the vessel that are continuous and nonfenestrated (Daneman and Prat, 2015). BBB is centrally positioned in the NVU and it is formed by a monolayer of tightly sealed endothelial cells around blood vessel of the vascular tree (Figure 1) (Zlokovic, 2011). This highly specialized membrane underlies the BBB and limits the entry of plasma components, red blood cells and immune cells like for example leukocytes into the brain resulting in a low paracellular (by means of inter-endothelial tight junctions (TJs)) and transcellular permeability. Moreover, the BBB control also the delivery into the CNS of circulating energy metabolites and essential nutrients that are required for normal neuronal and synaptic function (Zlokovic, 2005). At the capillary level, BBB integrity is maintained by pericytes, that work together with other components to prevent the entering of various potentially toxic macromolecules from the blood to the CNS and to promote their clearance from the CNS to the blood. In the human brain, total length of cerebral blood vessels is about 400 miles; the major contribute is from capillaries (85% of the vessel length) with about 12 m^2 of surface available for transport exchanges (Sweeney et al., 2019). In the NVU, both non-neuronal cells and neurons, play an integral role in all stages of BBB development and maintenance and act in concert to control BBB permeability. Indeed, dysfunction in these cell types often result in BBB impairment (Persidsky et al., 2006).

In light of these evidence, the BBB is not only a mechanical fence but also a dynamic biological entity, in which active metabolism and carrier-mediated transports occur (Masserini, 2013).

1.2 THE MOLECULAR COMPOSITION OF THE NVU

The endothelial cells (ECs) of the CNS have a unique molecular composition in comparison to the ECs of the other tissues. Between CNS ECs there are cellular adhesions, formed on the apical part of the lateral membrane by homotypic and heterotypic interactions of transmembrane molecules (i.e., Claudins, Occludins and Junctional Adhesion Molecules (JAMs)), linked to the actin cytoskeleton through interactions with cytoplasmic adaptors (i.e., Zonula Occludens-1 and -2 (ZO-1 and ZO-2))(Daneman and Prat, 2015).

Among the main transmembrane molecules there are (Fig. 3):

1) Claudins are a class of tretraspan transmembrane proteins characterized by a W-GLW-C-C domain in the first extracellular loop. Evidence in vitro suggests that claudins are essential for the paracellular barrier formation. The most relevant in the BBB are Claudin-5, Claudin-12 and Claudin-3;
2) Occludin is a tetraspanin highly expressed in CNS ECs compared with ECs in nonneural tissues, indicating that it may be an important component of the barrier and it is involved in the resistance of the BBB. In Occludin-deficient mice, there are calcifications of the CNS suggesting that perhaps Occludin specifically regulates calcium flux across the BBB;
3) JAMs are immunoglobulin superfamily members that form homotypic interactions at tight junctions in epithelial cells and ECs. JAMs have been shown to regulate leukocyte extravasation and paracellular permeability.

Among the main cytoplasmatic adaptors there is the Zonula Occludens (ZO) family. It includes multidomain scaffolding proteins, capable to form oligomers and to interact with thigh junctions (TJs)-associated membrane proteins, actin cytoskeleton and signaling proteins. In particular, ZO-1 and ZO-2 are involved in TJ assembly, that, in fact, is impaired in ZO-1-/ZO-2-deficient cells. These adhesions bring to the formation of thigh TJs that create a high-resistance paracellular barrier that restrict diffusion of water-soluble molecules and ions from blood to brain polarizing the luminal and abluminal compartments (Daneman and Prat, 2015).

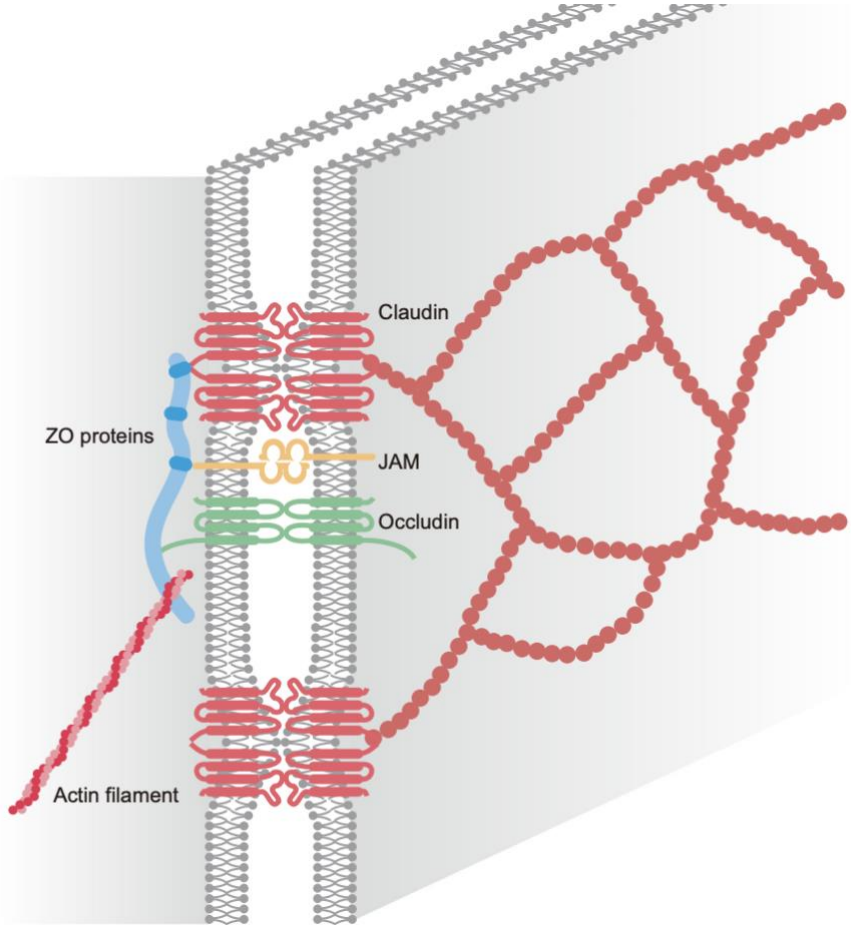

Figure 3. Structural organization of the tight Junctions (TJs). Claudins, Occludins, and JAMs are the major integral membrane proteins of TJs. Claudins form TJ strands, corresponding to membrane kissing points. TJ-associated membrane proteins are localized at apical cell–cell junctions by interacting with the ZO family of scaffolding proteins, serving as links between TJs and the actin cytoskeleton Text and figure adapted from (Otani and Furuse, 2020)

These peculiar characteristics require a transport system that allow the influx from the blood to the brain and the efflux from the brain to the blood of the substances.

Membrane transport proteins at the BBB are binned into two main categories: efflux and uptake transporters which have been studied extensively on one hand to elucidate brain function and on the other hand in order to use them for drug delivery or to study drug resistance mechanisms. Indeed, the restrictive nature of the BBB represents an obstacle for

drug delivery to the CNS, and, thus, major efforts have been made to generate methods to modulate or bypass the BBB for delivery of therapeutics (Larsen et al. 2014).

1) Efflux transporters: this category includes P-glycoprotein (P-gp or Mdr1), breast cancer resistant protein (BCRP) and the multidrug resistance-associated proteins (MRPs). They use the energy generated from ATP binding and hydrolysis to selectively transport solutes across the membrane. These transporters are mainly localized to the luminal side since they transport a wide array of substrates into the blood compartment.

2) Uptake transporters: this category includes mainly transporters (against their concentration gradient) of nutrients that cannot diffuse through due to their polarity. The ECs express a wide variety of these transporters to deliver very specific nutrients across the BBB into the CNS parenchyma. Many of these belong to the solute carrier class of facilitated transporters, including slc2a1 or glut 1 (glucose), one of the most studied since it is one of the highly expressed, slc16a1 (lactate, pyruvate), slc7a1 (cationic aminoacids), and slc7a5 (neutral aminoacids, L-DOPA) (Zlokovic 2008; Daneman 2012). In addition, CNS ECs express a variety of different receptor-mediated transport systems, including the transferrin receptor (transferrin/iron), Ager (amyloid), and low-density receptor-related lipoprotein (LRP)1/LRP8. Many of these transport systems are used for drug delivery across the BBB. Although most of these transporters provide nutrients from the blood to the brain (several are also important for removing waste products from the brain.

Another phenomenon of transport is the transcytosis but in normal conditions its rate in the CNS is drastically lower than in ECs in nonneural tissues. However, notably it is increased during injury and disease leading to BBB impairment. In the ECs transcytosis is mediated through caveolin-based vesicle trafficking (Daneman and Prat, 2015)

1.3 THE MAIN CELLULAR COMPONENTS OF THE NVU

The neurovascular unit (NVU) consists of neurons, astrocytes, pericytes, endothelial cells (ECs) and microglial cells (Fig. 1). Given the complexity of the fine CBF regulation mechanism and the barrier properties of the BBB, it is not surprising to find synergistic inductive functions involving more than one cell type. Indeed, the strong anatomical and chemical relationship between these elements allows the detection of brain needs and the consequent activation of the necessary fine orchestrated compensatory mechanisms.

Neurons: neurons are considered the "pacemaker" of the NVU (Muoio et al., 2014), due to the highly sophisticated mechanisms they use to regulate homeostasis of the CNS. They can detect little variations in the level of O_2 and nutritive compound and they generate signal in response to these. These signals can act directly or indirectly, trough interneurons, to other components of the NVU and allow to trigger compensatory response resulting in an increase of blood supply through modifications in vascular tone (Bell et al., 2020; Muoio et al., 2014).

Astrocytes: astrocytes, the most abundant cell type in the mammalian brain, are specialized glial cells that govern key steps in synapse formation and neuronal plasticity being intimately associated with synapses (Freeman, 2010). Indeed, the proper function of a synapse and the efficacy of its transmission are determined not only by the pre- and post-synaptic components but also by the environment in which a synapse is embedded. Astrocytes are involved in the up taking of glutamate from the synaptic cleft, in controlling homeostasis through movement of small molecules such as water, ions and soluble factors in the equilibration of osmotic gradients and in providing lactate to neurons, the main energy substrate. Through their highly ramified processes, one single astrocyte connects with several neuronal terminals forming the so-called tripartite synapse (Fig. 4), composed of pre-synaptic and post-synaptic processes with astrocytic processes enwrapping the synapses (Nanclares et al., 2021). In addition, astrocytes can sense neuronal activity by elevating their intracellular calcium concentration

through Gq-coupled protein mechanisms modulating neuronal function at the synaptic level through the calcium-dependent release of gliotransmitters (Fig. 4) (Bernardinelli et al., 2014).

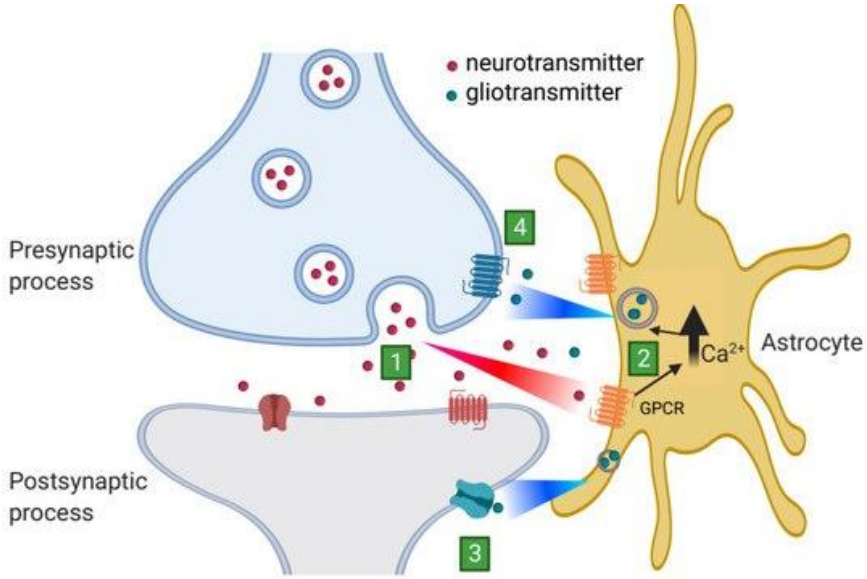

Figure 4. Schematic representation of a tripartite synapse. (1) The release of neurotransmitter from the pre-synaptic terminal acts on the post-synaptic terminal as well as with astrocytic receptors triggering an intracellular calcium increase via G-protein coupled receptors (GPCRs). (2) Then, intracellular calcium elevation triggers the release of gliotransmitters that bind with the post-synaptic (3) or presynaptic (4) receptors modulating synaptic transmission. Text and image adapted from (Nanclares et al., 2021)

Moreover, astrocytes have also an important role in BBB formation, in maintaining specific BBB features (i.e. tighter tight junctions formation, the regulation of the expression and polarized localization of transporters and of specialized enzyme systems, the correct association of endothelial cells) and in CBF regulation (Abbott et al., 2006). In light of this evidence, astrocytes have to communicate simultaneously with both neurons and blood vessels, establishing physical and chemical (gliotransmitters) connections enabling the interplay not only between neurons but also to the capillaries and pericytes (Muoio et al., 2014). Indeed, astrocytes occupy a strategic position between capillaries and neurons, showing various distinct phenotypes, depending on their location and association with other cell types (Abbott et al., 2006).

Regarding the signal transduction pathways involved in BBB modulation, a lot of studies have been done. The activation of several receptors on endothelial cells and astrocytes triggers an

increase of intracellular Ca^{2+}, which is one of the mechanisms involved in the cell- to-cell communications and in the modulation of adjacent cells' functions. This activation can be elicited by 5-hydroxytryptamine (5-HT, serotonin), glutamate, ATP or mechanical stimulation; some intracellular messengers, like inositol-1,4,5-trisphosphate (IP3), are small enough to diffuse through gap junctions mediating cell–cell spread of the Ca^{2+} wave, whereas other mediators, like glutamate or ATP, are locally released to adjacent cells (Abbott et al., 2006).

Astrocytes can be organized into syncytial structures of up to 100 units, that are strongly associated, anatomically by gap junctions and functionally through the spreading of calcium waves. Thanks to this organization the propagation of electrical signals through large distances and their transmission to the final effectors (smooth muscle cells of the vessels and pericytes) is possible (Muoio et al., 2014). The propagating rate of calcium waves spreading through the astrocytic syncytium is about 100 μm/s. Thus, this machinery is available for coordinating the activity within the NVU (Abbott et al., 2006).

Pericytes: pericytes are mural cells localized at the abluminal side of the perivascular space (embedded within the basement membrane) in blood microvessels. They are located at the interface between the brain parenchyma and the blood vessels acting as chemical sensors and mediator in the communication between the two other type of cells; they show distinct phenotypes (with different structure, expression profile and function) depending on their location along the vascular bed and their associations (Brown et al., 2019). Pericytes are multi-functional cells that have several important roles ranging from development and maintenance of BBB, regulation of CBF, trafficking of inflammatory cells (they can recruit immune cells allowing their extravasation into the brain), clearance of toxic waste products from the brain. They perform these functions through coordinated crosstalk with others cells within the NVU (Uemura et al., 2020).

In recent years, pericyte dysfunction is recognized as an important contributor to the progression of vascular diseases such as stroke and neurodegenerative diseases such as Alzheimer's disease (Brown et al., 2019).

Endothelial cells (ECs): the ECs are the first interface between blood and brain parenchyma since they line the capillary lumen by forming a monolayer; they have increased number of mitochondria in respect to the other ECs. They are characterized by the lack of fenestrations, the reduced number of pinocytotic vesicles (reduced micropinocytosis) and they are organized in a structure connected by tight junctions (TJs). TJs are the major responsible for the low paracellular permeability across the BBB restricting brain penetration of blood-derived elements.

Microglia: microglia are the principal immune cells of the CNS and they account for approximately 5–12% of brain cells, depending on the region (Colonna and Butovsky, 2017a; Hickman et al., 2018). Several fate mapping studies demonstrate that they have a myeloid origin and that they arise solely from yolk sac primitive macrophages.

Thus, microglia are a ontogenically distinct population, originating from a mesodermal origin, unlike all other brain parenchymal cells that have neuroectodermal origin (Ginhoux et al., 2010). Although microglia invade CNS during development, a recent study has demonstrated that, after selective depletion of microglia from the CNS (>99%) in adult mice, newborn microglia rapidly repopulate the whole brain to a homeostatic level (Huang et al., 2018).

Microglial cells play a crucial role in regulating homeostasis both in physiological and in pathological conditions. They monitor the cerebral parenchyma and are able to become activated following alterations in homeostasis, sensing the presence of insults or pathogens or CNS disorders. They are very plastic cells and they have several functions ranging from development to aging and they are able to change in healthy or disease.

During postnatal development, microglia play a key role in neurogenesis (synaptic plasticity) by synaptic pruning, that is the elimination of redundant synapses (with nonessential functions) with the strengthening of the others (Paolicelli et al., 2011). This function is very important for learning and memory processes. In the adult brain, microglia have a role in maintaining a healthy microenvironment: they actively survey the brain parenchyma, scanning for abnormalities, phagocytosing invading pathogens and clearing away debris and they make contact with synapses and neuronal soma (Wake et al., 2011). Therefore, in the last decade

the microglial has been defined as "active sensor and a versatile effector in both normal and pathological brain" (Hanisch and Kettenmann, 2007) as it plays a key role in maintenance of the integrity and homeostasis of the CNS. Under physiological conditions, microglial cells show highly ramified morphology (Savage et al., 2019) and are characterized by a reduced or absent expression of specific molecules of the "activated" state (Kreutzberg, 1996). During normal CNS function, microglia have a “resting” or homeostatic phenotype that basically reflects their surveilling activity.

Microglial cells are kept in this homeostatic state trough the action of neurons and astrocytes that constitutively release molecules known as "OFF signals” (Ransohoff and Cardona, 2010). OFF signals, such as CD200, SIRPα and CX3CL1, interact with their respective receptors that are for example CD200R, CD47, CX3CR1 and triggering receptor expressed on myeloid cells 2 (TREM2) (Kierdorf and Prinz, 2013). During alterations of physiological conditions when microglia must be activated to try to restore cerebral homeostasis, there is a reduction, o sometimes a stop, in the release of these molecules.

As opposed to OFF signals, there are "ON signals”, that regulate microglial activation. These stimuli can have different biochemical nature (peptides, lipoproteins, glycolipids, nucleotides) and can be released both in physiological and pathological conditions (Hanisch and Kettenmann, 2007). Among the ON signals, able to trigger innate immune responses, there are Pathogen Associated Molecular Patterns (PAMPs), molecules expressed or released by infectious agents, such as bacterial wall lipopolysaccharides (LPS), viral envelopes and bacterial or viral nucleic acid. These molecules are identified by specifics receptors, including Toll-like receptors (TLRs), receptor for advanced glycation endproducts (RAGE) and NOD-like receptors (NLRs). Other types of ON signals are proinflammatory cytokines (such as IFN-γ, released by Th1 lymphocytes), molecules released by damaged neurons (such as ATP and other purines) and intracellular constituents or molecules present only in particular situation or with abnormal forms in pathological situations (e.g., protein aggregates).

In particular ATP, which is released by both neurons and astrocytes following damage, acts as a paracrine signal and activates microglia by binding to P2X ionotropic receptors (P2X4 and P2X7) and metabotropic P2Y receptors (P2Y6 and P2Y12). ATP signaling is essential for the role

of microglia in surveillance, synaptic plasticity and damage response (Nimmerjahn et al., 2005). Microglia can acquire different activation or metabolic states depending on the type and duration of the stimulus that they receive from the surrounding environment. This activation involves profound changes in the morphology and in their functions and allows them to participate not only in mechanism of injury but also of tissue repair.

After activation, microglia can proliferate, acquire chemotactic abilities, release inflammatory cytokines or neurotrophic factors, activate other immune system cells by antigen presentation and engulf pathogens or damaged cells. Among the different states of activation of microglia there are two extreme phenotypes: a pro-inflammatory phenotype, called M1, and an anti-inflammatory phenotype, called M2, associated with tissue repair and remodeling. This categorization follows the hypothesis of polarization of macrophages, the peripheral counterpart of microglia (Fig. 5).

M1 activation promotes the release of proinflammatory cytokines, such as TNF-α, IL-6, IL-1β, IL-12, and CCL2. In the M1 microglia there is also an overexpression of the NADPH oxidase, which generates superoxide and reactive oxygen species (ROS), as well as inducible nitric oxidase, which converts arginase into nitric oxide (NO). NO increases the toxic effect of glutamate, thereby potentiating NMDA receptor–mediated neurotoxicity.

M2 activation promotes the release of anti- inflammatory cytokines, such as IL-10 and TGF-β, and induces arginase 1, which promotes the conversion of arginine into polyamines. M2 microglia secrete growth factors such as insulin-like growth factor I (IGF-I), fibroblast growth factor (FGF), and CSF1, as well as neurotrophic factors such as nerve growth factor (NGF), brain-derived neurotrophic factor (BDNF), neurotrophins (NT) 4/5, and glial cell–derived neurotrophic factor (GDNF). Neurotrophic factors engage a family of receptor tyrosine kinases known as Trk receptors, which regulate synaptic strength and plasticity (Colonna and Butovsky, 2017b).

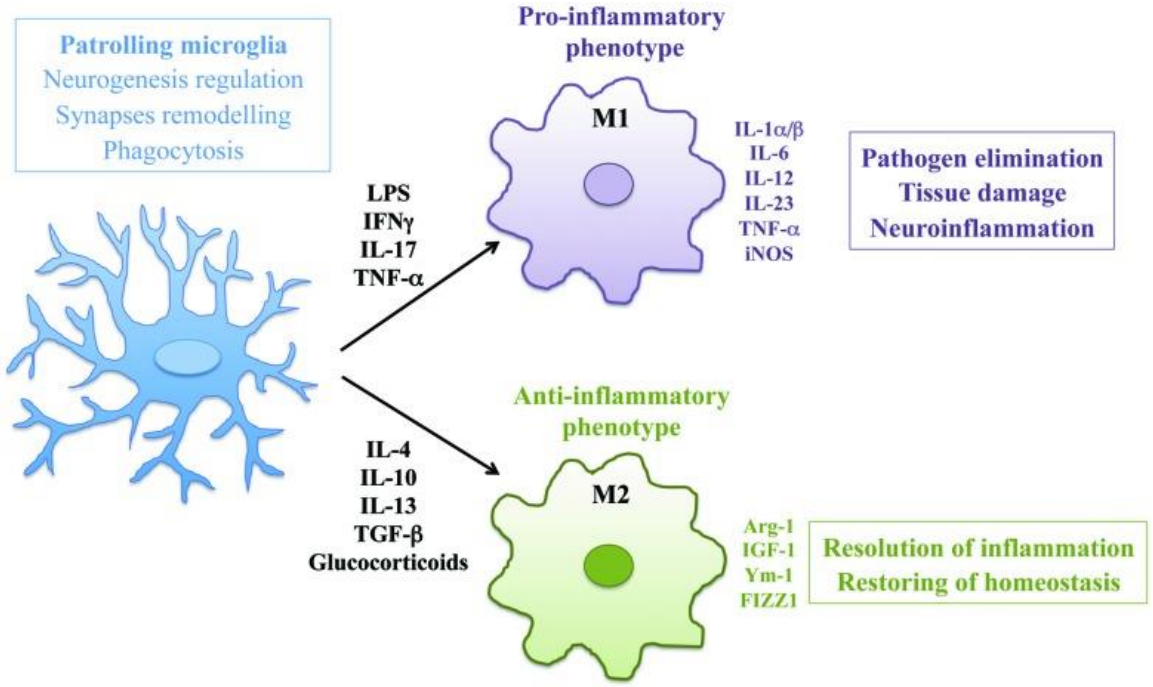

Figure 5. Schematic representation of microglial phenotype associated with different functional states. In physiological conditions surveying microglia regulate central nervous system (CNS) homeostasis. In neuroinflammation microglia assume ameboid morphology and acquire classical M1 or alternative M2 phenotype according to the nature of local milieu. Text and image adapted from (Salvi et al., 2017).

Although the M1 and M2 categories is useful to conceptualize microglia activities *in vitro*, it is increasingly accepted that the M1/M2 paradigm is inadequate to describe microglia activation *in vivo*, as microglia rarely display a significant polarization toward either the M1 or M2 phenotype and in models of neurodegeneration, can express at the same time both neurotoxic and neuroprotective phenotypes (Colonna and Butovsky, 2017b).

Therefore, the M1 / M2 dichotomy represents an over-simplification since the microglia can assume multiple phenotypes indicative of its dynamic functional heterogeneity and their activation is contex-dependent.

Since microglia can be either beneficial or detrimental to the brain according to the circumstances, their function is usually considered to be a “double-edged sword” (Kalsbeek et al., 2016).

2. THE NVU DYSFUNCTION IN THE ONSET AND PROGRESSION OF NEURODEGENARATION

Neurodegenerative diseases are brain disorders characterized by progressive neuronal dysfunction and loss of neuronal cells structure and function within the nervous system (Kovacs, 2018). At present, there is no effective cure for many neurodegenerative diseases, including Alzheimer's disease (AD), and this is a major concern considering that prevalence is increasing, as a result of world population getting old. In fact, due to increasing in life expectancy and lack of effective treatments, neurodegenerative diseases are predicted to massively grow over the next several decades (Gammon, 2014). Since there is strong evidence in the literature (Table 1) that NVU alterations lead to neuronal damage and brain dysfunction, there is growing interest in investigating the potential contribution of NVU dysfunction to neurodegeneration (de la Torre, 2017).

DISEASE	VASCULAR MORPHOLOGY	BLOOD-BRAIN BARRIER	CEREBRAL PERFUSION	SELECTED REFERENCES
ALZHEIMER'S DISEASE	Microvascular damage Microbleeds WM lesions ATS in cerebral arteries	↑ BBB permeability to Gd (early) ↑ Qalb (late, small)	↓ CBF before syntomps ↓ neurovascular coupling	(Janelidze et al., 2017; Kisler et al., 2017; Montagne et al., 2015; Roher et al., 2004; Toledo et al., 2013)

FRONTOTEMPORAL DEMENTIA	Microvascular damage Microbleeds WM lesions Perivascular astrocyte damage	↑ Qalb	↓ CBF before syntomps	(Dopper et al., 2016; Janelidze et al., 2017; Martinac et al., 2001; Sudre et al., 2017; Thal et al., 2015)
AMYOTROPHIC LATERAL SCLEROSIS	Microvascular damage RBC extravasation (some case)	↑ Qalb ↓ TJ protein Extravasation	↓ CBF α disease progression ↓neurovascular coupling	(Abrahams et al., 1996; Murphy et al., 2012; Rule et al., 2010; Winkler et al., 2013)
IDIOPATHIC PARKINSON DISEASE	Microvascular damage (late) ↑ endothelial cell nuclei in SN	↑ Qalb (late) BBB P-gp dysfunction ↑ VEGF in CSF	↓ CBF (early) = neurovascular coupling	(Janelidze et al., 2017; Kortekaas et al., 2005; Pisani et al., 2012; Rosengarten et al., 2010)

DEMENTIA WITH LEWY BODIES	Microvascular damage ATS in cerebral arteries	↑ Qalb	↓ CBF (early)	(Janelidze et al., 2017; Miners et al., 2014; Roquet et al., 2016)

Table 1. Evidence of neurovascular dysfunction in major neurodegenerative diseases. Abbreviations: ATS: atherosclerosis; Qalb: CSF/Plasma albumin ratio (index of BBB permeability); Gd: gadolinium; P-gp: P-glycoprotein efflux transporter; SN: substantia nigra; TJ: tight junctions; WM: white matter. Table adapted from (Iadecola, 2017)

Despite the abundance of evidence in the literature that neurodegeneration is associated with structural and functional alterations of the NVU, starting, in some cases, from the initial stages of the disease, many questions still remain open. Indeed, it is still to be clarified whether the dysfunction of the NVU is a collateral symptom of the degenerative process or a major contributor. The mechanisms by which this could occur, might be impaired cerebral perfusion, neurovascular uncoupling, dysfunction of the blood brain barrier, neurotrophic failure and impaired clearance capacity.

Moreover, the oxidative stress and inflammation, major causes of neurovascular dysfunction, have been virtually implicated in all neurodegenerative dysfunctions.

There is an urgent need to increase our knowledge in this field opening towards new avenues in the prevention, early diagnosis, and treatment of some of the most devastating illnesses affecting humankind (Iadecola, 2017)

2.1 TWO-HIT VASCULAR HYPOTHESIS OF ALZHEIMER'S DISEASE

Diseases associated with aging, such as dementia, are expected to be more prevalent due to increasing in life expectancy worldwide. In 2021 across the world there are over 50 million people affected by dementia. According to the World Health Organization (WHO), with nearly 10 million new cases every year, by 2030, 82 million people are predicted to be affected by AD (WHO, 2020). Dementia comprises a heterogeneous group of neurological disorders, such as Alzheimer's disease (AD) that is the most common cause of dementia (60–80% of all cases) in the elderly and the vascular dementia (VaD) is the second one (15% of cases). These disorders are characterized by abnormal changes in the brain that lead to memory loss and impaired cognitive abilities, including perception, language, and behavior (Apátiga-Pérez et al., 2022).

Considering the risk factors for cerebrovascular disorders and AD, a substantial overlap can be found. Indeed, type 2-diabetes, hypertension and obesity are risk factors that predispose to either cerebrovascular disorders or AD. It is also known that phenomena such as brain hypoperfusion–hypoxia, infarcts, silent or not, and transient ischemic or hypoxic attacks, all contribute to increase the risk of developing AD. Although the cellular and molecular events (including the single risk factors) underlying each step of AD are not entirely clear, it could be argued that all vascular risk factors converge at some point in the same final common path, characterized from dysfunction and/or vascular degeneration, as well as amyloid-β (Aβ) and tau pathology (Zlokovic, 2011).

Recently, accumulating evidence suggests that the vascular damage resulting from amyloid accumulation in the blood vessels could precede AD and VaD (Apátiga-Pérez et al., 2022).

According to the two-hit vascular hypothesis of AD there is an initial vascular dysfunction *("hit one"*) followed by the Aβ accumulation (*"hit two"*) that promote and precede neurodegeneration (Zlokovic, 2011).

Taking into account the *hit one*, it is suggested that vascular risk factors, such as hypertension, dyslipidemia and diabetes, could lead to several pathological events such as BBB dysfunction and the reduction in cerebral blood flow (CBF, also known as oligemia), the two main function of the NVU. Moreover, vascular impairment also reduces amyloid-β clearance at the BBB and

increases production of this peptide from the amyloid-β precursor protein (APP), leading to amyloid-β accumulation.

This accumulation (*hit two*) amplifies NVU and consequently neuronal dysfunction, accelerates neurodegeneration and dementia, and contributes to disease self-propagation.

Both hypoperfusion and/or Aβ accumulation can induce hyperphosphorylation of tau (p-tau), leading to neurofibrillary tangle formation (Apátiga-Pérez et al., 2022; Zlokovic, 2011).

Among the risk factors that can contribute to the so-called *hit 1* there are, not only vascular factors (hypertension, diabetes mellitus) but also several genetic risk factors for AD (mutations in apolipoprotein E4 gene, Presenilin-1, Phosphatidylinositol Binding Clathrin Assembly Protein, Clusterin) and environmental factors (e.g., air pollution, see chapter 3.2.1). These factors can contribute to NVU dysfunction and to small arteries, arterioles and brain capillaries damage trough Aβ-independent (*hit 1*) and/or Aβ-dependent (*hit 2*) pathway. Both pathways interact and converge on blood vessels and can independently or synergistically lead to neuronal injury, synaptic dysfunction and neurodegeneration contributing to dementia. AD affects different cell types of the NVU, ranging from endothelial cells, astrocytes, perycite, microglia and smooth muscle cells, compromising the cardinal function of the NVU, orchestrated by these cells. For example, degeneration of pericytes leads to loss of capillary dilation in response to neuronal stimuli, hypoperfusion and BBB breakdown with accumulation of blood-derived toxins and fluid in the perivascular spaces; endothelial damage leads to loss of endothelial-dependent vasodilation, CBF dysregulation and reduction; activation of astrocytes and microglia mediates inflammatory response and release of vasoactive cytokines and chemokines, further comprising CBF regulation and BBB integrity (Fig. 6) (Kisler et al., 2017).

Indeed, it must be taken into account also that abnormal vascular Aβ accumulation may trigger the inflammatory response, reactive oxygen species production, increase BBB permeability and lead to loss of integrity of the blood vessels, worsening the cognitive impairment (Iadecola and Gottesman, 2018).

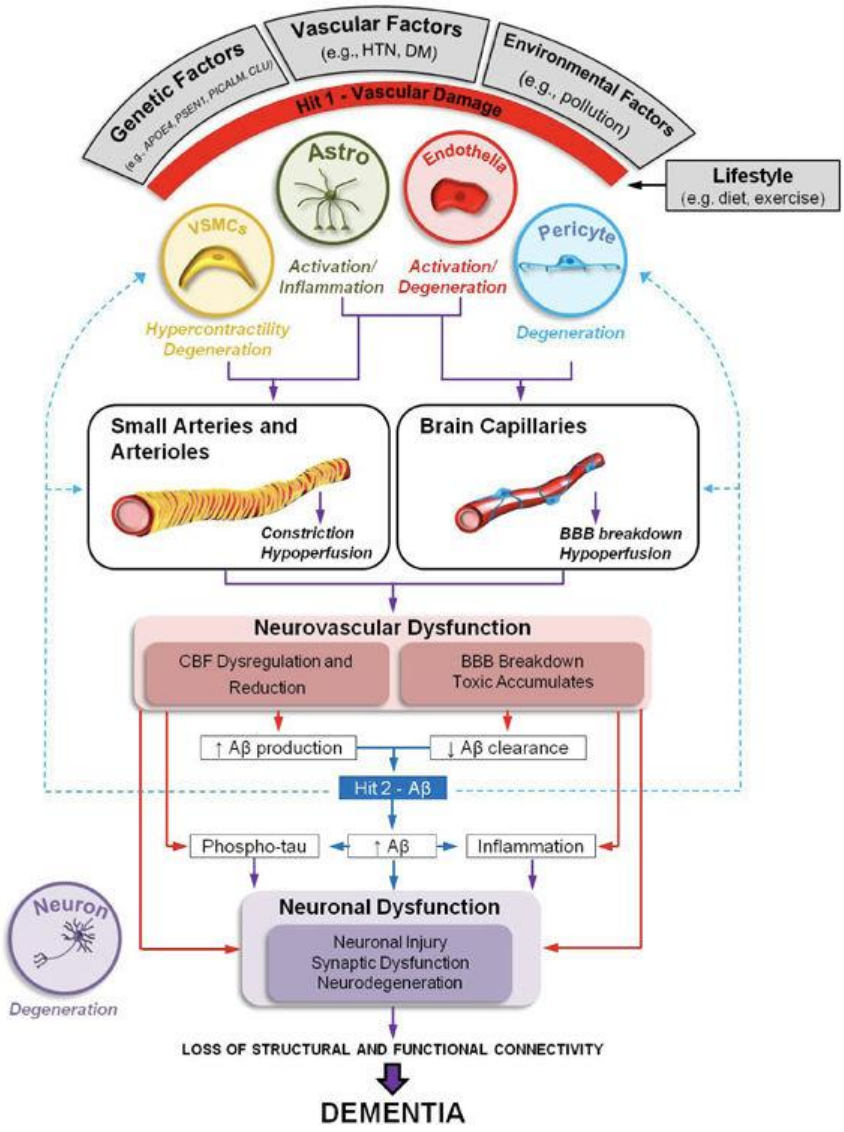

Figure 6. Neurovascular dysfunction in Alzheimer's disease: two-hit vascular hypothesis. Several genetic risk factors for AD (e.g., apolipoprotein E4 gene (APOE4), Presenilin-1 mutations (PSEN1), Phosphatidylinositol Binding Clathrin Assembly Protein (PICALM), Clusterin (CLU)), vascular factors (e.g., hypertension (HTN), diabetes mellitus (DM)), and environmental factors (e.g., pollution) lead to neurovascular dysfunction and damage to small arteries, arterioles and brain capillaries via Aβ-independent (*hit 1*, red) and/or Aβ-dependent (*hit 2*, blue) pathway. Both pathways interact and converge on blood vessels and can independently or synergistically (purple lines) lead to neuronal injury, synaptic dysfunction and neurodegeneration contributing to dementia. Damage to blood vessels can initiate a cascade of events leading to Aβ accumulation in brain (*hit 1*), which accelerates the Aβ-dependent pathway of neurodegeneration (*hit 2*). For example, BBB dysfunction in Aβ clearance receptors lipoprotein receptor and multidrug resistance protein 1 leads to faulty Aβ clearance and retention in brain. Text and image adapted from (Kisler et al., 2017)

2.2 NEUROINFLAMMATION AND NEURODEGENERATION

Although the exact mechanisms underlying many neurodegenerative diseases are not fully understood, several studies point out that neuroinflammation is considered a recurring hallmark of these diseases such as Alzheimer's, Parkinson's, Frontal Temporal Dementia, Amyotrophic Lateral Sclerosis (Kwon and Koh, 2020).

Neuroinflammation is described as a dynamic multi-stage physiological response orchestrated by several actors, including predominantly microglia and astrocytes and followed by a complex cascade of pro-inflammatory factors that modify the CNS milieu.

These factors prevent neuronal repair, resulting in synaptic impairment, oxidative damage and mitochondrial dysfunction, which in turn lead to neurodegeneration and neurotoxicity. In addition, chronic neuroinflammation can cause the blood-brain barrier dysfunction, which in itself can initiate or exacerbate neurodegenerative mechanisms (Bright et al., 2019)

Therefore, unravelling new mechanisms of neuro-inflammation and targeting these pathways are promising research trajectory for the treatment of CNS disorders.

Since the mediators involved, the time in which inflammation occurs, the mechanisms and the relationship between the various components are disease-specific, it is essential to understand for each pathology taken into account if inflammation is a causative factor, a consequent event an initial stimulus or condition that predisposes people to the onset of the disease (Thurgur and Pinteaux, 2019). However, substantial data in recent years have shown that immune-nervous system interactions are crucial for maintenance and development of healthy brain functions (Marin and Kipnis, 2013).

Since the initial trigger of neuroinflammation is often a cell-damaging process (i.e. infections, toxins, autoimmunity and alterations in neuronal activity) (Bright et al., 2019) and the consequent activation of microglia that survey brain parenchyma in physiological condition, microglial cells are among the main contributors to the architecture of the inflammatory response in brain. Dissecting their roles and their cross-talk with others elements can represent a keystone to understand the pathogenesis of many neurodegenerative diseases (Li and Barres, 2018).

Other key elements impacted by brain-derived inflammatory cytokines are astrocytes, pericytes and endothelial cells. Indeed, under neuroinflammatory condition, an elevation of cytokines in brain parenchyma can disrupt the functional relationship between these cells leading to increased BBB permeability and immune cells infiltration. In this context, changes in the endothelium-microglia interactions are associated with a variety of inflammation-related diseases in brain, where BBB permeability is compromised (da Fonseca et al., 2014).

The CNS has numerous unique immunological features that together make it an immune-privileged compartment in comparison to the others. Indeed, the transmission of blood-derived substances, including inflammatory factors, trough the blood–brain barrier (BBB) is strictly regulated by the endothelial cells that are connected by tight junction (TJ). Nevertheless, several studies highlight bidirectional communication between the brain, in particular microglia, and the peripheral immune system regardless the presence of the pathology (Cartier et al., 2014; Niranjan, 2018).

For these reasons, the original concept of the brain as an "immunologically privileged" organ has been overcome by the demonstrations that the peripheral immune cells, under different pathological conditions, can enter CNS parenchyma, modulating brain activity (Lauranzano et al., 2019). Therefore, neuroinflammation, that used to be considered as a local tissue response without any or with very limited involvement of the peripheral immune system, is believed to be influenced by a number of these peripheral factors.

3. THE NVU INTERACTION WITH NANOPARTICLE ELEMENTS

3.1 NANOMEDICINE AND NANOTECHNOLOGY IN DRUG DELIVERY

The awareness that several diseases may originate from alterations in biologic processes at the molecular or nanoscale level and that the actors, involved in the pathologies, may be in biologic systems that are protected by nanometer-size barriers, led to use nanomedicine as a promising therapeutic tool (Kim et al., 2010).

Therefore, the field of nanomedicine aims to use the chemical properties and physical characteristics (size and shape) of nanomaterials for the diagnosis and treatment of diseases at the molecular level taking advantages from the ability of these nanomaterials to pass through several biologic barriers, to reach the molecules, to mediate molecular interactions and to detect molecular changes in a sensitive, high-throughput manner (Kim et al., 2010).

The ability of nanomaterials to cross biological barriers is widely used in neurological disorders (including Alzheimer's disease and Parkinson's disease, strokes and brain cancers) treatment, since the penetration efficiency of most CNS drugs into the brain parenchyma is rather limited due to the existence of BBB (Xie et al., 2019).

Due to the presence of a tight vascular endothelium, most pharmaceuticals are excluded from CNS entry. Indeed, the efficiency of drug transportation across the BBB greatly depends on the properties of molecular size, hydrophilicity, dissociation degree (small hydrophilic compounds with a mass lower than 150 Da and highly hydrophobic compounds with a mass lower than 400–600 Da that can cross the membrane by passive diffusion (Masserini, 2013)). Moreover, several small highly lipophilic compound with ideal features to diffuse across the BBB, are recognize by efflux pumps and extruded from ECs.

In this scenario, nanomedicine has been played a pivotal role in developing strategies to deliver drugs to the CNS and nanoparticles (NPs) have been suggested as potential therapeutical tools of CNS diseases.

Among several NPs, liposomes, formed by phospholipids structured in mono- and multi-lamellar structures, have been used as transport systems for a long time for their high chemical

and biological stability, ability to incorporate different types of molecules and the possibility to be administered by virtually all routes (Sancini et al., 2016).

Liposomes are versatile structures that can be functionalized on their surface to guarantee high affinity with the target and a complete BBB over-crossing.

An example of the therapeutical potential of multifunctional liposomes is given from Balducci and colleagues (Balducci et al., 2014).

In this work, they conducted an *in vivo* study to explore the ability of multifunctional liposomes to target Aβ and interacting with aggregates promoting peptide removal across the BBB, helping its peripheral clearance in APP/PS1 transgenic mice, a mouse model of Alzheimer disease's. These liposomes were bifunctionalized with a peptide derived from the apolipoprotein-E receptor-binding domain (mApoE) for BBB targeting and with phosphatidic acid (PA), a high affinity ligand of Aβ, for its binding (Ross et al., 2018).

mApoE-PA-LIP were previously demonstrated to be able to inhibit peptide aggregation and to trigger the disaggregation of preformed aggregates, a property that was not exhibited by liposomes monofunctionalized with either mApoE or PA alone. This synergistic effect could be due to simultaneous interaction of the negatively charged PA phosphate group with positively charged aminoacidic residues on Aβ and of positively charged amino acids on mApoE with negatively charged regions of Aβ (Bana et al., 2014).

Following studies have shown that the underlying mechanism of mApoE-PA-LIP effect could be due to Aβ removal across the BBB. Indeed, peripheral administration of mApoE-PA-LIP increased the level of plasma Aβ without significant amounts of mApoE-PA-LIP entering the brain suggesting that they promote the removal of aggregates from the brain trough the BBB into the peripheral circulation (Mancini et al., 2016). This mechanism is known as "sink effect", according to which there is a reduction of Aβ burden by peripheral administration of a binding agent that draws excess Aβ out of the brain (Matsuoka et al., 2003).

However interestingly, treated mice also showed early memory restore, as it is demonstrated by novel object recognition test (Balducci et al., 2014), suggesting that are still missing other mechanisms underlying this effect (Forcaia et al., 2021).

Using functionalized liposomes as a therapeutic tool provides a valuable insight into future research studies in order to actively prevent amyloid plaque formation and restore vascular impairment that could occur with AD.

3.2 NANOTOXICITY

Although the use of engineered and multifuncionalized NPs could represent one of the main promising tools for innovative pharmacological strategies in neurology, it is important to underlie that physiologically the BBB represents a mechanism of defense of CNS against potentially neurotoxic substances. It follows that the benefit-risk balance diseases should be carefully evaluated for each type of new engineered NPs. During the assessment of potential neurotoxicity of NPs, it must take into account not only the core structure but also their surface functionalization, employed to reach the target and to make possible the crossing. Both of these elements can significantly alter the biological response (Masserini, 2013). Moreover, it is fundamental consider the multitude of variables that can occur when NPs interact with a complex structure such as the NVU which is responsible for maintaining a delicate balance.

According to a critical review by Calderón-Garcidueñas and colleagues, the information derived from the studies to investigate the behavior and toxicity of NPs developed for technological applications (including drug delivery and drug targeting) give fundamental information that represent the basis to study the mechanisms underlying neurotoxicity induced by anthropogenic NPs, such as air pollution (Fig. 7) (Calderón-Garcidueñas et al., 2019).

This fundamental information includes how these NPs overcome the barriers such as the BBB, considering also the pronounced changes of the NPs protein corona as they cross the BBB and the complexity of NPs interaction with soluble proteins, key organelles and NVU elements in general.

A profound knowledge of NVU is a requirement for understanding access of NPs to the CNS. The integrity of the NVU guarantees the proper function allowing the coupling between neural activity and blood flow. The orchestrated effort of multiple cells engaged in distinct signaling

pathways and effector systems across the entire cerebrovascular network is at the core of the NVU and anything that disturbs this complex but fragile network could have detrimental effect (Iadecola, 2017).

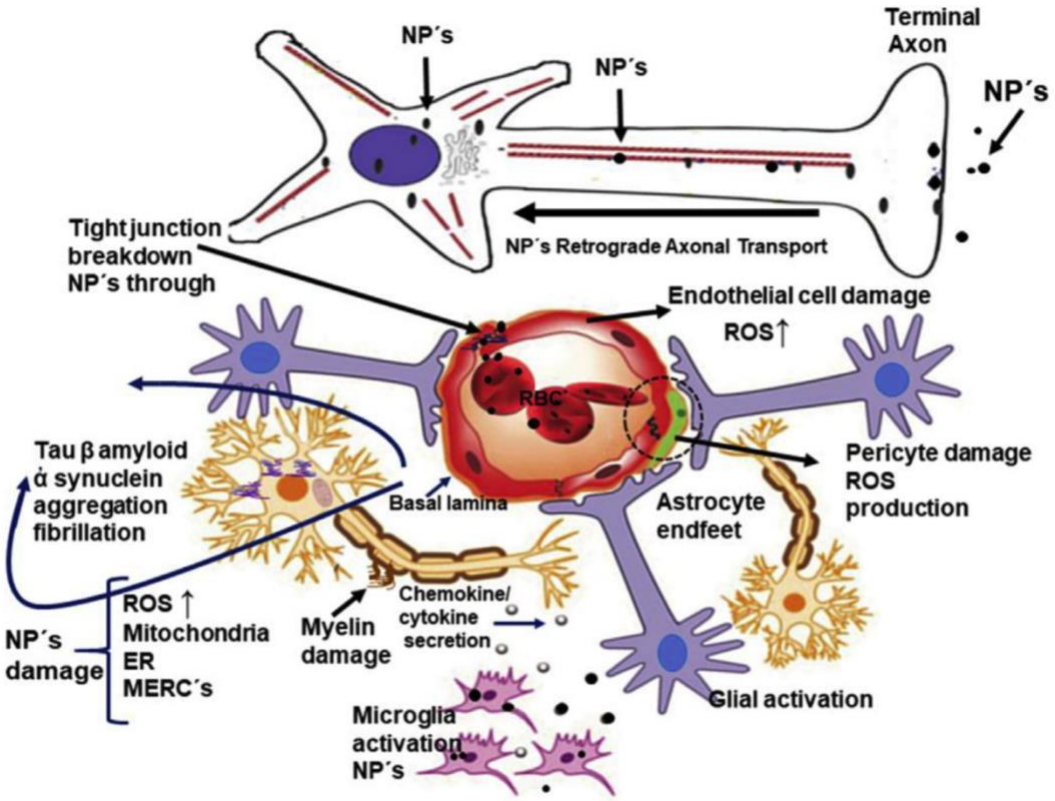

Figure 7. The Neurovascular Unit is the core of NPs-induced damage. The endothelial cells are an early target, along damage to neurons, glial and microglial cells. Binding of NPs to activated endothelial cells, astrocytic feet and choroid plexus damage the NVU and the blood brain barrier and contribute to the inflammatory process. Text and image modified from (Calderón-Garcidueñas et al., 2019)

3.2.1 AIR POLLUTION

Ambient air pollution (AP) is becoming the prominent environmental risk factor that affects public health; according to a document entitled "Ambient (outdoor) air pollution" and published the 22nd of September 2021 by the World Health Organization (WHO), every year in

both cities and rural areas, 4.2 million people prematurely die because of the effects of AP on health.

AP refers to the contamination of the outdoor environment by any chemical, physical or biological agent that modifies the natural characteristics of the atmosphere and that is harmful for living organisms. Among these, particulate matter (PM) of different size, gases, organic compounds and metals are those of major public health concern.

PM is a complex mixture of acids, organic chemicals, metals and soil or dust particles, which can be of natural or anthropogenic sources. The former includes volcanoes, fires, or dust storms, while the latter includes combustion in mechanical and industrial processes, tobacco smoke, and vehicle emissions. One of the main contributors to PM is represented by traffic-related pollutants, mostly ascribed to diesel exhaust particles (DEP).

PM is defined by its aerodynamic equivalent diameter (Ø), that is the Ø of a sphere, with the density of water (1 g/cm^3), which settles in still air at the same velocity as the particle in question; in particular, PM is classified in:

- PM10 is comprised of particles with Ø <10 μm, defined as “coarse”
- PM2.5 is comprised of particles with Ø <2.5 μm, defined as “fine”
- PM0.1 is comprised of particles with Ø < 100 nm, defined as “ultrafine” (UFPM)

It is important to underline the fact that PM10 represents all particles with Ø <10 μm, and thus contains coarse, fine and ultrafine PM fractions.

In recent years there is evidence that AP, as well as causing damages to respiratory and cardiovascular systems, may also affect the brain contributing to CNS diseases (Kim et al., 2010). Among the several pollutants, UFPM and PM2.5 are the most related to CNS diseases. UFPM is considered one of the most neurotoxic because it can penetrate deep into the lung, where it eventually enters the blood circulation and can get distributed throughout the body (Seigneur, 2009); PM2.5, besides increasing C-reactive protein and white blood cell associated with cardiovascular system-related inflammation markers, can also in dose-dependent manner increase IL-1β and TNF-α levels in the lungs, blood and brain, leading to neuroinflammation and affecting synaptic function integrity with consequences on spatial ability, learning and memory (Costa et al., 2020).

Air pollutants could affect the CNS either directly by transport of particles into the CNS or through systemic inflammations. Either of the effects can be caused by the physical characteristics of the particle itself or by toxic compounds adsorbed on them. Although the exact mechanisms underlying brain pathology are not fully understood, several lines of current evidence point out that neuroinflammation, oxidative stress, glial activation and cerebrovascular damage might be the primary pathways activated by inhaled AP (Hahad et al., 2020).

In last years, many studies have been made to establish the pathways trough which PM can affect the CNS. During respiration, the deposition of the particles depends on their size. The larger ones tend to remain in the upper part of the respiratory system causing local inflammation (rhinitis and rhinosinusitis). The smaller ones instead can reach the bronchioles and alveolar spaces causing pulmonary inflammation that helps the particles to cross the gas-blood barrier into the bloodstream (Shou et al., 2019).

There are two main aspects to consider:

1) Peripheral systemic inflammations: Although the CNS is considered an immunologically privileged organ, evidence show that microglia, the immunocompetent cells in the brain, are strongly affected by the inflammatory mediators released at the peripheral level (Dionisio-Santos et al., 2019). Moreover, several studies suggest that activation of the peripheral immune system elicits an increased inflammatory response in brain in aged but otherwise healthy subjects compared with younger cohorts. It has been hypothesized that the difference could be the reactive state of microglial cells in the aged brain. Thus, the aging process appears to serve as a "priming" stimulus for microglia, that causes, upon secondary trigger stimulus, a dysregulated response (Dilger and Johnson, 2008). According to these elements, sustained inflammation in the respiratory tract could also cause inflammatory effects in the brain, with proportionately worse consequences in relation to age.

Moreover, a sustained inflammation causes BBB disruption thus enhancing this bidirectional communication between the periphery and the brain (Fig. 8). The BBB may react to systemic inflammation in several ways; proportionally to the degree of structural disruption of the BBB, these include changes in signaling, enhanced cellular traffic, an increase in solute permeability and direct damage (Galea, 2021)

2) The role of the BBB: The entrance of these peripheral blood-derived substances, including inflammatory factors, into the CNS is strictly regulated by the endothelial cells that are connected by tight junction (TJ), forming the BBB with the function of preserving brain from potentially harmful factors (for anatomical and physiological characteristics see Chapter 1). The efficiency of this function depends on the integrity of the BBB.

According to a study conducted in a murine model, several components of diesel exhaust particles (DEP) could potentially disrupt BBB function. Indeed, cumulative effects from transient but repeated exposure to DEP may induce a state of sustained neurovascular inflammation that thus lastly contribute to the onset or progression of some neurological disorders (Heidari Nejad et al., 2015).

A lot of studies suggest that the exposure to a large number of air pollutants, especially fine and ultra-fine PM, may be an optional factor leading to BBB damage. Moreover, particles could pass through the BBB into the brain to trigger subsequent neuroinflammation and neurodegeneration. Several studies have confirmed that nanosized PM can physically penetrate the main barriers of the body (blood brain barrier and placental barrier) and therefore invade the brain parenchyma of adults (and fetuses) to directly induce effects in the brain (Han et al., 2022). On the other hand, peripheral inflammatory factors induced by PM exposure may also have easier pathway to affect the brain (Fig. 8). However, the mechanisms involved in air pollution-exposure mediated changes in the neurovascular system have not been fully elucidated (Shou et al., 2019)

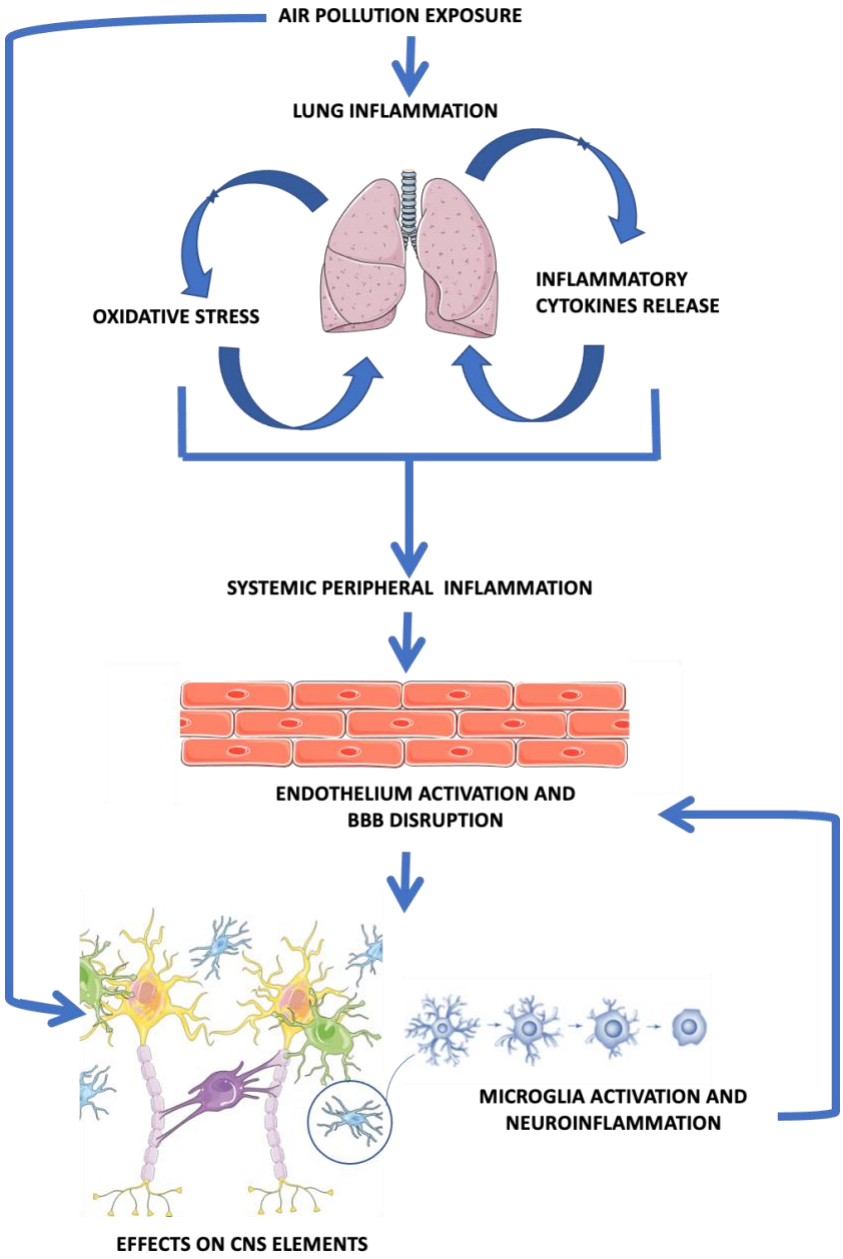

Figure 8. The principal routes of lung-brain axis. Air pollutants could affect the CNS either by direct transport of fine particles into the CNS trough endothelial cells or due to the indirect systemic inflammation. The interaction between particles and peripheral elements (i.e., lung) causes the production of inflammatory mediators that could affect endothelium and other CNS elements generating a cascade effect.

Most of the PM research focuses on the respiratory and cardiovascular diseases, although increasing experimental, clinical and epidemiological evidence has linked the adverse roles of continuous PM exposure with the increased morbidity and mortality of CNS diseases.

The potential CNS effects of ultrafine particles and the lack of studies investigating this important area of research should be addressed (Han et al., 2022).

According to a critical review by Calderón-Garcidueñas and colleagues, the information derived from the studies to investigate the behavior and toxicity of NPs developed for technological applications (including drug delivery and drug targeting) gives fundamental information that represent the basis to study the mechanisms underlying neurotoxicity induced by anthropogenic NPs, such as air pollution (Calderón-Garcidueñas et al., 2019).

In light of these considerations, the following part of the study aims at exploring the complex and correlated effects between nanosized elements of anthropogenic origin and NVU elements, taking advantages from the functional studies conducted to investigate the role of multifunctionalized liposomes, successfully used in a murine model of AD.

AIMS OF THE STUDY

Neurodegenerative diseases are brain disorders characterized by progressive neuronal dysfunction and loss of neuronal cells structure and function within the nervous system (Kovacs, 2018). At present, there is no effective cure for many neurodegenerative diseases, including Alzheimer's disease (AD), and this is a major concern considering that prevalence is increasing, as a result of world population getting old. Indeed, due to an increase in life expectancy and lack of effective treatments, neurodegenerative diseases are predicted to massively grow over the next several decades (Gammon, 2014). Since there is strong evidence in the literature that NVU alterations lead to neuronal damage and brain dysfunction, there is growing interest in investigating the potential contribution of NVU dysfunction to neurodegeneration (de la Torre, 2017).

The concept of the NVU is relatively recent and it is referred to multiple types of brain cells (endothelial cells, astrocytes, pericytes, neurons, microglia) that work together to regulate the transport through the blood–brain barrier (BBB) and the brain tissue homeostasis. Since the CNS has a high metabolic demand and is also extremely sensitive to a wide range of chemicals, it requires a highly regulated extracellular environment. Therefore, it is essential that the interface between the CNS and the peripheral circulatory system functions as a dynamic regulator of ion balance, a facilitator of nutrient transport, and a barrier to potentially harmful molecules. Since the NVU strategic role in regulating this delicate balance, it is clear that an alteration of this system could have deleterious effects to the whole brain. On one hand, the here proposed approach aims to counteract the alterations of this system when the disease is in course and on the other hand, to study what can alter this balance thus leading to the pathology. Indeed, we still lack a full understanding of the mechanisms dysregulated during neurodegenerative disease and it is often difficult to discern the causative factors from the caused ones during the pathology. This knowledge could be useful in identifying factors that contribute to the development and in designing effective therapeutic strategies to treat or prevent these diseases.

On these bases, this thesis aimed at advancing current knowledge in neurovascular unit dysfunction by characterizing the crosstalk and the relationship between its main component,

with the ultimate goal of uncovering novel and multimodal approaches in the field of the neurodegeneration.

In particular, the specific aims of the study are:

AIM 1) To explore the possibility that bi-functionalized liposomes mApoE-PA-LIP, acutely administered, may induce a functional response in neurons (Chapter RESULTS, part I).

Previous data published in our lab showed that liposomes (mApoE-PA-LIP) functionalized with a peptide derived from the apolipoprotein-E receptor-binding domain (mApoE) for BBB targeting and with phosphatidic acid (PA) for Aβ binding, promoted peptide removal across the BBB and its peripheral clearance in an *in vivo* model of AD with memory improvement (Balducci et al., 2014). Subsequent studies of our lab showed that mApoE-PA-LIP pre-treatment increased the ATP-evoked intracellular Ca^{2+} waves, both in presence and in absence of extracellular Ca^{2+}, indicating that this effect is mainly due to endogenous Ca^{2+} release from endoplasmic reticulum (ER) in hCMEC/D3, as an *in vitro* human BBB model, and in cultured astrocytes (Forcaia et al., 2021).

In lights of these results, we investigated whether mApoE-PA-LIP, acutely administered, may induce a functional response in neurons on 300 µm thick-brain slices from CD-1 mouse (P8-P30).

By whole-cell patch-clamp recordings both in voltage- and current-clamp configuration, we examined passive membrane properties and spontaneous excitatory and inhibitory postsynaptic currents (sEPSC and sIPSC) in mouse pyramidal cortical neurons in control condition and following mApoE-PA-LIP perfusion.

Data from this objective advanced our understanding of the mechanism by which after the pulmonary administration of mApoE-PA-LIP 3 times a week for 3 weeks in APP/PS1 Tg mice, a mouse model of AD, there is a recovery of cognitive impairment, as demonstrated by novel object recognition test and could give an additional support to promote mApoE-PA-LIP as effective therapeutic tool for AD.

AIM 2) To explore the effects of ambient (outdoor) air pollution on CNS elements and brain homeostasis *in vitro* by focusing on endothelial cells, that are the first interface between blood and brain, and on microglial cells, the main effector of neuroinflammation (Chapter RESULTS, part II).

Increasing evidence indicates that exposure to particulate matter (PM), combined with individual susceptibility and other possible contributing causes, correlates with the onset or progression of neurodegenerative diseases.

Among the different mechanisms proposed, the two mains are:

i) cerebrovascular damage (as demonstrate also in our previous studies according to which pulmonary PM- exposure in mice caused activation of the endothelium (Farina et al., 2013)), that can alter properties of the BBB (the so-called *hit one*, according to *two-hit vascular hypothesis* of AD) and ii) neuroinflammation that itself or exacerbating the direct damage to the endothelium can lead to neurological impairment.

In lights of this evidence, we investigated the direct effect of ambient air pollution (AP) on endothelial cells (hCMEC/D3) and microglial cells (BV2 and mouse primary cultures) using a standard reference material (SRM) of diesel exhaust particles (DEP), that is one of the main contributors of AP to have less variability and more controlled results. The identification of the DEP concentrations to be used in *in vitro* cell models is calculated as equivalent cumulative exposure dose that basically reflects the human exposure dose of highly polluted urban center. To have the possibility to study fine mechanisms underlying its deleterious effect e not from a toxicological point of view we before performed cell viability assays to verify that DEP at different concentration used did not affect cell viability (exposure to subacute doses).

By immunofluorescence and transmission electron microscopy (TEM) analysis we explored the morphological changes following DEP exposure on microglial and endothelial cells while by calcium imaging technique we characterized the intracellular calcium signalling, since the intracellular calcium concentration ($[Ca^{2+}]_i$) influences multiple fundamental cellular functions. These experiments enabled to define some of the direct effects of DEP on endothelial and microglial cells advancing our understanding in the mechanisms underlying DEP-induced

endothelial dysfunction and neuroinflammation, which may help to prevent, contain or reverse neurodegenerative disease processes exacerbated by ambient air pollution.

By means of nanomedicine and nanotoxicology approaches we can study the trigger mechanisms that potentially lead to CNS dysfunction and the strategies to counteract them.

MATERIALS AND METHODS

4. CELL CULTURE

4.1 ENDOTHELIAL CELLS

Immortalized human cerebral microvascular endothelial cell line (hCMEC/D3) was purchased from the Institute Cochin (INSERM, Paris, France). Cells were used only between passage 25th and 35th. All cultureware used for hCMEC/D3 cells were coated with 50 µg/mL of collagen (Collagen I Rat Tail, *Gibco*) diluted in 0.02 M Acetic acid (CH_3COOH, *Sigma-Aldrich*) and distilled water (dH_2O). The collagen solution was applied to the tissue culture flasks or well plates and they were incubated 1 h at room temperature covered from light. After 1 h the collagen solution was removed and the surfaces were rinsed with sterile Phosphate Buffered Saline (PBS, *EuroClone*). The hCMEC/D3 cells were cultured in complete media composed of Endothelial Cell Basal Medium-2 (EBM®-2, *Lonza*), supplemented with 10% heat-inactivated Foetal Calf Serum (FCS, *Eurobio*), 10 mM HEPES (pH 7.4) (*Gibco*), 100 U/mL Penicillin and 100 µg/mL Streptomycin (Penicillin-Streptomycin, *Gibco*), 1% Chemically Defined Lipid Concentrate (CD Lipid Concentrate, *Sigma-Aldrich*), 5 µg/mL Ascorbic Acid (*Sigma-Aldrich*), 1.4 µM Hydrocortisone (*Sigma-Aldrich*) solubilised in Ethanol (CH_3CH_2OH, *Sigma-Aldrich*) and 1 ng/mL of Recombinant Basic Fibroblast Growth Factor (bFGF, *Sigma-Aldrich*). Cells were seeded at a density of 25K–35K cells/cm^2 in T75 flasks and cultured at 37 °C, in a humidified incubator containing 5% CO_2 (Galaxy S+, *RSBiotech*); confluent hCMEC/D3 monolayers were obtained typically after 3-4 days of seeding. For passaging, cells were washed once with PBS, harvested with 0.25% trypsin/1 mM EDTA solution (Gibco), resuspended in culture medium and plated in T75 flask for expansion. For calcium imaging experiments, cells were seeded in Petri dishes (p35) at a density of 150K-200K for each Petri.

4.2 ASTROCYTES

Immortalized hippocampal astrocytes cell line (WT-iAstro) was kindly provided by Prof. Dmitry Lim (Department of Pharmaceutical Sciences, University of Piemonte Orientale, Novara, Italy)

and was obtained as described in (Rocchio et al., 2019). These lines have been established from hippocampi of wild-type control mice. Cells were used only between passage 16th and 22nd. The WT-iAstro cells were cultured in complete media composed of Dulbecco's Modified Eagle Medium (DMEM, *Euroclone*) supplemented with 10% heat-inactivated Foetal Bovine Serum (FBS, *Gibco*), 100 U/mL Penicillin and 100 µg/mL Streptomycin (Penicillin-Streptomycin, *Gibco)* and 2 mM L-glutamine (*Euroclone*). Cells were seeded at a density of 6K–7K cells/cm^2 in T75 flasks and cultured at 37 °C, in a humidified incubator containing 5% CO_2 (Galaxy S+, *RSBiotech*); confluent WT-iAstro monolayers were obtained typically after 2 days of seeding. For passaging, cells were washed once with PBS, harvested with 0.25% trypsin/1 mM EDTA solution (*Gibco*), resuspended in culture medium and plated in T75 flask for expansion. For calcium imaging experiments, cells were seeded in Petri dishes (p35) at a density of 15K-20K for each Petri.

4.3 MICROGLIAL CELLS

- Cell line: Immortalized murine microglial cells (BV2) were kindly provided by Prof. Dmitry Lim (Department of Pharmaceutical Sciences, University of Piemonte Orientale, Novara, Italy). Cells derived from C57/BL6 murine and are immortalized by v-raf/v-myc carrying J2 retrovirus. BV2 microglia cell line retains microglia morphological and functional characteristics. In accordance with v-raf/v-myc expressed characters, the metabolic and proliferation rate of in vitro BV-2 greatly exceeds that of other microglial cells. BV2 were used only between passage 16th and 22nd. Cells were cultured in complete media composed of Dulbecco's Modified Eagle Medium (DMEM, *Euroclone*) supplemented with with 10% heat-inactivated Foetal Bovine Serum (FBS, *Gibco*), 100 U/mL Penicillin and 100 µg/mL Streptomycin (Penicillin-Streptomycin, *Gibco*) and 2 mM L-glutamine (*Euroclone*). Cells were seeded at a density of 6K–7K cells/cm^2 in T75 flasks and cultured at 37 °C, in a humidified incubator containing 5% CO_2 (Galaxy S+, *RSBiotech*); confluent BV2 monolayers were obtained typically after 2 days of seeding. For passaging, cells were washed once with PBS, harvested in a fresh complete medium

with a cell scraper (*EuroClone*) and plated in T75 flask for expansion. For calcium imaging experiments, cells were seeded in Petri dishes (p35) at a density of 25K for each Petri.

- Primary cultures: Mixed glial cell cultures, containing both astrocytes and microglia, were established from one to three-day C57/BL6 pups (purchased from *Charles River*). Microglia were harvested by manual shaking and re-plated on poly-L-ornithine -coated tissue culture dishes (50 µg/mL, *Sigma-Aldrich*). Microglial cells were cultured in complete media composed of Minimum Essential Media (MEM, *Invitrogen*) supplemented with 20% Foetal Bovine Serum (FBS, *Gibco*), 100 U/mL Penicillin and 100 µg/mL Streptomycin (Penicillin-Streptomycin, *Gibco*) and 5.5 g/L of glucose (*Sigma-Aldrich*).

5. TREATMENTS

5.1 PREPARATION AND CHARACTERIZATION OF mApoE-PA-LIP

mApoE-PA-LIP are composed of sphingomyelin from bovine brain (Sm) and cholesterol (chol) Sm/Chol (1:1 molar ratio) mixed with 2.5 molar% of mal-PEG-PE (Re et al., 2011), and containing either 5 molar% of posphatidic acid (PA). Briefly, lipids were mixed in chloroform/methanol (2:1, v/v) and dried under a gentle stream of nitrogen followed by a vacuum pump for 3 hours to remove traces of organic solvent. The resulting lipid film was rehydrated in PSS, vortexed and then extruded 10 times through a polycarbonate filter (100-nm pore size diameter) under 20 bar nitrogen pressure, with an extruder. mApoE peptide was added to NL to give a final peptide: mal-PEG-PE molar ratio of 1.2:1 and incubated overnight at room temperature to form a thioether bond with mal-PEG-PE. mApoE peptide (CWGLRKLRKRLLR, MW 1698.18 g/mol) was synthetized by Karebay Biochem (*Monmouth Junction*). NL and ApoE-NL size and Polydispersity index (PDI) were obtained using a ZetaPlus particle sizer (*Brookhaven Instruments Corporation*) at 25 °C in H_2O by Dynamic Light Scattering

(DLS) with a 652 nm laser beam. For these experiments we use mApoE-PA-LIP with a diameter of 122.7± 4.85 nm and a PDI of 0.1 ± 0.02.

5.2 PREPARATION OF DIESEL EXHAUST PARTICLES (DEP)

Diesel exhaust particles (Standard Reference Material (SRM) 1650b) were purchased from National Institute of Standards Technology (NIST) (Gaithersburg, MD, USA). DEP 1650b is representative of heavy-duty diesel engine particulate emissions. The reported mean diameter (d (0.5), that is the particle-size distribution parameter indicating the particle size below which 50 % of the volume is present) of these particles was 0.18 µm with a specific Surface Area (S) of 108 m^2/g. DEP particles were weighed with a microbalance (Model: XB220A, *Precisa*) and re-suspended in sterile milli-Q water to a final concentration of 1 mg/mL. Two different ultrasonic systems were chosen to disperse DEP in the water, bath-type sonicator (SONICA *Soltec*) and a probe-type sonicator (Vibra-Cell™, *Sonics*, 3 kJ). The DEP suspension was stored at -20 C°.

6. CELL ASSAY

6.1 VITALITY ASSAY

The MTT assay is a colorimetric and quantitative assay used to measure cellular metabolic activity as an indicator of cell viability. It is based on the reduction of a yellow tetrazolium salt (3-(4,5-dimethylthiazol-2-yl)-2,5-diphenyltetrazolium bromide or MTT) to purple formazan crystals by metabolically active cells. The viable cells contain NAD(P)H-dependent oxidoreductase enzymes which reduce the MTT to formazan. The insoluble formazan crystals are dissolved using a solubilization solution and the resulting-coloured solution is quantified by measuring absorbance at 500-600 nm using a multi-well spectrophotometer (V-770 UV-Visible/NIR spectrophotometer, *Jasco Inc*.). The darker the solution, the greater the number of viable and metabolically active cells.

6.2 PROLIFERATION ASSAY

One day after plating on glass coverslips, microglial cells were co-exposed to DEP and to the thymidine analog EdU (Click-iT® EdU Assay, *Life Technologies*) for 24 h in proliferating medium. Cells were fixed with 4% paraformaldehyde and stained for EdU following the manufacturer's instructions. Coverslips were then incubated with DAPI (1 μg/mL, *Invitrogen*) to reveal total nuclei and mounted with a fluorescent mounting medium (*Dako*). 30-40 fields per coverslip were imaged at 20X magnification under an inverted fluorescence microscope (*Olympus*). Cell proliferation was assessed by quantifying EdU-DAPI double positive nuclei in at least two coverslips/condition, using ImageJ cell counter plugin.

6.3 IMMUNOCYTOCHEMISTRY

Microglia were plated on glass coverslips (1×10^5 cells/coverslip) and incubated overnight. Cells were treated with DEP (10 $\mu g/cm^2$) for 24 hours, then fixed with paraformaldehyde (4%), and immunolabeled overnight with rabbit polyclonal to Iba1, fluorescently tagged with goat anti-rabbit Alexa 555 (1:200) for 1 hour at room temperature and counterstained with DAPI staining (1 μg/mL) for 10 min. Cells were mounted and imaged using an epifluorescence microscope (40×), and morphological changes were qualitatively assessed.

7. CALCIUM IMAGING TECHNIQUE

Cell cultures were loaded with the calcium indicator dye acetoxy-methyl-ester Fura-2 (Fura-2 AM, *Invitrogen*, 2.5 μM, 30 minutes at 37°C, away from light), in phenol-red free Hank's balanced salt solution (HBSS, 140 mM NaCl, 5 mM KCl, 2 mM $CaCl_2$, 1 mM $MgCl_2{\cdot}6H_2O$, 10 mM glucose, 10 mM HEPES, pH 7.4). Fura-2 AM diffuses across the cell membrane and is de-esterified by cellular esterases to Fura-2 free acid (Fig. 9-a). After a washing in HBSS, cells will be disposed in a heated chamber at 37 °C and perfused with HBSS during the experiment. Fura-

2 fluorescence ratio (excitation at 340 and 380 nm; emission at 510 nm) will be observed by a wide-field fluorescence time lapse Nikon Eclipse FN1 upright microscope (*Nikon*) equipped with a 40X Nikon objective (water-immersion, 3.5 mm working distance, 0.80 numerical aperture) (Fig. 9-b,c). The excitation filters were mounted on a filter wheel (Lambda 10-2, *Sutter Instrument*). Images will be acquired for 50 ms with a 1.2 s interval between frames by CoolSNAP Photometrics CCD camera, which is controlled by MetaMorph software (*Molecular Devices*). The obtained data will be quantitatively analysed for changes of fluorescence intensities within the region of interest (ROI). Changes in intracellular Ca^{2+} concentration was evaluated after a trigger of 100 µM (or 200 µM) ATP, followed by washout of 30 minutes and a second ATP stimulus in control condition or after treatment with mApoE-PA-LIP or DEP.

For hCMEC/D3 physiological salt solution (PSS) (NaCl 150 mM; KCl 6 mM; $MgCl_2$ 1mM; $CaCl_2$ 1.5mM; HEPES 10 mM; Glucose 10 mM) was used. Ca^{2+}-free solution (0 $[Ca^{2+}]_e$ PSS) was obtained by substituting Ca^{2+} with 2 mM NaCl and by adding 0.5 mM EGTA.

For iAstro-WT and microglial cells Krebs Ringer Buffer (KRB) solution (125 mM NaCl, 5 mM KCl, 1mM NaH_2PO_4, 1mM $MgSO_4$, 2 mM $CaCl_2$, 5.5mM glucose, 20 mM HEPES) was used. All solutions were adjusted to pH 7.4 ± 0.01 with NaOH 1 M.

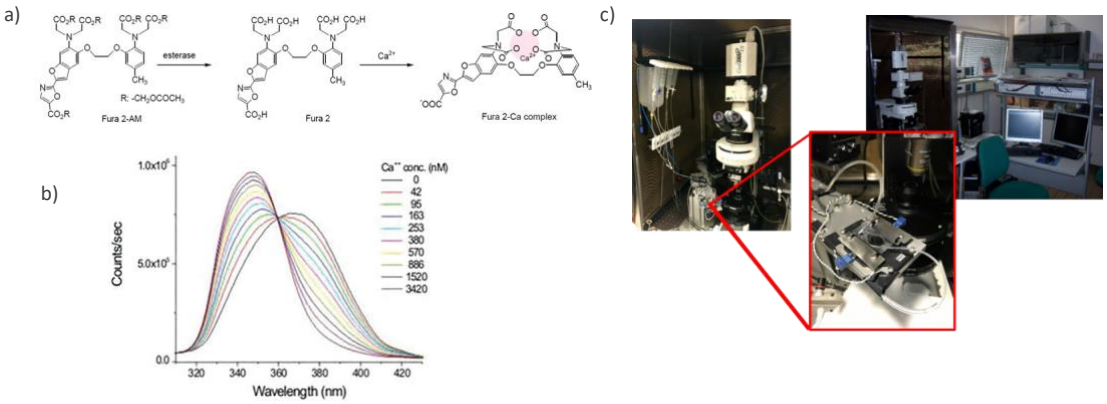

Figure 9. Basic elements of Calcium imaging technique. (a) The protection of carboxylic groups as Acetoxymethyl (AM) esters makes the dye neutral, so it can cross the cell membrane. Once inside the cell, esterases will cleave AM groups. This process gives place to charged compounds that are entrapped inside the cell. (b) Within Fura-2's spectrum it is possible to see that the fluorescence excitation has two peaks. These peaks directly reflect the binding of free ionic calcium in solution. At high free ionic calcium concentrations, the excitation peak of 340 nm is relatively high. When the free ionic calcium concentration is low, the excitation peak at 380 nm is increasing in relation to the peak at 340 nm. (c) Our experimental setup for calcium imaging measurement.

8. ANIMALS AND BRAIN SLICES PREPARATION

Male and female CD-1 mice (P8–21) (purchased from *Charles River*) were employed. All experimental procedures involving animals were performed in accordance with guidelines defined by European legislation (Directive 2010/63/EU) and Italian Legislation (LD no. 26/2014) and were designed to minimize the number of the animals and their suffering. Animals were anesthetized by inhalation of Isoflurane (2%, Isoflurane Veporizer, *Ugo Basile S.R.L*) and, after the loss of the tail-pinch reflex, were decapitated. The whole brain was removed and submerged in cold (∼4°C) carboxygenated (95% O_2, 5% CO_2, gas tanks provided from *Sapio*) cutting solution (NaCl 80 mM, KCl 2.5 mM, $NaH_2PO_4{\cdot}H_2O$ 1.25 mM, $NaHCO_3$ 26 mM, Glucose 15 mM, Sucrose 70 mM, $MgCl_2{\cdot}6H_2O$ 7 mM, $CaCl_2{\cdot}2H_2O$ 1 mM; pH 7.4). Coronal 300 µm-thick slices were prepared using a vibratome (OTS-5000, *Electron Microscopy Sciences*). Following cutting, the slices were allowed to equilibrate for 30 minutes at 35-37 °C and then at room temperature (∼23°C) in a recovery chamber filled with carboxygenated artificial cerebrospinal fluid (aCSF) medium (NaCl 125 mM, KCl 2.5 mM, $NaH_2PO_4{\cdot}H_2O$ 1.25 mM, $NaHCO_3$ 26 mM, Glucose 15 mM, $MgCl_2{\cdot}6H_2O$ 1.3 mM, $CaCl_2{\cdot}2H_2O$ 2.3 mM; pH 7.4).

9. PATCH-CLAMP RECORDINGS

All electrophysiological recordings (Fig. 10) were performed in the whole-cell configuration of the patch-clamp technique, in current-clamp or in voltage-clamp mode. Micropipettes (3-5 MΩ) were pulled from borosilicate capillaries (*Harvard Apparatus*) using a horizontal puller (p-97, *Sutter Instrument*) and filled with the intracellular solution K-based (K-gluconate 130 mM, NaCl 4 mM, $MgCl_2{\cdot}6H_2O$ 2 mM, EGTA 1 mM, Hepes 10 mM, Creatine Phosphate·$4H_2O$ 5 mM, $Na_2ATP{\cdot}H_2O$ 2 mM, $Na_3GTP{\cdot}H_2O$ 0.3 mM; pH adjusted to 7.3 ± 0.01 with KOH 1M). Recordings were performed at room temperature (∼23°C) in a recovery chamber perfused at 1.2 mL/min with aCSF, unless otherwise stated. The recording chamber was mounted on Nikon Eclipse FN1 upright microscope (*Nikon*) equipped with a 40X Nikon objective (water-immersion, 3.5 mm working distance, 0.80 numerical aperture) and connected to a near-infrared CCD camera. Recordings were made with a MultiClamp 700B amplifier (Axon Instruments *Molecular*

Devices) and digitized with a Digidata 1440A computer interface (*Molecular Devices*). Data were acquired using the software Clampex 9.2 (*Molecular Devices*), sampled at 20 kHz, filtered at 10 kHz, and analyzed with the software Clampfit 11.2 (*Molecular Devices*), Mini Analysis Program (*Synaptosof*) and OriginPro 2018 (*OriginLab Corporation*).

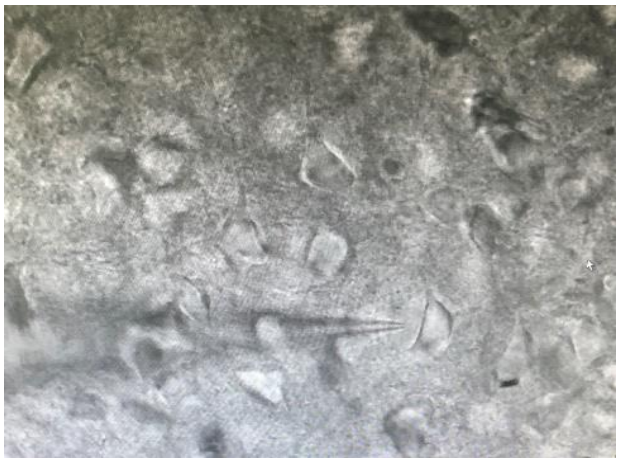

Figure 10. Rapresentative image of cortical neurons of a mouse brain slice. The approach with the glass micropipette (upright microscope) is shown.

10. STATISTYCAL ANALYSIS

Statistical analysis was performed with Microsoft Office Excel 2022 (*Microsoft*) and Prism 9 (*GraphPad Software, LLC*). All data throughout the text are expressed as mean ± SEM (standard error of the mean) and *n* indicates the number of cells analyzed for each experimental procedure. Before statistical analysis the Shapiro-Wilk test was used to assess the normal distribution of data. Statistical significance was assessed with one-way analysis of variance (ANOVA) at the indicated level of significance (p). Mann-Whitney non-parametric U test was used to evaluate data not showing a normal distribution. One-way ANOVA was used for multiple comparisons while two-tailed Student's t-test and Mann-Whitney non-parametric U test were used to compare pairs of data samples.

RESULTS

PRELIMINARY RESULTS

11. mApoE-PA-LIP MODULATION ON CALCIUM DYNAMICS IN hCMEC/D3 AND iASTRO-WT CELLS

IMPORTANT NOTE

This paragraph cites the following article, of which I am a co-author:

Multifunctional Liposomes Modulate Purinergic Receptor-Induced Calcium Wave in Cerebral Microvascular Endothelial Cells and Astrocytes: New Insights for Alzheimer's disease

Greta Forcaia[1], Beatrice Formicola[1], **Giulia Terribile[1]**, Sharon Negri[2], Dmitry Lim[3], Gerardo Biella[2], Francesca Re[1,4], Francesco Moccia[2], Giulio Sancini[1,4]

[1] School of Medicine and Surgery, University of Milano-Bicocca, via Cadore 48, 20900, Monza, MB, Italy.

[2] Department of Biology and Biotechnology "Lazzaro Spallanzani", University of Pavia, Pavia, Italy.

[3] Department of Pharmaceutical Sciences, University of Piemonte Orientale, Via Bovio, 6 28100, Novara, Italy.

[4] Nanomedicine Center, Neuroscience Center, School of Medicine and Surgery, University of Milano-Bicocca, via Cadore 48, 20900, Monza, MB, Italy.

11.1 mApoE-PA-LIP pre-treatment increases ATP-evoked calcium waves in hCMEC/D3 cells both in standard PSS and 0 $[Ca^{2+}]_e$ PSS

In the human immortalized endothelial cells (hCMEC/D3), used as a BBB model, the perfusion with 0.01 mg/mL of mApoE-PA-LIP for 5 minutes increased the Ca^{2+} dynamics evoked by a short (30 sec) ATP pulse in comparison to control conditions both in standard physiological salt solution (PSS) and in the absence of extracellular Ca^{2+} (0 $[Ca^{2+}]_e$ PSS).

We started our study in standard PSS and we analyzed the duration (Fig. 11-Ba) and the area under the curve (A.U.C.) (Fig. 11-Bc) of the Ca^{2+} response to ATP in control condition and after 5 min pretreatment with 0.01 mg/mL of mApoE-PA-LIP. A significant increase of the duration of the ATP-evoked Ca^{2+} waves was found in presence of mApoE-PA-LIP (144 ± 3.03 s, n = 87) in comparison to controls (130 ± 2.19 sec, n = 139) (Fig. 11-Ba). Notably, the pre-treatment with mApoE-LIP (without PA functionalization) did not increase the mean duration of the ATP-induced Ca^{2+} response in hCMEC/D3 cells (125 ± 1.95 sec, n = 52) (Fig. 11-Bb). In agreement with the elongation of the intracellular Ca^{2+} wave, we observed a significant increase in the A.U.C. value after the mApoE-PA-LIP pre-treatment (38.26 ± 5.06) in comparison to controls (25.44 ± 2.82) (Fig. 11-Bc). Moreover, we found again that the pre-treatment with mApoE-PA-LIP also in 0 $[Ca^{2+}]_e$ PSS increased the duration of ATP-evoked Ca^{2+} waves (192.7 ± 6.38 sec, n = 21) in comparison to controls (101.5 ± 9.2 sec, n = 16) (Fig. 12-Ba). Likewise, also the A.U.C increased (26.97 ± 5.88) in comparison to controls (13.29 ± 0.33) (Fig. 12-Bb).

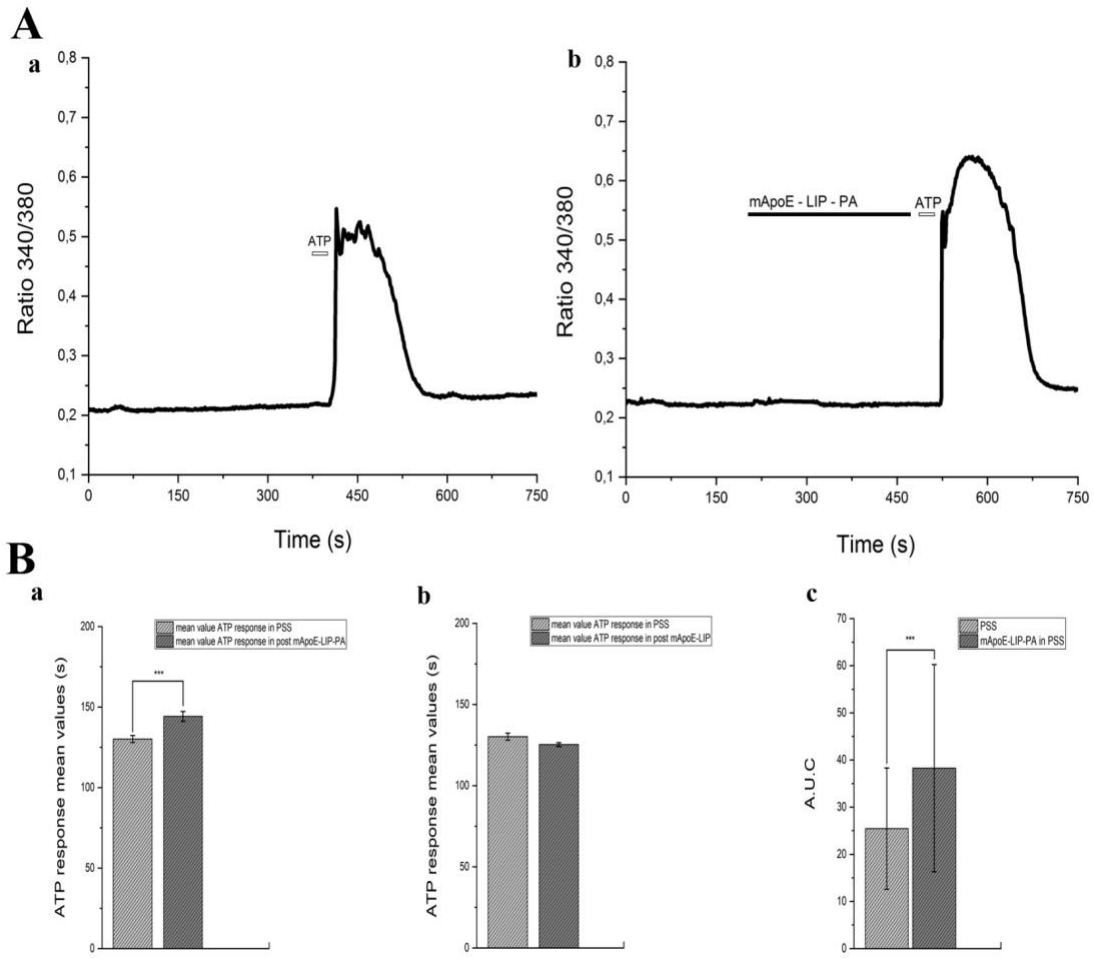

Figure 11. mApoE-PA-LIP pre-treatment increases ATP-evoked calcium waves in hCMEC/D3 cells in standard PSS. (A-a) hCMEC/D3 representative trace of Ca^{2+} response after a trigger of 50 µM ATP in standard PSS is shown. (A-b) hCMEC/D3 representative trace of Ca^{2+} response after a trigger of 50 µM ATP after pre-treatment with 0.01mg/mL mApoE-PA-LIP in standard PSS is shown. (B-a) Bar histogram of the ATP response mean values ± SE in PSS and after a mApoEPA-LIP pre-treatment. (B-b) Bar histogram of the ATP response mean values ± SE in PSS and after a mApoE-LIP (without PA) pre-treatment. (B-c) Bar histogram of the A.U.C mean values ± SE in PSS and after a mApoE-PA-LIP pre- treatment. Unpaired t test, differences were considered significant at ***p value < 0.001.

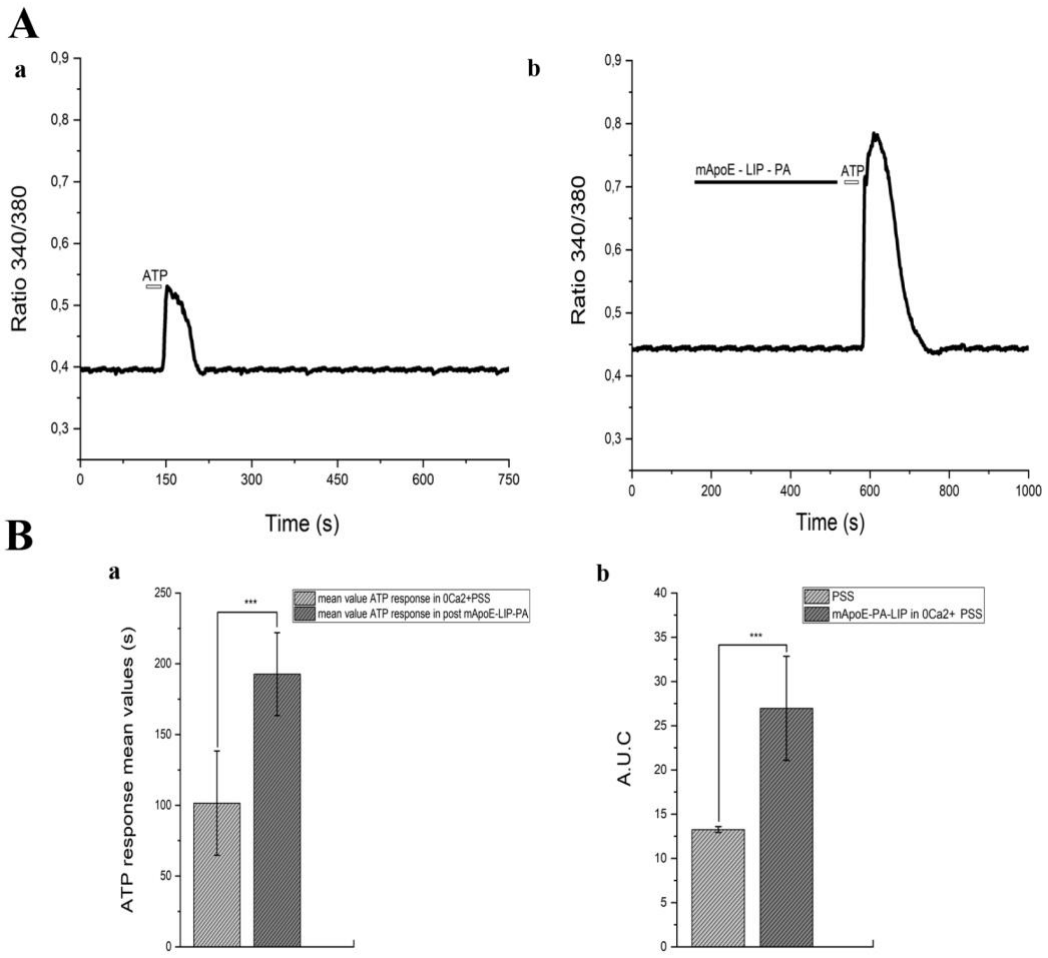

Figure 12. mApoE-PA-LIP pre-treatment increases ATP-evoked calcium waves in hCMEC/D3 cells in 0 [Ca2+]e PSS. (A-a) hCMEC/D3 representative trace of Ca^{2+} response after a trigger of 50 µM ATP in 0 $[Ca^{2+}]_e$ PSS is shown. (A-b) hCMEC/D3 representative trace of Ca^{2+} response after a trigger of 50 µM ATP after pre-treatment with 0.01mg/mL mApoE-PA-LIP in standard 0 $[Ca^{2+}]_e$ PSS is shown. (B-a) Bar histogram of the ATP response mean values ± SE in PSS without Ca2+ and after a mApoEPA-LIP pre-treatment. (B-b) Bar histogram of the A.U.C mean values ± SE in PSS and after a mApoE-PA-LIP pre-treatment. Also, in 0 $[Ca^{2+}]_e$, the pretreatment with mApoE-PA-LIP increased the calcium dynamics evoked by ATP stimulus in comparison to control. Unpaired t test, differences were considered significant at **p value < 0.01.

11.2 mApoE-PA-LIP pre-treatment increases ATP-evoked calcium waves in iASTRO-WT cells both in normal KRB and 0 $[Ca^{2+}]_e$ KRB

Also in the murine immortalized astocytes (iASTRO-WT), the perfusion with 0.01 mg/mL of mApoE-PA-LIP for 5 minutes increased the Ca^{2+} dynamics evoked by a short (30 sec) ATP pulse in comparison to control conditions both in standard Krebs Ringer Buffer (KRB) solution and in the absence of extracellular Ca^{2+} (0 $[Ca^{2+}]_e$ KRB). We observed a significant increase in the duration of ATP-evoked Ca^{2+} waves in presence of mApoE-PA-LIP (277 ± 26.63 sec, n = 34) in comparison to controls (137 ± 4.65 sec, n = 56) (Fig. 13-Ba). We then confirmed that also the A.U.C. (Fig. 13-Bb) of the Ca^{2+} response to ATP increased after pre-treatment with mApoE-PA-LIP in standard KRB. After the pre-treatment, indeed, A.U.C increased (4.35 ± 0.41) in comparison to control (2 ± 0.09). We confirmed that the pre-treatment with mApoEPA-LIP in 0 $[Ca^{2+}]_e$ KRB increased ATP-evoked Ca^{2+} waves in comparison to control (Fig. 14-A). The ATP response duration (Fig. 14-Ba) was significantly increased (130.68 ± 3.25 sec, n = 21) in comparison to control (102.47 ± 5.98 sec, n = 38). Under this condition, also the A.U.C value increased (1.71 ± 0.07) in comparison to control (1± 0.08) (Fig. 14-Bb)

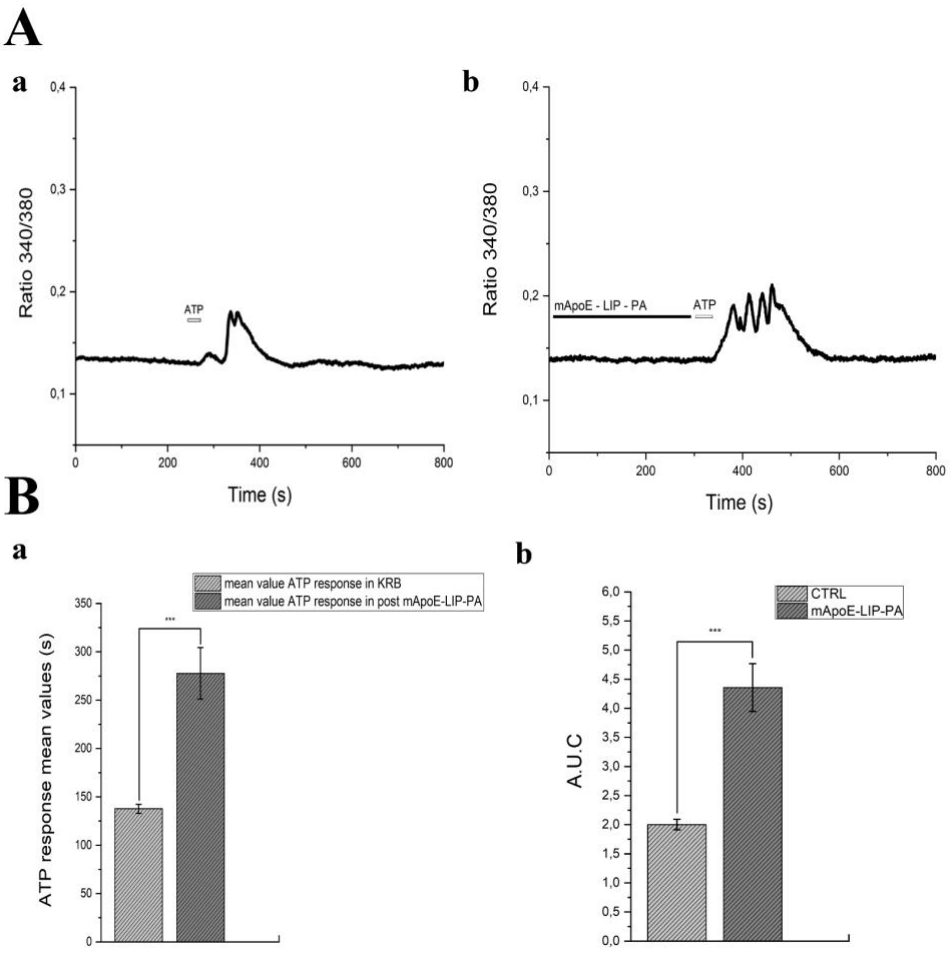

Figure 13. mApoE-PA-LIP pre-treatment increases ATP-evoked calcium waves in iASTRO-WT cells in normal KRB

(A-a) iAstro-WT representative trace of Ca^{2+} response after a trigger of 100 µM ATP in standard KRB is shown. (A-b) iAstro-WT representative trace of Ca^{2+} response after a trigger of 100 µM ATP after the pre-treatment with 0.01mg/mL mApoE-PA-LIP in standard KRB is shown. (B-a) Bar histogram of the ATP response mean values ± SE in KRB and after mApoE-PA-LIP pre-treatment. (B-b) Bar histogram of the A.U.C mean values ± SE in KRB and after mApoE-PA-LIP pre-treatment. Unpaired t test, differences were considered significant at ***p value < 0.001.

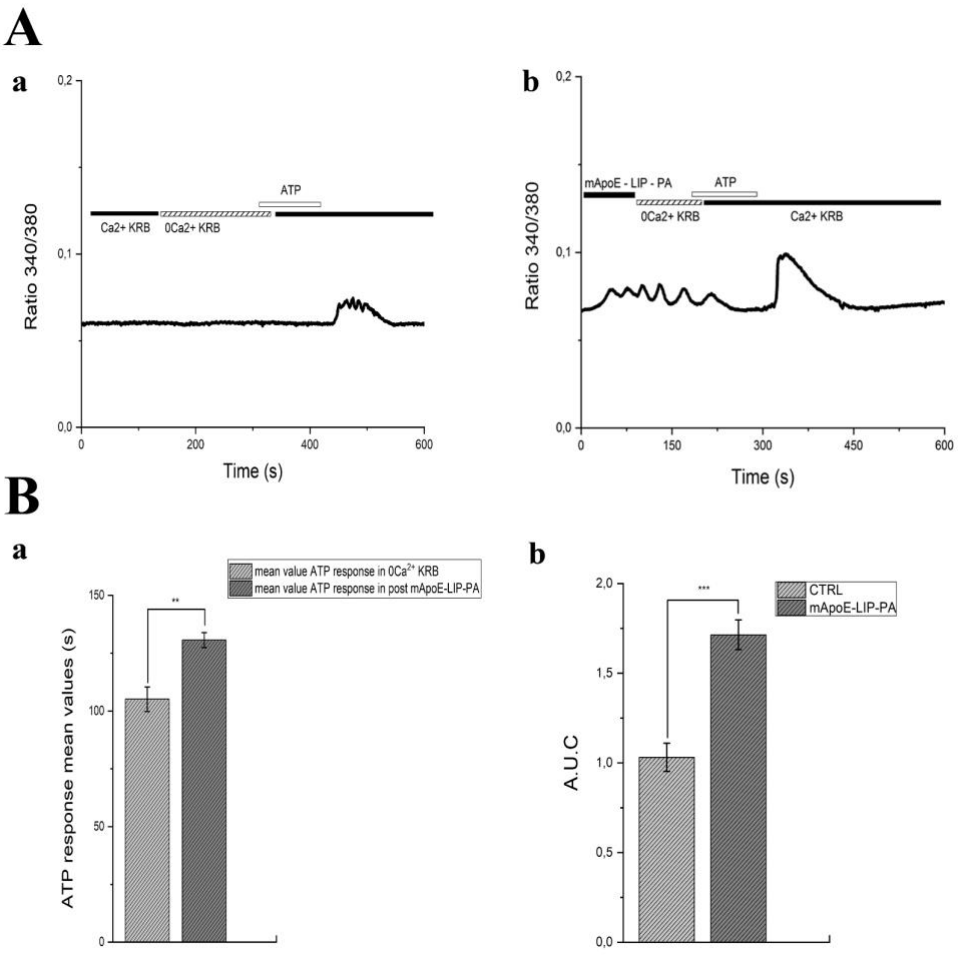

Figure 14. mApoE-PA-LIP pre-treatment increases ATP-evoked calcium waves in iASTRO-WT cells also in 0 0 $[Ca^{2+}]_e$ KRB. (A-a) iAstro-WT representative trace of Ca^{2+} response after a trigger of 100 µM ATP in 0 $[Ca^{2+}]_e$ KRB is shown. (A-b) iAstro-WT representative trace of Ca^{2+} response after a trigger of 100 µM ATP after the pre-treatment with 0.01mg/mL mApoE-PA-LIP in 0 $[Ca^{2+}]_e$ KRB is shown. (B-a) Bar histogram of the ATP response mean values ± SE in KRB and after mApoE-PA-LIP pre-treatment in 0 $[Ca^{2+}]_e$ KRB. (B-b) Bar histogram of the A.U.C mean values ± SE in KRB and after mApoE-PA-LIP pretreatment in 0 $[Ca^{2+}]_e$. Unpaired t test, Differences were considered significant at **p value < 0.01, and ***p value < 0.001.

11.3 mApoE-PA-LIP pre-treatment modulates Ca^{2+} dynamics only when SERCA is active both in hCMEC/D3 cells and iAstro-WT

In order to confirm that the endoplasmic reticulum (ER) represents the main endogenous Ca^{2+} store targeted by ATP, we then evaluated the Ca^{2+} response to ATP in presence of Cyclopiazonic Acid (CPA), that specifically binds to and inhibits Sarco-Endoplasmic Reticulum Calcium ATPase (SERCA), in normal standard solution and in 0 $[Ca^{2+}]_e$ (PSS for hCMEC/D3 and KRB for iASTRO-WT) both in hCMEC/D3 cells (Fig. 15) and in iAstro-WT (Fig. 16). In the presence of extracellular Ca^{2+}, CPA evoked an initial increase in $[Ca^{2+}]_i$ followed by a prolonged plateau phase, which were due to passive ER Ca^{2+} release and store-operated calcium entry (SOCE) activation respectively (Fig. 15-A and Fig. 16-A). As expected, the Ca^{2+} response to CPA adopted transient kinetics under 0 $[Ca^{2+}]_e$ conditions (Fig. 15-B). However, ATP failed to trigger intracellular Ca^{2+} signaling upon depletion of the ER Ca^{2+} store with CPA in hCMEC/D3 and in iASTRO-WT cells both in standard solution and in 0 $[Ca^{2+}]_e$.

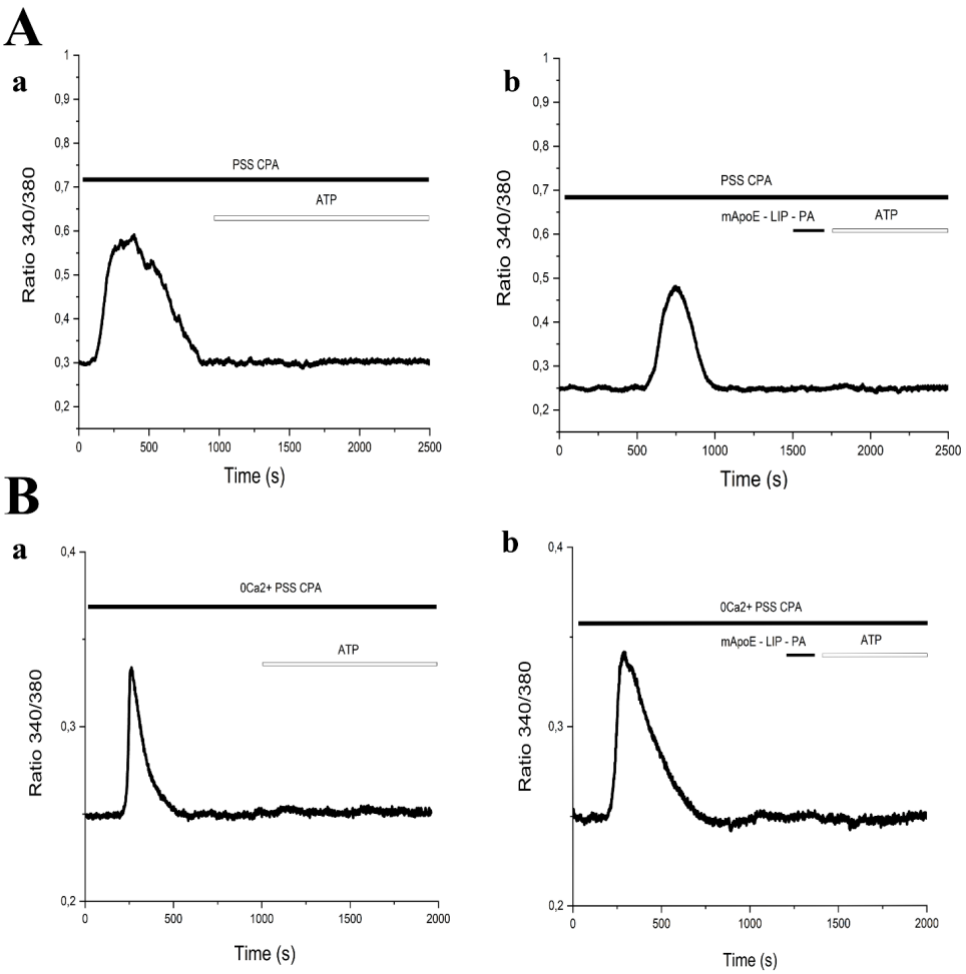

Figure 15. CPA effect on hCMEC/D3 cells. (A-a) CPA (10 µM) response under extracellular Ca^{2+} conditions. ATP-evoked response is blocked by CPA perfusion. (Ab) CPA (10 µM) response after pre-treatment with 0.01 mg/mL of mApoE-PA-LIP, also in these conditions there is no ATP response. (B-a) CPA (10 µM) response under 0 $[Ca^{2+}]_e$ conditions. (B-b) CPA (10 µM) response after pre-treatment with 0.01 mg/mL of mApoE-PA-LIP in 0 $[Ca^{2+}]_e$ PSS. With CPA both in presence and absence of extracellular calcium, ATP failed to activate calcium wave.

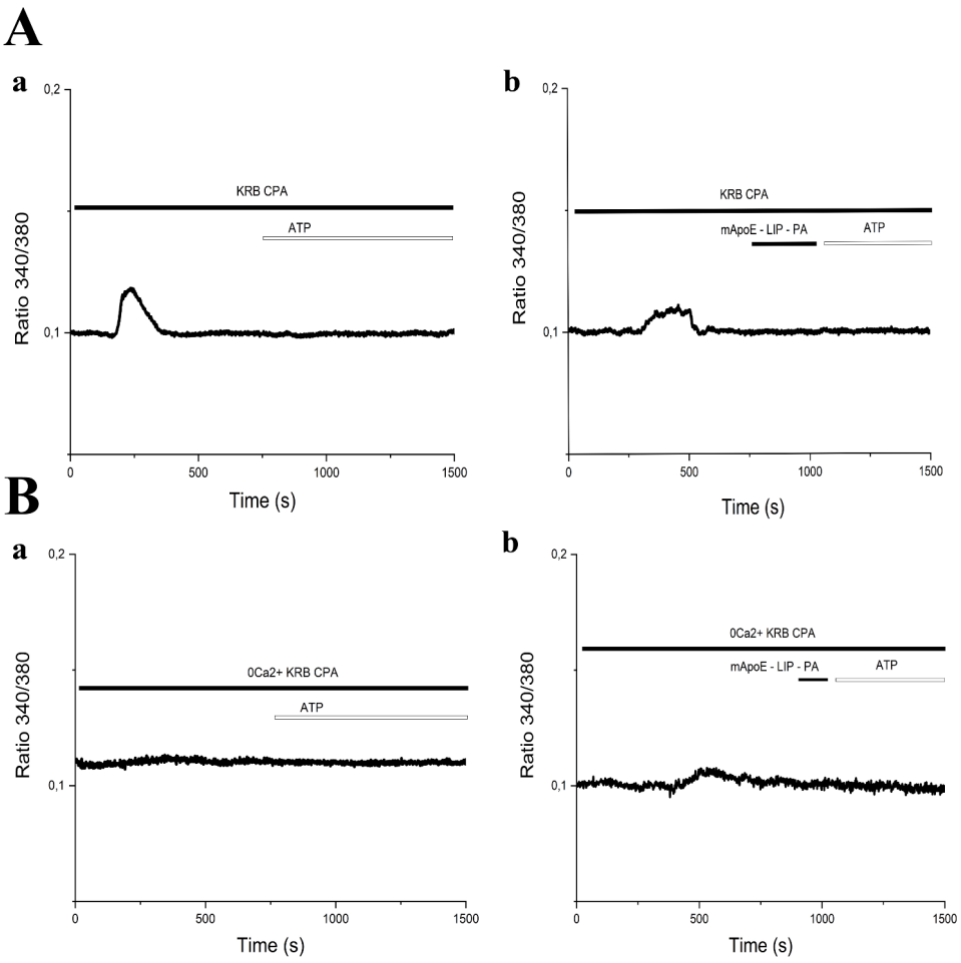

Figure 16. CPA effect on iASTRO-WT cells. (A-a) CPA (10 µM) response under extracellular Ca^{2+} conditions. ATP-evoked response is blocked by CPA perfusion. (A-b) CPA (10 µM) response after pre-treatment with 0.01 mg/mL mApoE-PA-LIP, also in these conditions there is no ATP response. (B-a) CPA (10 µM) administration under 0 $[Ca^{2+}]e$ conditions. ((B-b) CPA (10 µM) response after pre-treatment with 0.01 mg/mL of mApoE-PA-LIP in 0 $[Ca^{2+}]_e$ KRB. With CPA both in presence and absence of extracellular calcium, ATP failed to activate calcium wave.

With these preliminary results we assessed mApoE-PA-LIP activities on hCMEC/D3 as an in vitro human BBB model and on cultured astrocytes in order to evaluate mApoE-PA-LIP ability of modulating the intracellular Ca^{2+} dynamics within two main cellular constituents of the NVU. Our results proved that mApoE-PA-LIP actively modulate the intracellular Ca^{2+} waves triggered by extracellular ATP in cultured hCMEC/D3 and astrocytes.

A trigger stimulus of 50 and 100 µM ATP for both hCMEC/D3 and astrocytes respectively, increased the duration and the A.U.C of the Ca^{2+} wave when both hCMEC/D3 and astrocytes were pre-treated with mApoE-PA-LIP at the final concentration of 0.01 mg/mL. Interestingly, pretreatment with mApoE-LIP without PA functionalization failed to increase both the duration and the A.U.C of the intracellular Ca^{2+} wave triggered by ATP. mApoE-PA-LIP increased the ATP-evoked intracellular Ca^{2+} waves in cultured hCMEC/D3 and astrocytes even under 0 $[Ca^{2+}]_e$ conditions, thus indicating that the increased intracellular Ca^{2+} wave triggered by ATP is mainly due to endogenous Ca^{2+} release from ER. Indeed, when SERCA activity was blocked by CPA, the extracellular application of ATP failed to trigger any intracellular Ca^{2+} waves.

RESULTS PART I

12. mApoE-PA-LIP modulation on pyramidal cortical neurons on mouse brain slices

In order to explore the possibility that mApoE-PA-LIP, acutely administered, may induce a functional response in neurons, whole-cell patch-clamp recordings of passive membrane properties and spontaneous excitatory and inhibitory postsynaptic currents (sEPSC and sIPSC) were performed on mouse pyramidal cortical neurons in control condition and following mApoE-PA-LIP perfusion. All the experiments were carried out on mouse brain slices. Although the cortex exhibits a remarkable heterogeneity of neuronal populations, during patch-clamp experiments, pyramidal neurons were visually identified by the use of infrared differential interference contrast (IR-DIC) microscopy, based on their morphological characteristics such as the triangular-shaped cell body and a, partially visible, pronounced apical dendrite. In addition, their cellular identity was confirmed considering their intrinsic membrane properties, including large action potential amplitudes and strong adaptation (Fig. 17). In this way it was possible to easily distinguish pyramidal neurons from other cell types contained in the cortex, such as the bipolar neurons, with rounded soma and two emerging extensions or the glial cells with their multiradiate symmetry and the absence of action potentials. Only healthy neurons with a stable resting membrane potential (V_{rest}) of about −70, a stable firing level and overshooting action potentials were included in the study. During recording, mApoE-PA-LIP was perfused at the concentration of 0.01 mg/mL for approximately 10 minutes. Data shown in Fig. 18 refers to the same cell in control condition and after the perfusion and indicates that the mApoE-PA-LIP perfusion doesn't alter the firing responses.

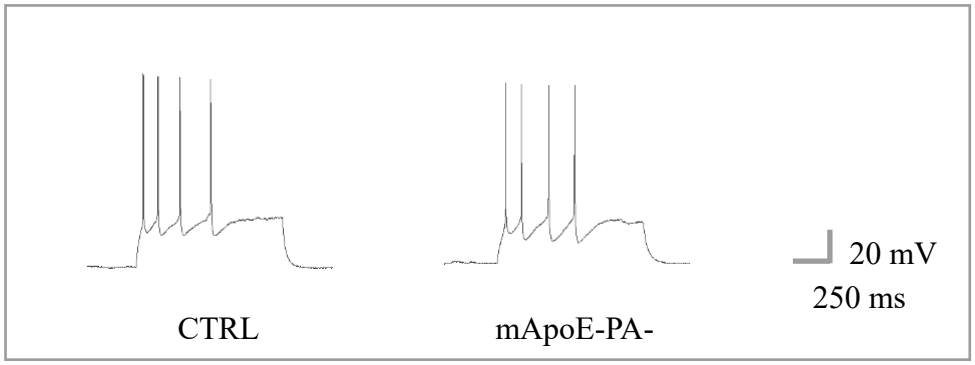

Figure 17. Firing pattern of a cortical pyramidal neuron. Current clamp recording of firing pattern evoked by the injection of just over-threshold depolarizing current step before and after mApoE-PA-LIP perfusion [0.01 mg/mL].

12.1 mApoE-PA-LIP perfusion does not affect passive membrane properties

The possible effects of the mApoE-PA-LIP on the passive membrane properties of the cortical pyramidal neurons have been investigated using whole-cell patched-clamp experiments performed on mouse brain slices. Passive membrane properties determine the size and time course of the voltage response of the neuron, the distance that the voltage response can travel and the speed of voltage response propagation.

The main passive properties that have been considered include:

i) the resting membrane potential (V_{rest}, expressed in mV), that is the relatively static electrical potential difference across the plasma membrane, when the cell is quiescent in a non-excited state. For a direct electrical estimation of the V_{rest}, a whole-cell patch recording initially achieved under voltage clamp condition, is switched to current clamp configuration. The output signal obtained at zero current (I=0) returns the V_{rest} of the recorded neuron;

ii) the cell membrane capacitance (C_m, expressed in pF) that is the ability of the cell membrane to store charge. C_m has been estimated by applying a square wave voltage to the membrane during voltage clamp recordings, allowing the charging and discharging of the cell membrane to be measured by studying the current that flows in response to the voltage step;

iii) the membrane resistance (R_m, expressed in MΩ) that depends on the amount of charge that can leak through the cell membrane. R_m has been estimated applying a square wave voltage to the membrane during voltage clamp recordings. The obtained current response has been used to calculate R_m according to Ohm's law;

iv) the membrane time constant (τ_m, expressed in ms) dictates how fast the cell membrane potential responds to the injection of current stimuli. τ_m has been estimated by exponential fitting of the decay voltage response to current steps during current clamp recordings. In this study, the passive membrane properties of

the neurons have been analyzed before and after the perfusion of the mApoE-PA-LIP [0.01 mg/mL].

From the data obtained (Fig. 18) it was possible to conclude that the exposure of neurons to mApoE-PA-LIP did not determine any significant change in the passive properties considered.

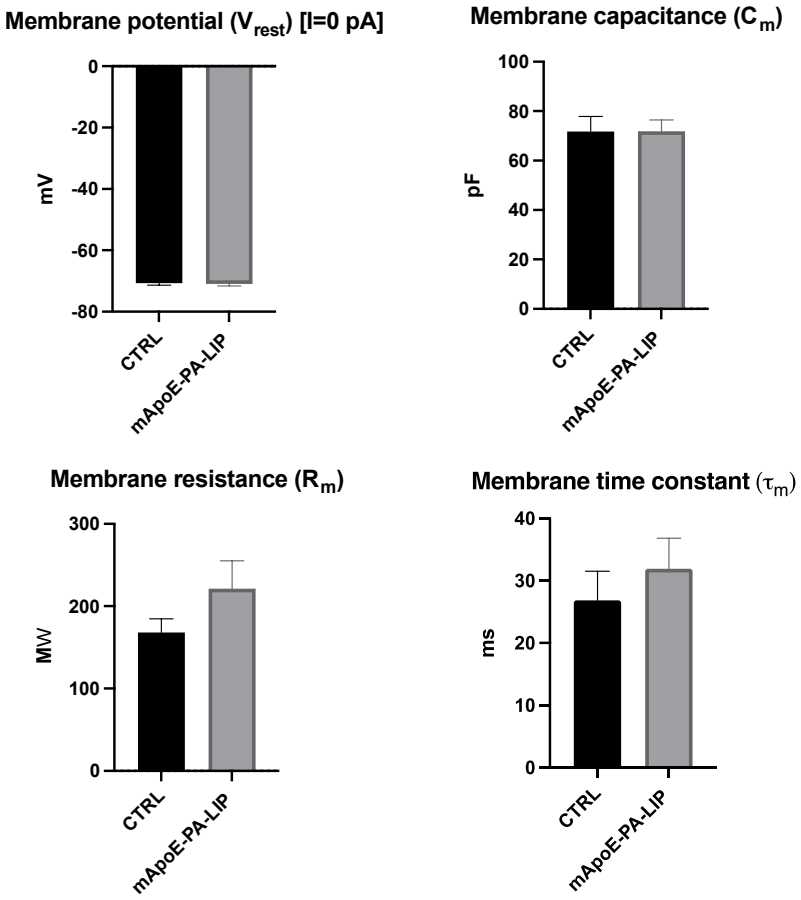

Figure 18. Passive properties (V_{rest}, C_m, R_m, τ_m) at V_h -70 mV, in pyramidal neurons (N=15) before and after liposomes perfusion [0.01 mg/mL]. The histograms show that the mApoE-PA-LIP perfusion did not produce effects on passive properties of the membrane in the tested cells. The average values of V_{rest} were: -70.70 ± 0.68 mV in cells in control condition, -70.93 ± 0.70 mV after the perfusion with mApoE-PA-LIP; the average values of C_m were: 71.78 ± 6.09 pF in cells in control condition, 71.89 ± 4.58 pF after the perfusion with mApoE-PA-LIP; the average values of R_m were: 168.17 ± 16.37 MΩ in cells in control condition, 221.43 ± 0.70 MΩ after the perfusion with mApoE-PA-LIP; the average values of τ_m were: 26.85.70 ± 4.65 ms in cells in control condition, 31.93.93 ± 4.90 ms after the perfusion with mApoE-PA-LIP. All results are plotted as mean ± SEM, statistical evaluations were obtained using the paired t-test.

12.2 mApoE-PA-LIP perfusion increases the frequency but not the amplitude of sEPSCs recorded from mouse cortical pyramidal neurons at -70 mV

To determine any possible short-term effect induced by mApoE-PA-LIP on synaptic transmission, mApoE-PA-LIP [0.01 mg/mL] have been perfused for 10 minutes, during whole-cell patch-clamp recordings performed on mouse cortical pyramidal neurons.

The excitatory spontaneous activity was monitored in voltage-clamp configuration by holding the cell membrane potential at -70 mV. At this holding potential, the contribution of the inhibitory synaptic (GABAergic) currents could be considered negligible on the basis of the chloride (Cl-) reversal potential calculated for the solutions used for the recordings. In this way it has been possible to record just the spontaneous excitatory postsynaptic currents (sEPSCs), mediated by the activation of ionotropic glutamate receptors (AMPA) and that appear as inward currents (Fig. 19). Under these experimental conditions, mApoE-PA-LIP application increased the frequency of sEPSCs (Fig. 20-A) by 33.3±5.8% (n = 15 neurons) with no change in their amplitude (Fig. 20-B).

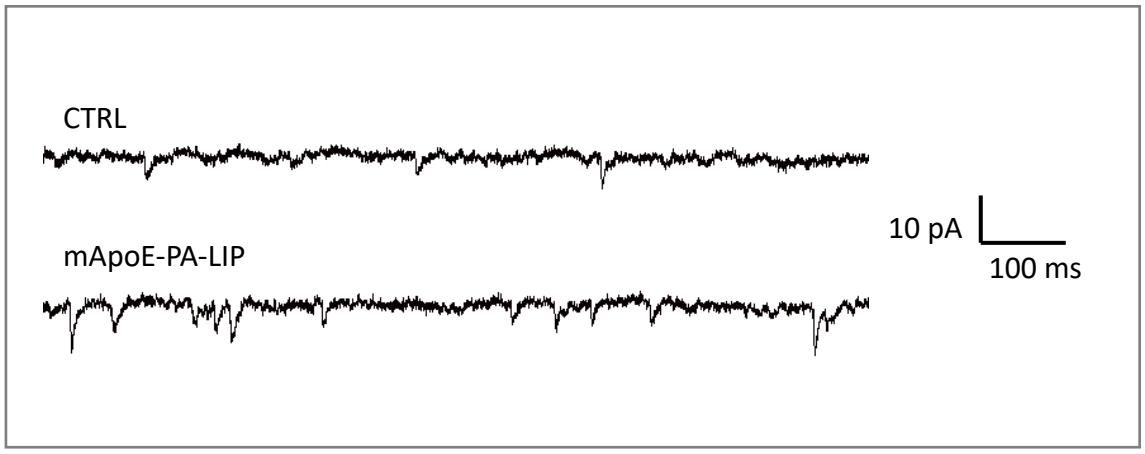

Figure 19. sEPSCs recorded from mouse cortical pyramidal neuron at -70 mV. Representative current traces of sEPSC recorded from a mouse cortical pyramidal neuron at the holding potential of -70 mV in control conditions (CTRL, top trace) and after liposomes perfusion [0.01 mg/mL] (mApoE-PA-LIP, bottom trace).

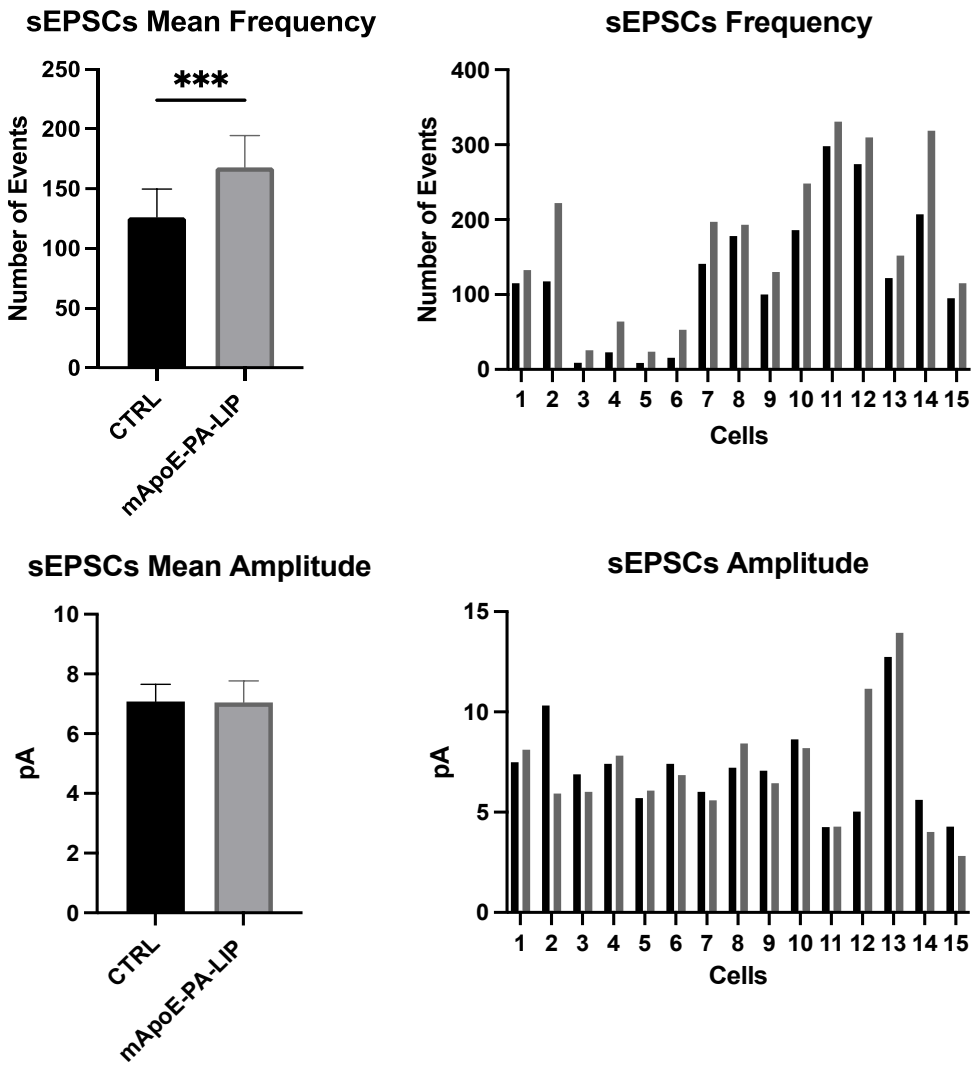

Figure 20. sEPSCs recorded from mouse cortical pyramidal neuron at -70 mV. sEPSCs frequency and amplitude (n = 15) at V_h -70 mV, comparing cortical neurons before and after mApoE-PA-LIP perfusion. All results are plotted as mean ± SEM, paired t-test, differences were considered significant at *** p value < 0.001.

12.3 mApoE-PA-LIP perfusion modifies the kinetics of the sEPSCs event

The kinetic analysis of sEPSCs was performed by measuring rise time and time constant of decay. It has been observed (Fig. 21) that in the presence of mApoE-PA-LIP the decay time is significantly slower compared to the control condition. On the contrary, no difference was found in the rise time kinetics between the control and mApoE-PA-LIP condition.

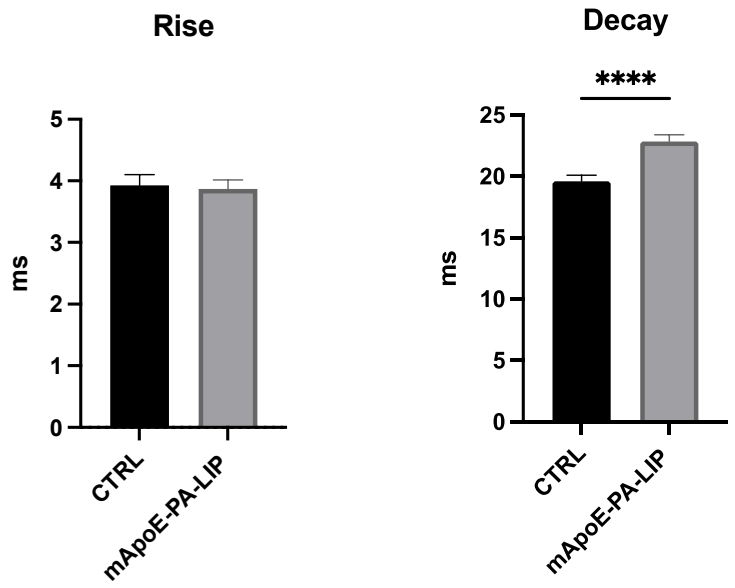

Figure 21. Kinetics of the sEPSCs event. Rise and decay at V_h -70 mV, comparing cortical neurons before and after mApoE-PA-LIP perfusion. All results are plotted as mean ± SEM, paired t-test, differences were considered significant at **** p value < 0.0001.

12.4 mApoE-PA-LIP perfusion does not increase the frequency and the amplitude of sEPSCs in presence of NBQX at -70 mV

We next identified the neurotransmitter receptors involved in this response using pharmacology. As shown in Fig. 22, when AMPA transmission was blocked by 10 µM 2,3-dihydroxy-6-nitro-7-sulfamoyl-benzo[f]quinoxaline- 2,3-dione (NBQX), the sEPSCs mean frequency was dramatically reduced and in this condition mApoE-PA-LIP perfusion failed to increase the frequency of the remaining sEPSCs. This result could suggest that the mApoE-PA-LIP-mediated increase in sEPSCs frequency could involve AMPAergic transmission.

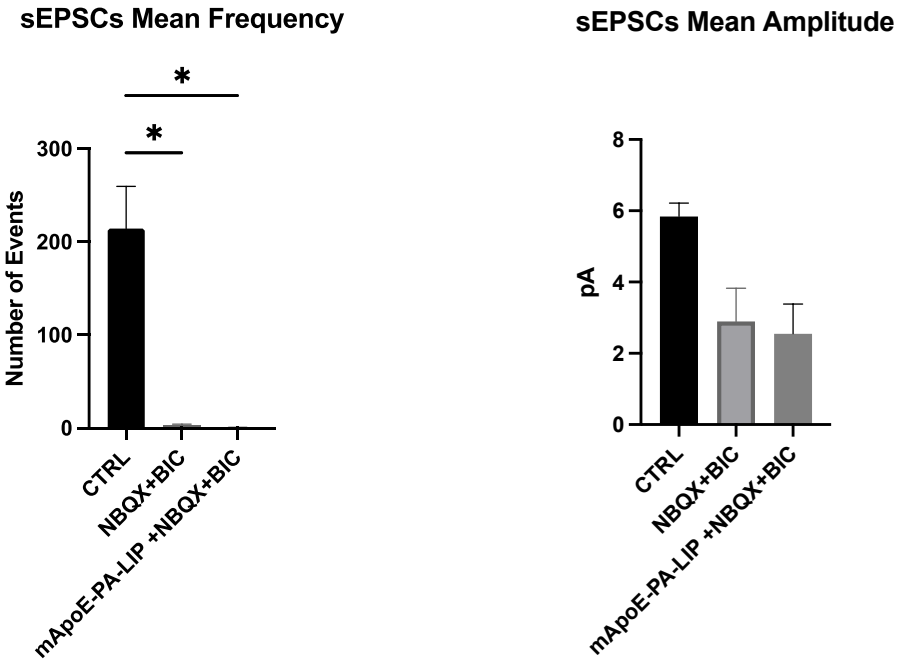

Figure 22. sEPSCs recorded from mouse cortical pyramidal neuron at -70 mV in presence of NBQX. sEPSCs frequency and amplitude at V_h -70 mV, comparing cortical neurons (N=6) before and after liposomes perfusion and applying a selective blocker (NBQX) of glutamate receptors AMPA/Kainato. All results are plotted as mean ± SEM, one-way ANOVA, differences were considered significant at * p value < 0.05.

12.5 mApoE-PA-LIP perfusion increases the frequency but not the amplitude of sEPSCs recorded from mouse cortical pyramidal neurons at -50 mV

To investigate any possible NMDA contribution to the observed increase induced by mApoE-PA-LIP on synaptic transmission, mApoE-PA-LIP [0.01 mg/mL] have been perfused for 10 minutes, during whole-cell patch-clamp recordings performed on mouse cortical pyramidal neurons. Spontaneous activity was monitored in voltage-clamp configuration by holding the cell membrane potential at -50 mV. When V_h is depolarized to –50 mV, Mg^{2+} block is removed, thus activating NMDA receptors. Under these experimental conditions, mApoE-PA-LIP application increased the frequency of sEPSCs (n = 6 neurons) with no change in their amplitude (Fig. 23).

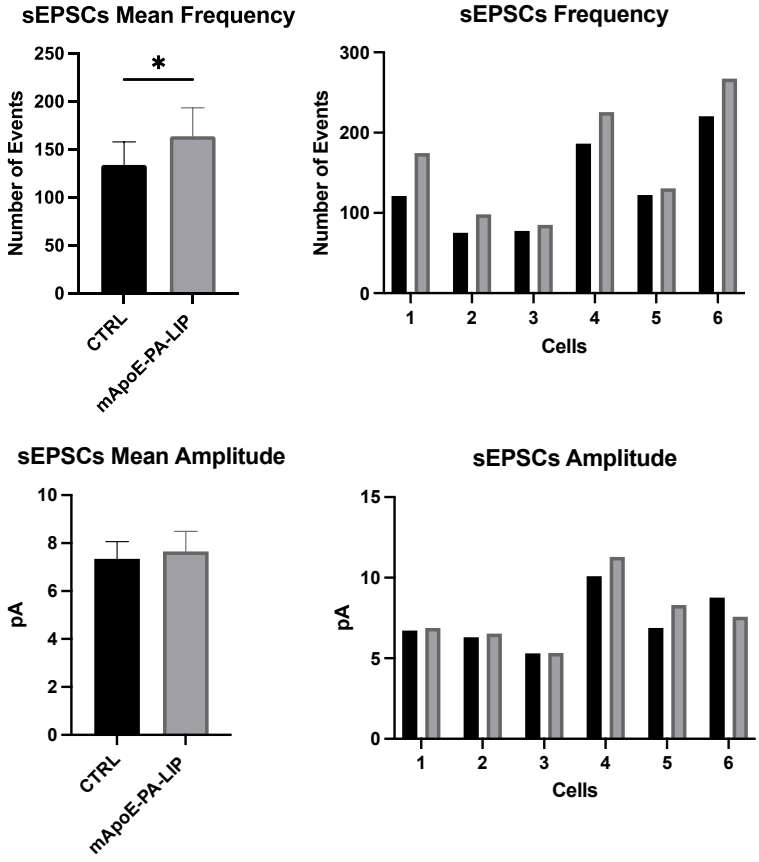

Figure 23. sEPSCs recorded from mouse cortical pyramidal neuron at -50 mV sEPSCs frequency, amplitude at V_h -50 mV, comparing cortical neurons (N=6) before and after liposomes perfusion. All results are plotted as mean ± SEM, paired t-test, differences were considered significant at * p value < 0.05.

12.6 mApoE-PA-LIP perfusion increases the frequency but not the amplitude of sIPSCs recorded from mouse cortical pyramidal neurons at -50 mV

In the same experimental conditions, monitoring the spontaneous activity in voltage-clamp configuration by holding the cell membrane potential at -50 mV, spontaneous inibitory postsynaptic currents (sIPSCs) were also analysed. Indeed, spontaneous currents were recorded at -50 mV, which is less negative than the reversal potential for inhibitory post-synaptic potentials and so outward currents were considered as sIPSCs.

Under these conditions, mApoE-PA-LIP application increased the frequency of sIPSCs (n = 6 neurons) with no change in their amplitude (Fig. 24).

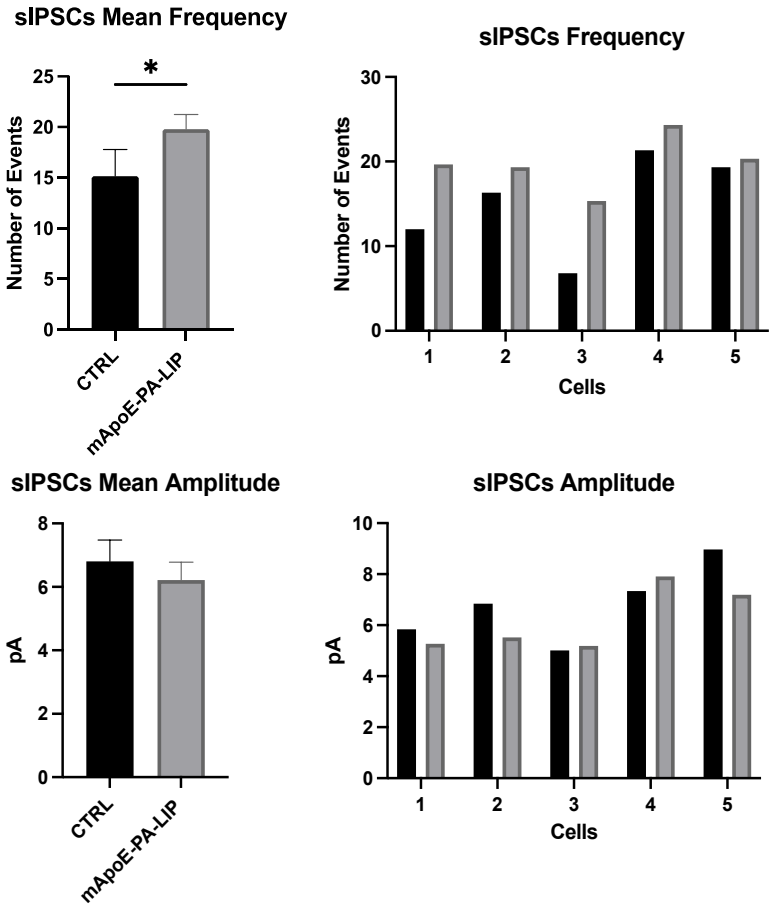

Figure 24. sIPSCs recorded from mouse cortical pyramidal neuron at -50 mV. sIPSCs frequency, amplitude at V_h -50 mV, comparing cortical neurons (N=6) before and after liposomes perfusion. All results are plotted as mean ± SEM, paired t-test, differences were considered significant at * p value < 0.05.

RESULTS PART II

13. In vitro diesel exhaust particles effect on microglial and endothelial cells

To investigate the molecular mechanisms through which diesel exhaust particles (DEP) exert harmful action on the brain, cells in primary culture and in cell lines were used, because they are both powerful systems that allow to dissect the direct effects on a specific cell type. In particular, in order to explore the direct effects of DEP on CNS element endothelial and microglial cells were employed. Our characterization started with endothelial cells because they are the first interface between blood and brain parenchyma and with microglial cells because they are the main effectors of inflammatory response in the brain. BV2, primary culture of microglial cells and hCMEC/D3 were treated with different concentrations of DEP. The identification of the DEP concentrations to be used in in-vitro cell models is calculated as equivalent cumulative exposure dose that basically reflects the human exposure dose of highly polluted urban center. In the experiments, DEP was used at the concentration of 5 $\mu g/cm^2$ or 10 $\mu g/cm^2$ for 3 hours to explore short term effects and for 24 hours to explore long term effect. Data refers to separate groups in control condition and in incubation with DEP.

13.1 DEP incubation does not affect cell viability in BV2 and hCMEC/D3

In order to be sure to not use a toxic dose for the experiments, DEP was tested at different concentration to not affect cell viability (exposure to subacute doses). BV2 and hCMEC/D3 cells viability was assessed by MTT assay. Data obtained show that the two DEP concentrations did not significantly affect cell viability on both cell types (Fig. 25).

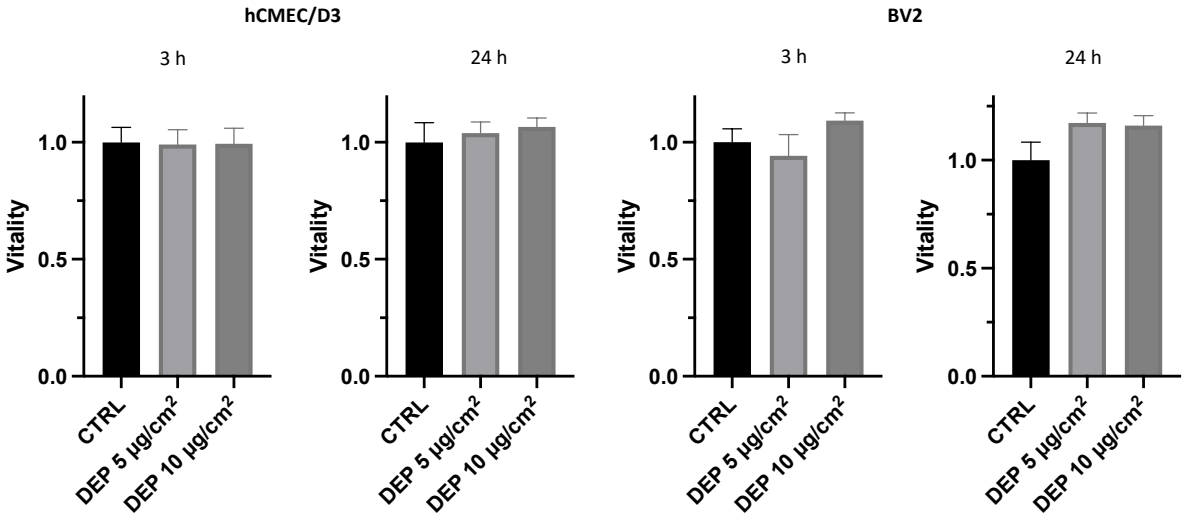

Figure 25. DEP incubation does not affect cell viability. Effects of DEP on cell viability measured by MTT assay at different time points (3 and 24 hours). Histograms represent the ratio, compared to control cells, of viable cells after the exposure to 5 and 10 µg/cm^2 of DEP 1650b. Cells without any treatment were used as control (CTRL). All results are plotted as mean ± SEM (n = 2 in triplicate).

13.2 DEP incubation inhibits cell proliferation in primary microglial cells

To investigate the molecular mechanisms through which DEP could affect neuroinflammation, we started studying the effects on microglial proliferation. Microglial proliferation is a major part in the evolution of chronic neurodegeneration, with direct implications for understanding the contribution of the CNS innate immune response to disease progression. Indeed, microglial cells play a key role in the development and maintenance of this inflammatory response showing enhanced proliferation and activation. The action of DEP on microglial proliferation was assessed in microglial cells exposed to 10 µg/cm^2 of DEP and to the proliferation marker EdU for 24 hours (Fig. 26). Surprisingly, quantification of microglial cells positive for EdU showed that DEP inhibited the proliferation of cultured microglia by 50% (Fig. 27-B). This is an unexpected result because microglial activation is usually accompanied by an increase in cell proliferation, which in some pathologies becomes uncontrolled. However, this result can be explained, in accordance with what was found in alveolar macrophages, treated with ultra-fine carbon particles, by a dysfunctional alteration of the cytoskeleton, due to high phagocytosis, which causes swelling of the cells and marked rigidity (Moller, 2002).

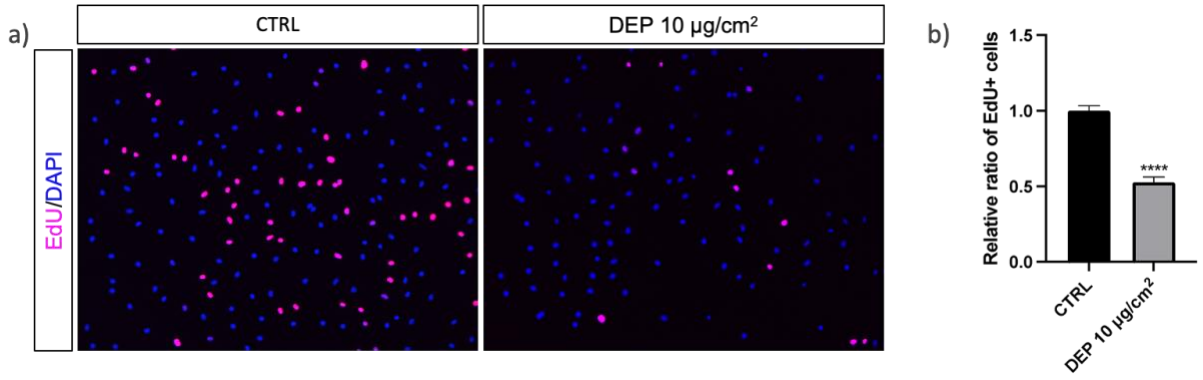

Figure 26. DEP impact on primary microglia proliferation. (a) Fluorescence images of cultured primary microglia incubated with EdU (red), fixed and stained for DAPI (blue) after 24hrs exposure to DEP 10 µg/cm^2. (b) The histograms show the percentage of EdU+ microglial cells exposed or not to DEP. Data have been normalized to control (number of experiments n = 2; All results are plotted as mean ± SEM, paired t-test, differences were considered significant at **** p value < 0.0001.

13.3 DEP incubation induces morphological changes in BV2 and primary microglia

Cell morphology and particles deposition was investigated through microscopic analysis after BV2 cells exposure to DEP (10 µg/cm^2). Our preliminary data suggest, as shown in Fig. 27, that BV2 cells actively interact with DEP after 24 hours treatment. DEP seems to be a chemoattractant factor for BV2 and we also observed morphological changes after DEP exposure, such as the emission of longer tunneling nanotubes (TNT). TNT are dynamic connections between cells, which represent a novel route for cell-to-cell communication, not only in physiological conditions but also in pathological processes. The most studied functions of TNT are the propagation of calcium flux and the transfer of cargos.

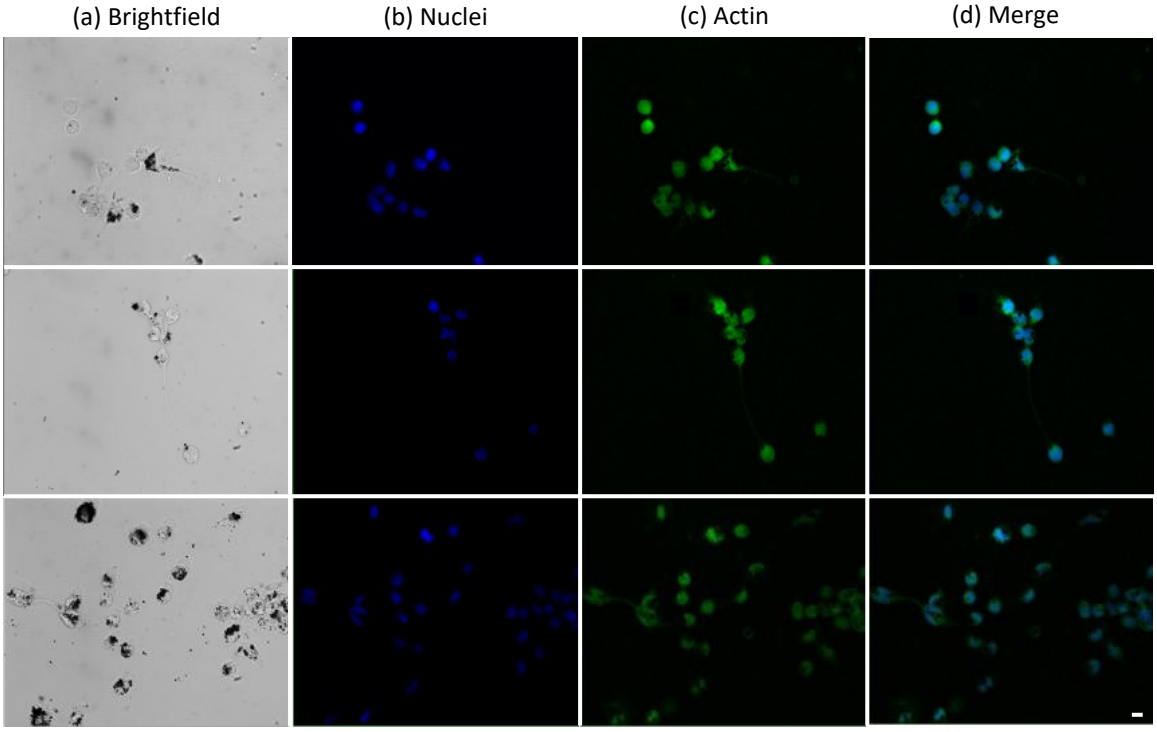

Figure 27. BV2 morphology after DEP exposure. Fluorescence images of BV2 cells exposed to 10 µg/cm^2 of DEP 1650b for 24 hrs. Nuclei were stained with DAPI (blue), and membrane with actin (green). Scale bar = 20 µm.

When activated, microglia change from a ramified state to an amoeboid shape, moving through a series of changes from increased proliferation, the retraction of extensions, increased mobility, and finally, the ability to phagocytose debris (Stence et al., 2001).

To determine the effect of DEP on microglia, cells were immunocytochemically labeled for Iba1 and imaged using fluorescence microscopy. Compared to control microglia, those treated with DEP were qualitatively larger, more spherical, lacked extensions and contained DEP particles, suggestive of a phagocytotic state (Fig. 28). These results suggest that DEP induces morphological changes indicative of microglia activation.

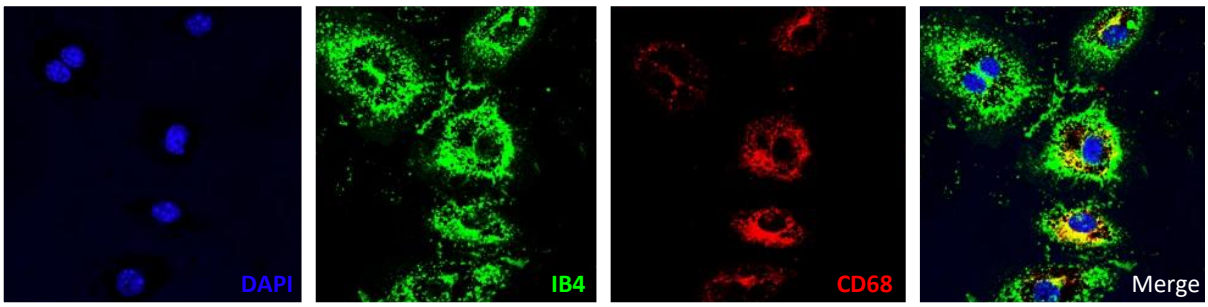

Figure 28. Primary microglia morphology after DEP exposure. Fluorescence images of microglial cells exposed to 10 µg/cm^2 of DEP 1650b for 24 hours. Nuclei were stained with DAPI (blue). Cells were immunocytochemically labeled for IB4 (green) and CD68 (red).

13.4 DEP is uptaken by hCMEC/D3

In order to see what happens when DEP comes into contact with the endothelial cells, that are the first interface between blood and brain parenchyma, hCMEC/D3 were treated with the DEP and were observed under the electron transmission microscope (TEM). Unexpectedly, the images reveal that the DEP is internalized by the hCMEC/D3 and that it tends to accumulate and persist in vesicular structures also in the perinuclear region (Fig. 29). The most surprising element is the ability of these cells to carry inside elements that are not functionalized to cross the BBB, unlike for example multi-functionalized liposomes, that are made to cross the BBB.

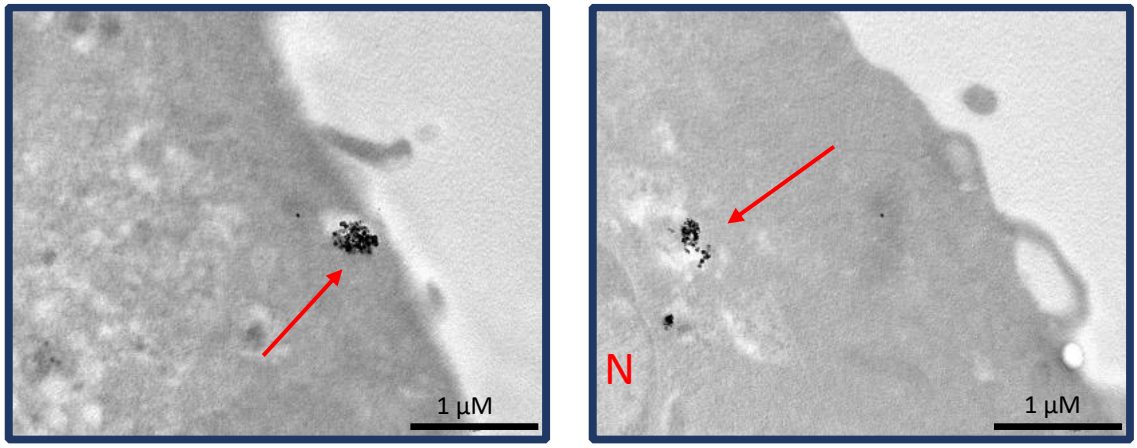

Figure 29. Uptake of DEP by hCMEC/D3 cells. hCMEC/D3 cells were incubated with DEP and investigated with electron microscopy. Images show that DEP is internalized and localized in morphologically distinct intracellular vesicles, also near perinuclear region. In the figure, "N" indicates the nucleus. Scale bar = 1 µm.

13.5 Calcium dynamics: DEP exposure decreases ATP-evoked calcium waves both in primary microglial cells and hCMEC/D3

To study the impact of microglial activation on receptor-mediated Ca^{2+} signaling, untreated primary microglial cells were compared with those incubated with DEP (10 μg/cm^2 for 24 hours). For eliciting transient increases in the $[Ca^{2+}]_i$, ATP was applied. ATP has functional receptors on microglia, which are linked to calcium signaling, namely metabotropic purinergic receptors. Addition of ATP (100 μm) to the bath solution induced reproducible transient increases in the fura-2-based calcium signal. An example of a trace (R 340/380) as recorded from an individual microglial cell under control conditions is given in Fig. 30-b. Data showed that DEP-activated microglia generated much smaller $[Ca^{2+}]_i$ signals after ATP trigger, revealeing a significant suppression of the receptor-evoked calcium signals, probably due to an increase in the resting $[Ca^{2+}]_i$, associated with microglial activation (Hoffmann et al., 2003).

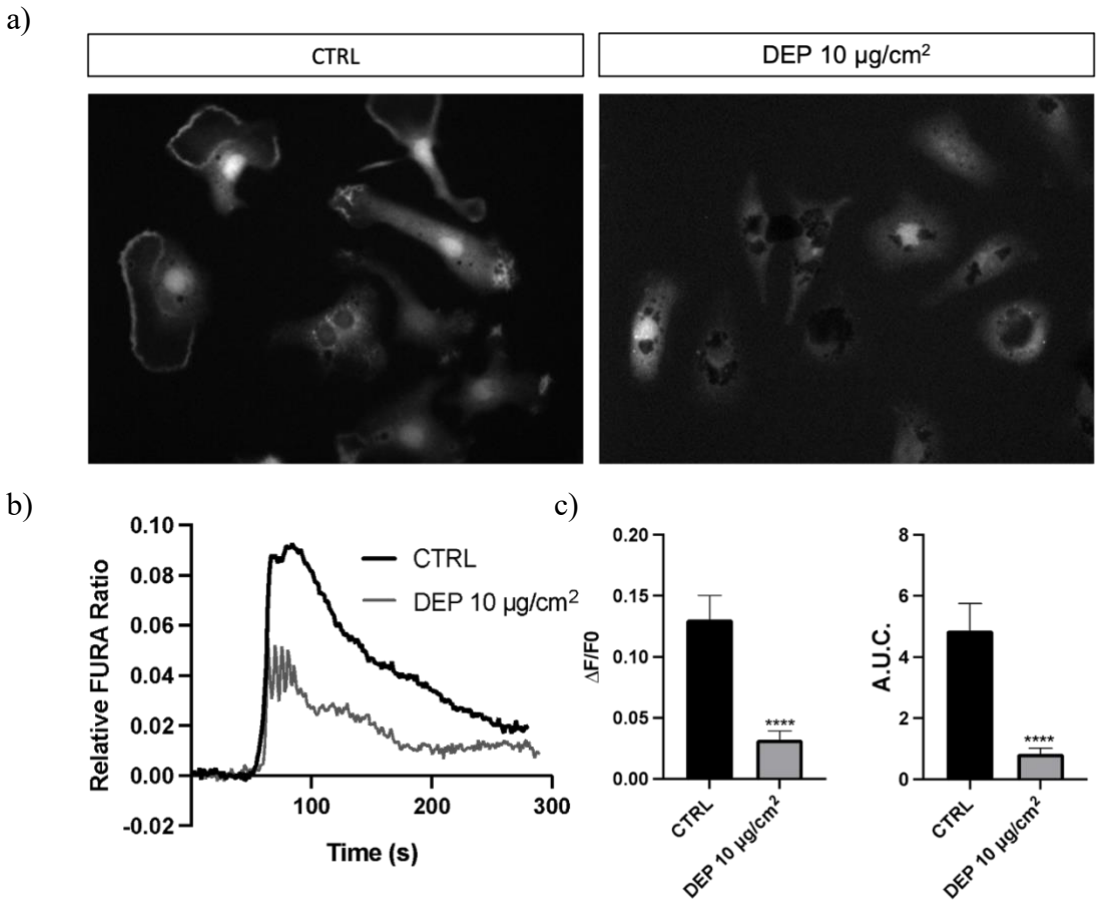

Figure 30. DEP effects on primary microglia calcium dynamics studied trough calcium Imaging technique after 24 hours exposure to DEP 10 µg/cm². Fluorescence images of cultured microglia loaded with FURA-2AM (Cf: 2,5 µM) and representative traces of Ca^{2+} response after a trigger of 100 µM ATP are shown in a) and b) respectively. For direct comparison, an overlay of the two graphs (CTRL and cells treated with 10 µg/cm² of DEP) is illustrated in b). Histograms in c) show the normalized Ca^{2+} wave peak and the area under the curve (A.U.C.) of the response of microglia in cultures exposed or not to DEP 1650b. All results are plotted as mean ± SEM (n = 9 for CTRL and n = 11 for treated cells), Unpaired t-test, **** p value < 0.0001

The same experiment was performed exactly in the same way on hCMEC/D3 (Fig. 31) and the results were comparable, indicating that the direct exposure to DEP causes also endothelium activation.

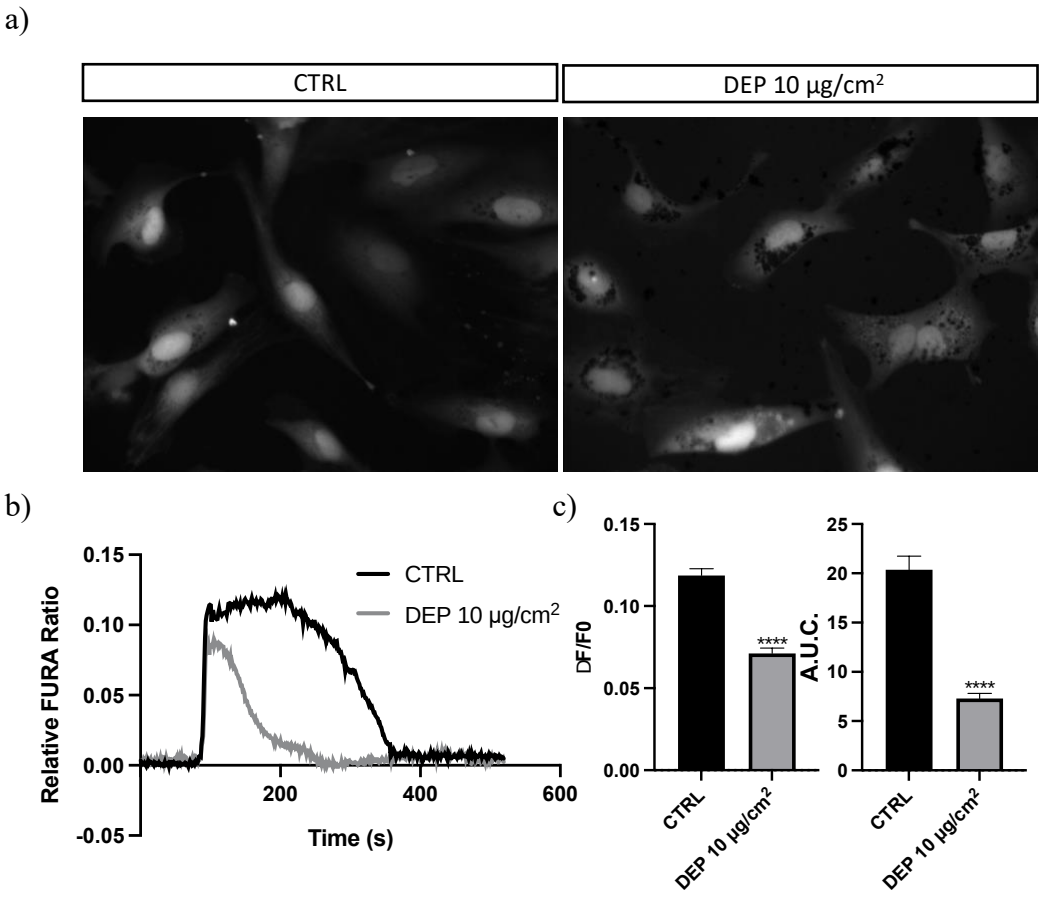

Figure 31. DEP effects on hCMEC/D3 calcium dynamics studied trough calcium imaging technique after 24 hours exposure to DEP 10 µg/cm². Fluorescence images of cultured hCMEC/D3 loaded with FURA-2AM (Cf: 2,5 µM) and representative traces of Ca^{2+} response after a trigger of 100 µM ATP are shown in a) and b) respectively. For direct comparison, an overlay of the two graphs (CTRL and cells treated with 10 µg/cm² of DEP) is illustrated in b). Histograms in c) show the normalized Ca^{2+} wave peak and the area under the curve (A.U.C.) of the response of hCMEC/D3 in cultures exposed or not to DEP 1650b. All results are plotted as mean ± SEM (n = 65 for CTRL and n = 45 for treated cells), Unpaired t-test, **** p value < 0.0001

DISCUSSION

Neurodegenerative diseases are brain disorders characterized by progressive neuronal dysfunction, loss of neuronal cells structure and functional deficit within the nervous system (Kovacs, 2018). Although the clinical impact of such pathologies is constantly growing, as a consequence of the progressive aging of the world population, many of the pathogenetic mechanisms underlying these neurodegenerations are still unclear, making it difficult to identify potential pharmacological treatments for many of them.

A proposed hypothesis to explain the pathogenesis of neurodegenerative disease and the diversity of its phenotypes, is based on seven main propositions: i) neurodegenerative disease is associated with multiple risk factors, ii) age is the most important of the risk factors, iii) aging differentially affects neuroanatomical pathways, iv) degeneration of these pathways results in the formation of pathogenic proteins, v) pathogenic proteins spread along anatomical pathways, vi) the phenotypes of familial and sporadic forms of disease are similar and vii) neurodegenerative disease is characterized by heterogeneity, overlapping phenotypes and multiple pathology. According to this hypothesis, the most cases of neurodegenerative disease would be multifactorial processes in which interactions between external environmental and internal genetic risk factors act cumulatively over a lifetime to determine the 'allostatic load' of an individual (A. Armstrong, 2013).

In light of these considerations, it is urgent to identify possible new drug targets or pathways that can be modulated in the treatment and to adopt early strategies to prevent the onset of neurodegeneration.

In recent years, great attention has focused on the role of the neurovascular unit (NVU) in the neurodegenerative process. The concept of *unit* is relatively recent in neuroscience and it was formally introduced in 2001 to emphasize the close developmental, structural and functional association between brain cells and the microvasculature and their consequent coordinated reaction to injury (Bell et al., 2020). Each component is intimately and reciprocally linked to each other, establishing an anatomical and functional whole, which results in a highly efficient system, involved in several functions with the primary aim to preserve the homeostasis of the brain’s microenvironment. Among these, there are two processes that display an intimate involvement: the neurovascular coupling (NVC) involved in cerebral blood flow (CBF)

regulation and the barrier function accomplished through the blood-brain-barrier (BBB) (Bell et al., 2020).

Strong evidence (Iadecola, 2017) points at the NVU alterations as a broad bridge to neuronal damage and brain dysfunction onset, therefore in the last years is growing the interest in investigating the mechanisms by which the NVU dysfunction brings to the neurodegeneration (de la Torre, 2017). Though the NVU has been recognized as a key player in the neurodegeneration, it still remains to be clarified whether the NVU dysfunctions is a collateral endpoint of the degenerative process or instead a major contributor to the onset of the process itself. The mechanisms by which this could occur might be related to the neurovascular uncoupling thus triggering an impaired cerebral perfusion, ending to the neurotrophic failure of the BBB and its related impaired clearance capacity.

This is indeed quite well documented for Alzheimer disease (AD) for which are available a lot of experimental and clinical studies showing that vascular dysfunction is an early manifestation of the disease and may promote AD pathology (Iadecola, 2017). Although the cellular and molecular events (including the single risk factors) underlying each step of AD are not entirely clear, it could be argued that all vascular risk factors converge at some point in the same final common path, characterized from dysfunction and/or vascular degeneration, as well as amyloid-β (Aβ) and tau pathology (Zlokovic, 2011). So, in the last years, accumulating evidence suggests that the vascular damage resulting from amyloid accumulation in the blood vessels could precede AD (Apátiga-Pérez et al., 2022). Indeed, according to the *two-hit vascular hypothesis* of AD, there is an initial vascular dysfunction (*hit one*) followed by the Aβ accumulation (*hit two*) that promotes and precedes neurodegeneration (Zlokovic, 2011). Nevertheless, the role of cerebrovascular pathology in the clinical expression of AD (if vascular lesions lower the threshold for cognitive deficits or if the two processes amplify each other) has not yet been clarified. Shedding light on these aspects could be fundamental to increase the knowledge we lack and which could help in identifying new therapies.

Therefore, if there is a need to act on NVU as a whole, it is mandatory to move towards new strategies able to modulate simultaneously several pathways involved in NVU dysfunction itself. At the first hand it has to take into account that the barrier function of the vascular

component of the NVU excludes most pharmaceuticals from CNS entry and mainly extrudes xenobiotic from the CNS by mean of efflux pumps.

In this scenario, nanomedicine plays a pivotal role in developing new strategies to deliver drugs to the CNS and indeed nanoparticles (NPs) have been suggested as potential therapeutical tools of CNS diseases' treatment (Masserini, 2013). Among several NPs, liposomes, made by phospholipids structured in mono- and multi-lamellar structures, have been proposed as transport for their high chemical and biological stability, their ability to incorporate different types of molecules and the possibility to be administered by virtually all routes (Sancini et al., 2016). Liposomes are versatile structures that can be functionalized on their surface to guarantee high affinity with the target and a complete BBB over-crossing.

Previous findings hinted at mApoE–PA–LIP, bifunctionalized liposomes composed of sphingomyelin and cholesterol, as a well-tolerated valuable new nanotechnological tools for AD therapy (Balducci et al., 2014), in light of their ability to bind amyloid-β (Aβ) and to target and cross the BBB (Bana et al., 2014; Gobbi et al., 2010; Re et al., 2011).

These characteristics are provided by their functionalization with a peptide derived from the apolipoprotein-E receptor-binding domain (mApoE) for BBB targeting and with phosphatidic acid (PA) for Aβ binding.

The therapeutic effectiveness of mApoE–PA–LIP in transgenic AD mouse models has been previously reported, demonstrating their effects on brain Aβ burden reduction and memory improvement (Balducci et al., 2014).

Starting from this evidence and looking to the mApoE-PA-LIP mechanism of action at the NVU, we assessed mApoE-PA-LIP activities on hCMEC/D3 as an in vitro human BBB model and on cultured astrocytes to evaluate their ability of modulating the intracellular Ca^{2+} dynamics within two main cellular constituents of the NVU.

Our preliminary results proved that mApoE-PA-LIP actively modulate the intracellular Ca^{2+} waves triggered by extracellular ATP in cultured hCMEC/D3 and astrocytes. Indeed, a trigger stimulus of 50 and 100 μM ATP for hCMEC/D3 and astrocytes respectively, increased the duration and the area under the curve (AUC) of the Ca^{2+} wave when both hCMEC/D3 and

astrocytes were pre-treated with mApoE-PA-LIP at the final concentration of 0.01 mg/mL. Interestingly, pretreatment with mApoE-LIP, without PA functionalization, failed to increase both the duration and the AUC of the intracellular Ca^{2+} wave triggered by ATP.

In light of this results we speculate that PA related to mApoE-PA-LIP i) might modulate the cell membrane curvature and promote membranes fusion, thus regulating the activity of different proteins involved in the vesicle docking; ii) could accumulate and form microdomains highly negatively charged, which potentially serve as membrane retention sites for several key proteins for exocytosis, such as the SNARE protein syntaxin-1 (Lam et al., 2008) or other membrane remodeling processes (Jenkins and Frohman, 2005); iii) could promote the transcellular trafficking of Aβ acting as to biological membranes.

Furthermore, when Sarco-Endoplasmic Reticulum Calcium ATPase (SERCA) activity was blocked by Cyclopiazonic acid, the extracellular application of ATP failed to trigger any intracellular Ca^{2+} waves in hCMEC and astrocytes, indicating that metabotropic purinergic receptors (P2Y) are mainly involved in the mApoE-PA-LIP-induced increase of the Ca^{2+} wave triggered by ATP. We might then speculate that mApoE-PA-LIP modulate intracellular Ca^{2+} dynamics evoked by ATP when SERCA is active through inositol-1,4,5-trisphosphate-dependent (IP3) endoplasmic reticulum Ca^{2+} release.

Considering that P2Y receptors represent important pharmacological targets to treat cognitive dysfunctions and that P2Y receptors have neuroprotective effects in neuroinflammatory processes, the enhancement of purinergic signaling provided by mApoE-PA-LIP could counteract Aβ-induced vasoconstriction and related reduction in CBF.

This evidence could indeed improve the Aβ clearance, that is reduced due to vascular impairment (*hit one*) providing new insight to explain the “sink effect” as well established by *in vitro* and *in vivo* study in mice models of AD (Balducci et al., 2014).

Moreover, being the P2Y2 receptors involved in: i) promotion of the degradation of amyloid precursor protein (APP) assisted by α-secretase, thus ending to soluble sAPPα protein rather than the neurotoxic Aβ1–42 peptide, that is enhanced due to vascular impairment (*hit one*) ii) microglial activation iii) binding of monocytes to the endothelial wall and their diapedesis, the

gain of function of the P2Y2 pathway triggered by mApoE-PA-LIP may promote a substantial enhancement of the overall neuroprotective action (Weisman et al., 2012).

Indeed, the increased duration and AUC of the Ca^{2+} wave triggered by ATP, when both hCMEC/D3 and iAstro-WT were pre-treated with mApoE-PA-LIP, would at the end be specifically involved in the neuroprotective effect.

It could be of great impact that our mApoE-PA-LIP induced a positive modulation of the ATP-triggered Ca^{2+} waves both in hCMEC/D3 cells and astrocytes. Indeed, P2Y receptors, due to their subcellular expression, acting on voltage-gated membrane channels, are able to modulate neurotransmitter release, modulate dendritic integration, facilitate neuronal excitability and affect other various neuronal functions such as synaptic plasticity or gene expression (Guzman and Gerevich, 2016).

Indeed interestingly, the mApoE-PA-LIP administration in APP/presenilin 1 transgenic mice also confirmed early memory restore, as it is demonstrated by novel object recognition test (Balducci et al., 2014), suggesting that there may be further mechanisms underlying this effect.

In order to disclose the specificity of mApoE-PA-LIP in modulating neuronal synaptic transmission, we investigated whether mApoE-PA-LIP, acutely administered, may induce a functional response in neurons on 300 µm thick-brain slices from CD-1 mouse (P8-P30).

By whole-cell patch-clamp recordings both in voltage- and current-clamp configuration, we examined passive membrane properties and spontaneous excitatory and inhibitory postsynaptic currents (sEPSC and sIPSC) in mouse pyramidal cortical neurons in control condition and following mApoE-PA-LIP [0.01 mg/mL] perfusion for a period of at least 10 minutes.

The excitatory spontaneous activity was monitored in voltage-clamp configuration by holding the cell membrane potential at -70 mV. At this holding potential, the contribution of the inhibitory synaptic (GABAergic) currents could be considered negligible on the basis of the chloride (Cl-) reversal potential calculated for the solutions used for the recordings. In this way it has been possible to record just the spontaneous excitatory postsynaptic currents (sEPSCs), mediated by the activation of ionotropic glutamate receptors (AMPA) and that appear as

inward currents. Under these experimental conditions, mApoE-PA-LIP application increased the frequency of sEPSCs by 33.3±5.8% (n = 15 neurons) with no change in their amplitude.

The kinetic analysis of sEPSCs was performed by measuring rise time and time of decay. It has been observed that in the presence of mApoE-PA-LIP the decay time is significantly slower compared to the control condition. On the contrary, no difference was found in the rise time kinetics between the control and mApoE-PA-LIP condition.

We next identified the neurotransmitter receptors involved in this response by means of pharmacology. When AMPA transmission was blocked by 10 µM 2,3-dihydroxy-6-nitro-7-sulfamoyl-benzo[f]quinoxaline- 2,3-dione (NBQX), mApoE-PA-LIP perfusion failed to increase the frequency of the remaining sEPSCs. This result could suggest that the mApoE-PA-LIP-mediated increase in sEPSCs frequency could involve AMPAergic transmission.

To investigate any possible NMDA contribution to the observed increase induced by mApoE-PA-LIP on synaptic transmission, mApoE-PA-LIP [0.01 mg/mL] have been perfused for 10 minutes, during whole-cell patch-clamp recordings performed on mouse cortical pyramidal neurons. Spontaneous activity was monitored in voltage-clamp configuration by holding the cell membrane potential at -50 mV. When V_h is depolarized to –50 mV, Mg^{2+} block is removed, thus activating NMDA receptors.

Under these experimental conditions, mApoE-PA-LIP application increased the frequency of sEPSCs with no change in their amplitude.

In the same experimental conditions, monitoring the spontaneous activity in voltage-clamp configuration by holding the cell membrane potential at -50 mV, spontaneous inibitory postsynaptic currents (sIPSCs) were also analysed.

Indeed, spontaneous currents were recorded at -50 mV, which is less negative than the reversal potential for inhibitory post-synaptic potentials and so outward currents were considered as sIPSCs.Under these conditions, mApoE-PA-LIP application increased the frequency of sIPSCs without changing their amplitude.

Overall, our results show that mApoE-PA-LIP application increased the frequency of sEPSCs and sIPSCs with no change in their amplitude at holding potential of both -70 mV and -50 mV, without affecting the passive properties of the neuron’s membrane.

According to these observations, the modulatory activity of mApoE-PA-LIP could occur at the presynaptic level increasing the probability of neurotransmitter release. This action could be explained, not only due to the intrinsic action of PA, as explained before, but also through the active involvement of astrocytes. Indeed, the roles that astrocytic calcium elevations overall play in neurophysiology and especially in modulation of neuronal activity have been intensely put on evidence in the recent years (Agulhon et al., 2008).

Starting from our previous results we know that the treatment with mApoE-PA-LIP in astrocytes increases the intracellular Ca^{2+} levels (Forcaia et al., 2021) and we know from literature that astrocytes, by elevating their intracellular Ca^{2+} concentration through Gq-coupled protein mechanisms, can modulate neuronal function at the synaptic level through the Ca^{2+}-dependent release of gliotransmitters (Bernardinelli et al., 2014).

Astrocytes have many G protein-coupled receptors (GPCRs) linked to Ca^{2+} mobilization from internal stores, most of them being Gq-coupled GPCRs (Gq GPCRs). Since Gq GPCR agonist application elicited Ca^{2+} increases in astrocytes, which in turn correlated with changes in neuronal ionotropic glutamate receptor (iGluR) activity, there is evidence for an astrocytes-mediated effect on synaptic transmission through the Gq GPCR-mediated Ca^{2+}-dependent release of neuroactive molecules (Agulhon et al., 2008).

However, it is very difficult to determine the effect of selectively stimulating astrocytic ca^{2+} signaling cascades on physiological processes such as synaptic transmission, since astrocytes and other neural cells (e.g., neurons, microglia) exhibit a similar array of Gq GPCRs linked to Ca^{2+} mobilization. Among the several approaches used to selectively increase astrocytic Ca^{2+} there is Ca^{2+} loading via patch-clamp pipettes into astrocytes (uncaging caged IP3 or ca^{2+}) (Fiacco and McCarthy, 2006). This method evokes in single astrocyte a global intracellular astrocytic Ca^{2+} increase that triggers an increase in the frequency of spontaneous excitatory postsynaptic AMPA currents (sEPSCs) of CA1 neurons (Fiacco and McCarthy, 2004). As a proof of concept indeed the incubation with group I mGluR antagonists blocked the astrocyte-induced increase in AMPA sEPSC frequency, suggesting that astrocytes-released glutamate activates mGluRs on neighboring presynaptic terminals to

elevate presynaptic Ca^{2+} and increase the probability of neurotransmitter release (Agulhon et al., 2008; Fiacco and McCarthy, 2006). Moreover, these Ca^{2+} waves spreading through the astrocytic syncytium represent a machinery for coordinating the activity within the NVU (Abbott et al., 2006).

Thus, we can hypothesize that astrocytes might modulate neuronal spontaneous post synaptic excitatory currents (sEPSCs) through their intracellular calcium elevations due to the direct mApoE-PA-LIP-mediated effect on P2Y purinergic receptors. Further experiments are required to confirm this hypothesis.

The here outlined results advanced our understanding of the mechanism of action by which the mApoE-PA-LIP administration in APP/presenilin 1 transgenic mice promotes significant recovery of the cognitive impairment, thus providing an additional support to promote mApoE-PA-LIP as effective therapeutic tool for AD.

Conducting these cross-sectional studies on nanoparticles that interact with a such complex structure as the NVU has also given us the tools to investigate the interaction of nanometer-sized structures from anthropogenic source with the NVU itself.

Indeed, most of the information we have about the behavior and toxicity of NPs are from the studies related to nanomedicine and nanotechnology. Since integrity of the NVU guarantees the coupling between neural activity and blood flow, the orchestrated effort of multiple cells engaged in distinct signaling pathways and effector systems across the entire cerebrovascular network are at the core of the NVU; anything that disturbs this complex and yet fragile network has detrimental consequences (Calderón-Garcidueñas et al., 2019; Iadecola, 2017).

According to the *two-hit vascular hypothesis* of AD (Zlokovic, 2011), environmental air pollutants (AP) are one of the possible causes leading to vascular impairment (Iadecola and Gottesman, 2018). For this reason we decided to investigate the possible functional alterations induced by AP. Increasing evidence indicates that exposure to particulate matter (PM), combined with individual susceptibility and other possible contributing causes, correlates with the onset or progression of neurodegenerative diseases (Costa et al., 2020).

Among the different proposed mechanisms, two main ones strictly correlate with the NVU: i) the cerebrovascular damage, that can cause altered properties of the BBB (the so-called “hit one”, according to *two-hit vascular hypothesis* of AD) and ii) the overall neuroinflammation that by itself or by exacerbating the direct damage to the endothelium can trigger the onset and progression of the neurological impairment.

Considering this evidence, we investigated the direct effect of PM on endothelial cells (hCMEC/D3) and microglial cells (BV2 and mouse primary cultures) using a standard reference material (SRM) of diesel exhaust particles (DEP), that is one of the main contributors of PM coming from highly polluted city kerbsides. The identification of the DEP concentrations to be used in *in vitro* cell models is calculated as equivalent cumulative exposure dose that basically reflects the human exposure dose of highly polluted urban center. In order to study the fine mechanisms underlying DEP sustained and prolonged effect on mammalian cell homeostasis we performed cell viability assays to verify that DEP at different concentration used did not significantly affect cell viability (i.e., looking at exposures to subacute doses).
Our study therefore focused on the endothelium, because of its characteristic of being the first interface between CNS and periphery and on microglia, which is the main effector of neuroinflammation.

The original concept of the brain as an *immunologically privileged* organ has been overcome by the demonstrations that the innate immune cells, brain-resident, microglia influence nervous system functions by secreting a variety of chemical messengers, and that peripheral immune cells, under different pathological conditions, enter the CNS parenchyma, modulating brain activity (Lauranzano et al., 2019).
For all these reasons, the barrier properties and neuroinflammation effects appear as complex processes whose treatment cannot be separated from each other (da Fonseca et al., 2014).
Since multiple studies indicate that BBB dysfunction is an early key event in the pathogenesis of neurodegenerative diseases, exploratory studies are required to assess the correlation

between PM exposure and vascular impairment of the BBB, thereby helping to elucidate the association between PM and neurodegenerative diseases (Calderón-Garcidueñas et al., 2019).

Our study of the PM effects on the human cerebral microvascular endothelial cells (hCMEC/D3) takes the advantage from the results coming from previous investigations conducted in our laboratory which clearly demonstrates that the administration of PM by the pulmonary route led to broad systemic effects as confirmed by ET-1 and HO-1 increased levels in the brain (Farina et al., 2013).

Currently, it is still not clear if the effects we have seen *in vivo* are the result of a direct mechanism of PM on the cerebral microvasculature or of an indirect mechanism mediated by inflammatory processes at the level of peripheral tissues which in turn causes inflammation at the BBB.

Our data show that PM can be actively internalized by endothelial cells (probably trough a non-specific absorption mechanism), as demonstrated by images obtained through transmission electron microscopy (TEM) (Fig. 30). This internalization could lead to the barrier dysfunctionality which would no longer be a physical barrier to the entry of harmful substances and which would lose the dynamism and fluidity required for the effective regulation of exchanges between blood and brain parenchyma.

Indeed, in light of our results we might speculate that the exposure to DEP causes loss of membrane fluidity. Indeed, during the assessment of the action of DEP on microglial proliferation we found that 24 hours-exposure to 10 $\mu g/cm^2$ of DEP inhibited the proliferation of cultured microglia by 50%. This is an unexpected result because microglial activation is usually accompanied by an increase in cell proliferation, which in some pathologies becomes uncontrolled. However, this result can be explained, in accordance with what was found in alveolar macrophages, treated with ultra-fine carbon particles, by a dysfunctional alteration of the cytoskeleton, due to high phagocytosis, which causes swelling of the cells and marked rigidity (Moller, 2002). However, prolonged endothelial inflammation promotes overwhelming and uncontrolled inflammation, such as the 'cytokine storm', which eventually leads to endothelial dysfunction and further impairs endothelial integrity (A. Armstrong, 2013).

Since through the *in vitro* experiments conducted on hCMEC with mApoE–PA–LIP we were able to study the purinergic pathway and its fundamental role in neuroprotection mechanisms, we went to see DEP-induced effects on the same pathway.

To study the impact of microglial activation on receptor-mediated Ca^{2+} signaling, we compared untreated primary microglial cells with those incubated with DEP (10 μg/cm^2 for 24 hours). For eliciting transient increases in the $[Ca^{2+}]_i$, ATP was applied. Addition of 100 μm ATP to the bath solution induced reproducible transient increases in the fura-2-based calcium signal. Our data showed that DEP-activated microglia generated much smaller $[Ca^{2+}]_i$ signals after ATP trigger, revealing a significant suppression of the receptor-evoked calcium signals, probably due to an increase in the resting $[Ca^{2+}]_i$, associated with microglial activation (Hoffmann et al., 2003), that in our experiments could be confirmed also from the morphological analysis that reveal ameboid phenotype (Fig. 28).

The same experiment was performed exactly on hCMEC/D3 and the results were comparable, indicating that the direct exposure to DEP causes also endothelium activation.

The here outlined results relating to the DEP-induced effects on endothelial and on microglial cells show that, although DEP does not directly produce toxicity, it causes small alterations which, adding together, could lead to the lowering of individual threshold to the onset of pathologies affecting the SNC.

Indeed, our data suggest that the direct treatment of the cells with DEP causes their activation, as evidenced by the altered ability to respond to a stimulus, such as ATP. For microglial cells, it is also evident from morphological studies that reveal MG amoeboid phenotype.

These results enabled to define some of the direct effects of DEP on cerebral endothelial and microglial cells advancing our understanding of the mechanisms underlying DEP-induced endothelial dysfunction and neuroinflammation, which may help to prevent, contain or reverse neurodegenerative disease processes exacerbated by ambient air pollution long lasting exposure. A throughout knowledge of the NVU is an essential requirement for understanding its role in neurodegeneration ranging from the onset to progression of the pathologies and from the prevention to the cure approaches.

Considering all our observations, the enhancement of purinergic signalling provided by mApoE-PA-LIP together with their modulatory effect at the presynaptic level by increasing the probability of neurotransmitter release could act simultaneously on several dysregulated processes in the progression of the disease. Indeed, P2Y receptors are important pharmacological targets to treat cognitive dysfunctions having protective effects in neuroinflammatory processes and counteracting Aβ-induced vasoconstriction and related reduction in CBF. These actions could improve the Aβ clearance, that is reduced due to vascular impairment (*hit one*) providing new insight to explain the *sink effect* as well established by *in vitro* and *in vivo* study in mice models of AD (Balducci et al., 2014).

Moreover, the action on brain synaptic transmission could be explained by: i) the intrinsic action of PA, that, acting on voltage-gated membrane channels, is able to modulate neurotransmitter release, dendritic integration, neuronal excitability and synaptic plasticity (Guzman and Gerevich, 2016); ii) the active involvement of astrocytes that, by elevating their intracellular Ca^{2+} concentration through Gq-coupled protein mechanisms, can modulate neuronal function at the synaptic level through the Ca^{2+}-dependent release of gliotransmitters (Bernardinelli et al., 2014).

All these observations provide a multi-modal approach to counteract simultaneously neurodegeneration effects of brain disease acting at the dynamic relationship between endothelium, astrocyte, microglia and neuron.

However, it is important to consider that there are also factors that force the progression of the disease. Indeed, substantial overlap exists among risk factors for cerebrovascular disorder and Alzheimer's disease. For example, midlife diabetes, hypertension and obesity are vascular risk factors that predispose individuals to Alzheimer's disease and vascular dementia. Among these, one of the conditions that appears to be particularly involved is the exposure to atmospheric particulate matter.

In light of this evidence, we take advantage from our previous characterization of mApoE-PA-LIP protective effect to study the same pathways that we tried to finely modulate with mApoE-PA-LIP to counteract the disease progression. Interestingly, we found alterations in these pathways. Both microglial and endothelial cells show a significant suppression of the purinergic

signling after an ATP trigger, probably due to an increase in the resting $[Ca^{2+}]_i$, associated with their activation.

Indeed, when we look at nanodimension we are faced with two components of the same phenomenon: the highly innovative and extremely interesting aspect of nanomedicine from a therapeutic point of view, but also the aspect of nanotoxicology that focuses on fine alterations that over time can cause a series of events that accumulating can lead to pathology. Understanding the weight of these alterations is extremely important to develop useful strategies, not only to contain and limit, but also to prevent, neurodegenerative processes.

BIBLIOGRAPHY

A. Armstrong, R., 2013. Review article What causes alzheimer's disease? fn 3, 169–188. https://doi.org/10.5114/fn.2013.37702

Abbott, N.J., Rönnbäck, L., Hansson, E., 2006. Astrocyte–endothelial interactions at the blood–brain barrier. Nat Rev Neurosci 7, 41–53. https://doi.org/10.1038/nrn1824

Abrahams, S., Goldstein, L.H., Kew, J.J.M., Brooks, D.J., Lloyd, C.M., Frith, C.D., Leigh, P.N., 1996. Frontal lobe dysfunction in amyotrophic lateral sclerosis: A PET study. Brain 119, 2105–2120. https://doi.org/10.1093/brain/119.6.2105

Agulhon, C., Petravicz, J., McMullen, A.B., Sweger, E.J., Minton, S.K., Taves, S.R., Casper, K.B., Fiacco, T.A., McCarthy, K.D., 2008. What is the role of astrocyte calcium in neurophysiology? Neuron 59, 932–946. https://doi.org/10.1016/j.neuron.2008.09.004

Apátiga-Pérez, R., Soto-Rojas, L.O., Campa-Córdoba, B.B., Luna-Viramontes, N.I., Cuevas, E., Villanueva-Fierro, I., Ontiveros-Torres, M.A., Bravo-Muñoz, M., Flores-Rodríguez, P., Garcés-Ramirez, L., de la Cruz, F., Montiel-Sosa, J.F., Pacheco-Herrero, M., Luna-Muñoz, J., 2022. Neurovascular dysfunction and vascular amyloid accumulation as early events in Alzheimer's disease. Metab Brain Dis 37, 39–50. https://doi.org/10.1007/s11011-021-00814-4

Balducci, C., Mancini, S., Minniti, S., La Vitola, P., Zotti, M., Sancini, G., Mauri, M., Cagnotto, A., Colombo, L., Fiordaliso, F., Grigoli, E., Salmona, M., Snellman, A., Haaparanta-Solin, M., Forloni, G., Masserini, M., Re, F., 2014. Multifunctional Liposomes Reduce Brain -Amyloid Burden and Ameliorate Memory Impairment in Alzheimer's Disease Mouse Models. Journal of Neuroscience 34, 14022–14031. https://doi.org/10.1523/JNEUROSCI.0284-14.2014

Bana, L., Minniti, S., Salvati, E., Sesana, S., Zambelli, V., Cagnotto, A., Orlando, A., Cazzaniga, E., Zwart, R., Scheper, W., Masserini, M., Re, F., 2014. Liposomes bi-functionalized with phosphatidic acid and an ApoE-derived peptide affect Aβ aggregation features and cross the blood–brain-barrier: Implications for therapy of Alzheimer disease. Nanomedicine: Nanotechnology, Biology and Medicine 10, 1583–1590. https://doi.org/10.1016/j.nano.2013.12.001

Bell, A.H., Miller, S.L., Castillo-Melendez, M., Malhotra, A., 2020. The Neurovascular Unit: Effects of Brain Insults During the Perinatal Period. Front. Neurosci. 13, 1452. https://doi.org/10.3389/fnins.2019.01452

Bernardinelli, Y., Muller, D., Nikonenko, I., 2014. Astrocyte-synapse structural plasticity. Neural Plast 2014, 232105. https://doi.org/10.1155/2014/232105

Bright, F., Werry, E.L., Dobson-Stone, C., Piguet, O., Ittner, L.M., Halliday, G.M., Hodges, J.R., Kiernan, M.C., Loy, C.T., Kassiou, M., Kril, J.J., 2019. Neuroinflammation in frontotemporal dementia. Nat Rev Neurol 15, 540–555. https://doi.org/10.1038/s41582-019-0231-z

Brown, L.S., Foster, C.G., Courtney, J.-M., King, N.E., Howells, D.W., Sutherland, B.A., 2019. Pericytes and Neurovascular Function in the Healthy and Diseased Brain. Front Cell Neurosci 13, 282. https://doi.org/10.3389/fncel.2019.00282

Calderón-Garcidueñas, L., Reynoso-Robles, R., González-Maciel, A., 2019. Combustion and friction-derived nanoparticles and industrial-sourced nanoparticles: The culprit of Alzheimer and Parkinson's diseases. Environmental Research 176, 108574. https://doi.org/10.1016/j.envres.2019.108574

Cartier, N., Lewis, C.-A., Zhang, R., Rossi, F.M.V., 2014. The role of microglia in human disease: therapeutic tool or target? Acta Neuropathol 128, 363–380. https://doi.org/10.1007/s00401-014-1330-y

Colonna, M., Butovsky, O., 2017a. Microglia Function in the Central Nervous System During Health and Neurodegeneration. Annu. Rev. Immunol. 35, 441–468. https://doi.org/10.1146/annurev-immunol-051116-052358

Colonna, M., Butovsky, O., 2017b. Microglia Function in the Central Nervous System During Health and Neurodegeneration. Annu. Rev. Immunol. 35, 441–468. https://doi.org/10.1146/annurev-immunol-051116-052358

Costa, L.G., Cole, T.B., Dao, K., Chang, Y.-C., Coburn, J., Garrick, J.M., 2020. Effects of air

pollution on the nervous system and its possible role in neurodevelopmental and neurodegenerative disorders. Pharmacol Ther 210, 107523. https://doi.org/10.1016/j.pharmthera.2020.107523

da Fonseca, A.C.C., Matias, D., Garcia, C., Amaral, R., Geraldo, L.H., Freitas, C., Lima, F.R.S., 2014. The impact of microglial activation on blood-brain barrier in brain diseases. Front Cell Neurosci 8, 362. https://doi.org/10.3389/fncel.2014.00362

Daneman, R., Prat, A., 2015. The blood-brain barrier. Cold Spring Harb Perspect Biol 7, a020412. https://doi.org/10.1101/cshperspect.a020412

de la Torre, J. c., 2017. Are Major Dementias Triggered by Poor Blood Flow to the Brain? Theoretical Considerations. JAD 57, 353–371. https://doi.org/10.3233/JAD-161266

D'Esposito, M., Deouell, L.Y., Gazzaley, A., 2003. Alterations in the BOLD fMRI signal with ageing and disease: a challenge for neuroimaging. Nat Rev Neurosci 4, 863–872. https://doi.org/10.1038/nrn1246

Dilger, R.N., Johnson, R.W., 2008. Aging, microglial cell priming, and the discordant central inflammatory response to signals from the peripheral immune system. Journal of Leukocyte Biology 84, 932–939. https://doi.org/10.1189/jlb.0208108

Dionisio-Santos, D.A., Olschowka, J.A., O'Banion, M.K., 2019. Exploiting microglial and peripheral immune cell crosstalk to treat Alzheimer's disease. J Neuroinflammation 16, 74. https://doi.org/10.1186/s12974-019-1453-0

Dopper, E.G.P., Chalos, V., Ghariq, E., den Heijer, T., Hafkemeijer, A., Jiskoot, L.C., de Koning, I., Seelaar, H., van Minkelen, R., van Osch, M.J.P., Rombouts, S.A.R.B., van Swieten, J.C., 2016. Cerebral blood flow in presymptomatic MAPT and GRN mutation carriers: A longitudinal arterial spin labeling study. NeuroImage: Clinical 12, 460–465. https://doi.org/10.1016/j.nicl.2016.08.001

Farina, F., Sancini, G., Battaglia, C., Tinaglia, V., Mantecca, P., Camatini, M., Palestini, P., 2013.

Milano Summer Particulate Matter (PM10) Triggers Lung Inflammation and Extra Pulmonary Adverse Events in Mice. PLoS ONE 8, e56636. https://doi.org/10.1371/journal.pone.0056636

Fiacco, T.A., McCarthy, K.D., 2006. Astrocyte calcium elevations: Properties, propagation, and effects on brain signaling. Glia 54, 676–690. https://doi.org/10.1002/glia.20396

Forcaia, G., Formicola, B., Terribile, G., Negri, S., Lim, D., Biella, G., Re, F., Moccia, F., Sancini, G., 2021. Multifunctional Liposomes Modulate Purinergic Receptor-Induced Calcium Wave in Cerebral Microvascular Endothelial Cells and Astrocytes: New Insights for Alzheimer's disease. Mol Neurobiol 58, 2824–2835. https://doi.org/10.1007/s12035-021-02299-9

Freeman, M.R., 2010. Specification and morphogenesis of astrocytes. Science 330, 774–778. https://doi.org/10.1126/science.1190928

Galea, I., 2021. The blood–brain barrier in systemic infection and inflammation. Cell Mol Immunol 18, 2489–2501. https://doi.org/10.1038/s41423-021-00757-x

Gammon, K., 2014. Neurodegenerative disease: Brain windfall. Nature 515, 299–300. https://doi.org/10.1038/nj7526-299a

Ginhoux, F., Greter, M., Leboeuf, M., Nandi, S., See, P., Gokhan, S., Mehler, M.F., Conway, S.J., Ng, L.G., Stanley, E.R., Samokhvalov, I.M., Merad, M., 2010. Fate Mapping Analysis Reveals That Adult Microglia Derive from Primitive Macrophages. Science 330, 841–845. https://doi.org/10.1126/science.1194637

Gobbi, M., Re, F., Canovi, M., Beeg, M., Gregori, M., Sesana, S., Sonnino, S., Brogioli, D., Musicanti, C., Gasco, P., Salmona, M., Masserini, M.E., 2010. Lipid-based nanoparticles with high binding affinity for amyloid-β1–42 peptide. Biomaterials 31, 6519–6529. https://doi.org/10.1016/j.biomaterials.2010.04.044

Guzman, S.J., Gerevich, Z., 2016. P2Y Receptors in Synaptic Transmission and Plasticity: Therapeutic Potential in Cognitive Dysfunction. Neural Plasticity 2016, 1–12. https://doi.org/10.1155/2016/1207393

Hahad, O., Lelieveld, J., Birklein, F., Lieb, K., Daiber, A., Münzel, T., 2020. Ambient Air Pollution Increases the Risk of Cerebrovascular and Neuropsychiatric Disorders through Induction of Inflammation and Oxidative Stress. IJMS 21, 4306. https://doi.org/10.3390/ijms21124306

Hajipour, F., Giannouli, E., Moussavi, Z., 2020. Acoustic characterization of upper airway variations from wakefulness to sleep with respect to obstructive sleep apnea. Med Biol Eng Comput 58, 2375–2385. https://doi.org/10.1007/s11517-020-02234-5

Han, B., Li, X., Ai, R.-S., Deng, S.-Y., Ye, Z.-Q., Deng, X., Ma, W., Xiao, S., Wang, J.-Z., Wang, L.-M., Xie, C., Zhang, Yan, Xu, Y., Zhang, Yuan, 2022. Atmospheric particulate matter aggravates CNS demyelination through involvement of TLR-4/NF-kB signaling and microglial activation. eLife 11, e72247. https://doi.org/10.7554/eLife.72247

Hanisch, U.-K., Kettenmann, H., 2007. Microglia: active sensor and versatile effector cells in the normal and pathologic brain. Nat Neurosci 10, 1387–1394. https://doi.org/10.1038/nn1997

Heidari Nejad, S., Takechi, R., Mullins, B.J., Giles, C., Larcombe, A.N., Bertolatti, D., Rumchev, K., Dhaliwal, S., Mamo, J., 2015. The effect of diesel exhaust exposure on blood-brain barrier integrity and function in a murine model: Diesel exhaust and blood brain barrier integrity. J. Appl. Toxicol. 35, 41–47. https://doi.org/10.1002/jat.2985

Hickman, S., Izzy, S., Sen, P., Morsett, L., El Khoury, J., 2018. Microglia in neurodegeneration. Nat Neurosci 21, 1359–1369. https://doi.org/10.1038/s41593-018-0242-x

Hoffmann, A., Kann, O., Ohlemeyer, C., Hanisch, U.-K., Kettenmann, H., 2003. Elevation of Basal Intracellular Calcium as a Central Element in the Activation of Brain Macrophages (Microglia): Suppression of Receptor-Evoked Calcium Signaling and Control of Release Function. J. Neurosci. 23, 4410–4419. https://doi.org/10.1523/JNEUROSCI.23-11-04410.2003

Huang, Y., Xu, Z., Xiong, S., Sun, F., Qin, G., Hu, G., Wang, J., Zhao, L., Liang, Y.-X., Wu, T., Lu, Z., Humayun, M.S., So, K.-F., Pan, Y., Li, N., Yuan, T.-F., Rao, Y., Peng, B., 2018. Repopulated microglia are solely derived from the proliferation of residual microglia after acute depletion.

Nat Neurosci 21, 530–540. https://doi.org/10.1038/s41593-018-0090-8

Iadecola, C., 2017. The Neurovascular Unit Coming of Age: A Journey through Neurovascular Coupling in Health and Disease. Neuron 96, 17–42. https://doi.org/10.1016/j.neuron.2017.07.030

Iadecola, C., Gottesman, R.F., 2018. Cerebrovascular Alterations in Alzheimer Disease. Circ Res 123, 406–408. https://doi.org/10.1161/CIRCRESAHA.118.313400

Janelidze, S., Hertze, J., Nägga, K., Nilsson, K., Nilsson, C., Wennström, M., van Westen, D., Blennow, K., Zetterberg, H., Hansson, O., 2017. Increased blood-brain barrier permeability is associated with dementia and diabetes but not amyloid pathology or APOE genotype. Neurobiology of Aging 51, 104–112. https://doi.org/10.1016/j.neurobiolaging.2016.11.017

Jenkins, G.M., Frohman, M.A., 2005. Phospholipase D: a lipid centric review. Cell. Mol. Life Sci. 62, 2305–2316. https://doi.org/10.1007/s00018-005-5195-z

Kalsbeek, M.J.T., Mulder, L., Yi, C.-X., 2016. Microglia energy metabolism in metabolic disorder. Mol Cell Endocrinol 438, 27–35. https://doi.org/10.1016/j.mce.2016.09.028

Kierdorf, K., Prinz, M., 2013. Factors regulating microglia activation. Front. Cell. Neurosci. 7. https://doi.org/10.3389/fncel.2013.00044

Kim, B.Y.S., Rutka, J.T., Chan, W.C.W., 2010. Nanomedicine. N Engl J Med 363, 2434–2443. https://doi.org/10.1056/NEJMra0912273

Kisler, K., Nelson, A.R., Montagne, A., Zlokovic, B.V., 2017. Cerebral blood flow regulation and neurovascular dysfunction in Alzheimer disease. Nat Rev Neurosci 18, 419–434. https://doi.org/10.1038/nrn.2017.48

Kortekaas, R., Leenders, K.L., van Oostrom, J.C.H., Vaalburg, W., Bart, J., Willemsen, A.T.M., Hendrikse, N.H., 2005. Blood-brain barrier dysfunction in parkinsonian midbrain in vivo. Ann Neurol. 57, 176–179. https://doi.org/10.1002/ana.20369

Kovacs, G.G., 2018. Concepts and classification of neurodegenerative diseases, in: Handbook of Clinical Neurology. Elsevier, pp. 301–307. https://doi.org/10.1016/B978-0-12-802395-2.00021-3

Kreutzberg, G.W., 1996. Microglia: a sensor for pathological events in the CNS. Trends in Neurosciences 19, 312–318. https://doi.org/10.1016/0166-2236(96)10049-7

Kwon, H.S., Koh, S.-H., 2020. Neuroinflammation in neurodegenerative disorders: the roles of microglia and astrocytes. Transl Neurodegener 9, 42. https://doi.org/10.1186/s40035-020-00221-2

Lam, A.D., Tryoen-Toth, P., Tsai, B., Vitale, N., Stuenkel, E.L., 2008. SNARE-catalyzed Fusion Events Are Regulated by Syntaxin1A–Lipid Interactions. MBoC 19, 485–497. https://doi.org/10.1091/mbc.e07-02-0148

Lauranzano, E., Campo, E., Rasile, M., Molteni, R., Pizzocri, M., Passoni, L., Bello, L., Pozzi, D., Pardi, R., Matteoli, M., Ruiz-Moreno, A., 2019. A Microfluidic Human Model of Blood–Brain Barrier Employing Primary Human Astrocytes. Adv. Biosys. 1800335. https://doi.org/10.1002/adbi.201800335

Li, Q., Barres, B.A., 2018. Microglia and macrophages in brain homeostasis and disease. Nat Rev Immunol 18, 225–242. https://doi.org/10.1038/nri.2017.125

Lipp, L.L., 2014. Brain Perfusion and Oxygenation. Critical Care Nursing Clinics of North America 26, 389–398. https://doi.org/10.1016/j.ccell.2014.04.008

Mancini, S., Minniti, S., Gregori, M., Sancini, G., Cagnotto, A., Couraud, P.-O., Ordóñez-Gutiérrez, L., Wandosell, F., Salmona, M., Re, F., 2016. The hunt for brain Aβ oligomers by peripherally circulating multi-functional nanoparticles: Potential therapeutic approach for Alzheimer disease. Nanomedicine: Nanotechnology, Biology and Medicine 12, 43–52. https://doi.org/10.1016/j.nano.2015.09.003

Marin, I., Kipnis, J., 2013. Learning and memory … and the immune system. Learn. Mem. 20,

601–606. https://doi.org/10.1101/lm.028357.112

Martinac, J.A., Craft, D.K., Su, J.H., Kim, R.C., Cotman, C.W., 2001. Astrocytes degenerate in frontotemporal dementia: possible relation to hypoperfusion. Neurobiology of Aging 22, 195–207. https://doi.org/10.1016/S0197-4580(00)00231-1

Masserini, M., 2013. Nanoparticles for brain drug delivery. ISRN Biochem 2013, 238428. https://doi.org/10.1155/2013/238428

Matsuoka, Y., Saito, Mitsuo, LaFrancois, J., Saito, Mariko, Gaynor, K., Olm, V., Wang, L., Casey, E., Lu, Y., Shiratori, C., Lemere, C., Duff, K., 2003. Novel Therapeutic Approach for the Treatment of Alzheimer's Disease by Peripheral Administration of Agents with an Affinity to β-Amyloid. J. Neurosci. 23, 29–33. https://doi.org/10.1523/JNEUROSCI.23-01-00029.2003

McConnell, H.L., Kersch, C.N., Woltjer, R.L., Neuwelt, E.A., 2017. The Translational Significance of the Neurovascular Unit. J Biol Chem 292, 762–770. https://doi.org/10.1074/jbc.R116.760215

Miners, J.S., Palmer, J.C., Tayler, H., Palmer, L.E., Ashby, E., Kehoe, P.G., Love, S., 2014. AÎ^2 degradation or cerebral perfusion? Divergent effects of multifunctional enzymes. Front. Aging Neurosci. 6. https://doi.org/10.3389/fnagi.2014.00238

Moller, W., 2002. Ultrafine Particles Cause Cytoskeletal Dysfunctions in Macrophages. Toxicology and Applied Pharmacology 182, 197–207. https://doi.org/10.1006/taap.2002.9430

Montagne, A., Barnes, S.R., Sweeney, M.D., Halliday, M.R., Sagare, A.P., Zhao, Z., Toga, A.W., Jacobs, R.E., Liu, C.Y., Amezcua, L., Harrington, M.G., Chui, H.C., Law, M., Zlokovic, B.V., 2015. Blood-Brain Barrier Breakdown in the Aging Human Hippocampus. Neuron 85, 296–302. https://doi.org/10.1016/j.neuron.2014.12.032

Muoio, V., Persson, P.B., Sendeski, M.M., 2014. The neurovascular unit - concept review. Acta Physiol (Oxf) 210, 790–798. https://doi.org/10.1111/apha.12250

Murphy, M.J., Grace, G.M., Tartaglia, M.C., Orange, J.B., Chen, X., Rowe, A., Findlater, K., Kozak,

R.I., Freedman, M., Lee, T.-Y., Strong, M.J., 2012. Widespread cerebral haemodynamics disturbances occur early in amyotrophic lateral sclerosis. Amyotrophic Lateral Sclerosis 13, 202–209. https://doi.org/10.3109/17482968.2011.625569

Nanclares, C., Baraibar, A.M., Araque, A., Kofuji, P., 2021. Dysregulation of Astrocyte–Neuronal Communication in Alzheimer's Disease. IJMS 22, 7887. https://doi.org/10.3390/ijms22157887

Nimmerjahn, A., Kirchhoff, F., Helmchen, F., 2005. Resting Microglial Cells Are Highly Dynamic Surveillants of Brain Parenchyma in Vivo. Science 308, 1314–1318. https://doi.org/10.1126/science.1110647

Niranjan, R., 2018. Recent advances in the mechanisms of neuroinflammation and their roles in neurodegeneration. Neurochemistry International 120, 13–20. https://doi.org/10.1016/j.neuint.2018.07.003

Otani, T., Furuse, M., 2020. Tight Junction Structure and Function Revisited. Trends in Cell Biology 30, 805–817. https://doi.org/10.1016/j.tcb.2020.08.004

Paolicelli, R.C., Bolasco, G., Pagani, F., Maggi, L., Scianni, M., Panzanelli, P., Giustetto, M., Ferreira, T.A., Guiducci, E., Dumas, L., Ragozzino, D., Gross, C.T., 2011. Synaptic Pruning by Microglia Is Necessary for Normal Brain Development. Science 333, 1456–1458. https://doi.org/10.1126/science.1202529

Persidsky, Y., Ramirez, S.H., Haorah, J., Kanmogne, G.D., 2006. Blood-brain barrier: structural components and function under physiologic and pathologic conditions. J Neuroimmune Pharmacol 1, 223–236. https://doi.org/10.1007/s11481-006-9025-3

Pisani, V., Stefani, A., Pierantozzi, M., Natoli, S., Stanzione, P., Franciotta, D., Pisani, A., 2012. Increased blood-cerebrospinal fluid transfer of albumin in advanced Parkinson's disease. J Neuroinflammation 9, 670. https://doi.org/10.1186/1742-2094-9-188

Ransohoff, R.M., Cardona, A.E., 2010. The myeloid cells of the central nervous system parenchyma. Nature 468, 253–262. https://doi.org/10.1038/nature09615

Re, F., Cambianica, I., Sesana, S., Salvati, E., Cagnotto, A., Salmona, M., Couraud, P.-O., Moghimi, S.M., Masserini, M., Sancini, G., 2011. Functionalization with ApoE-derived peptides enhances the interaction with brain capillary endothelial cells of nanoliposomes binding amyloid-beta peptide. Journal of Biotechnology 156, 341–346. https://doi.org/10.1016/j.jbiotec.2011.06.037

Rocchio, F., Tapella, L., Manfredi, M., Chisari, M., Ronco, F., Ruffinatti, F.A., Conte, E., Canonico, P.L., Sortino, M.A., Grilli, M., Marengo, E., Genazzani, A.A., Lim, D., 2019. Gene expression, proteome and calcium signaling alterations in immortalized hippocampal astrocytes from an Alzheimer's disease mouse model. Cell Death Dis 10, 24. https://doi.org/10.1038/s41419-018-1264-8

Roher, A.E., Esh, C., Rahman, A., Kokjohn, T.A., Beach, T.G., 2004. Atherosclerosis of Cerebral Arteries in Alzheimer Disease. Stroke 35, 2623–2627. https://doi.org/10.1161/01.STR.0000143317.70478.b3

Roquet, D., Sourty, M., Botzung, A., Armspach, J.-P., Blanc, F., 2016. Brain perfusion in dementia with Lewy bodies and Alzheimer's disease: an arterial spin labeling MRI study on prodromal and mild dementia stages. Alz Res Therapy 8, 29. https://doi.org/10.1186/s13195-016-0196-8

Rosengarten, B., Dannhardt, V., Burr, O., Pöhler, M., Rosengarten, S., Oechsner, M., Reuter, I., 2010. Neurovascular Coupling in Parkinson's Disease Patients: Effects of Dementia and Acetylcholinesterase Inhibitor Treatment. JAD 22, 415–421. https://doi.org/10.3233/JAD-2010-101140

Ross, C., Taylor, M., Fullwood, N., Allsop, D., 2018. Liposome delivery systems for the treatment of Alzheimer’s disease. IJN Volume 13, 8507–8522. https://doi.org/10.2147/IJN.S183117

Rule, R.R., Schuff, N., Miller, R.G., Weiner, M.W., 2010. Gray matter perfusion correlates with disease severity in ALS. Neurology 74, 821–827.

https://doi.org/10.1212/WNL.0b013e3181d3e2dd

Salvi, V., Sozio, F., Sozzani, S., Del Prete, A., 2017. Role of Atypical Chemokine Receptors in Microglial Activation and Polarization. Front. Aging Neurosci. 9, 148. https://doi.org/10.3389/fnagi.2017.00148

Sancini, G., Dal Magro, R., Ornaghi, F., Balducci, C., Forloni, G., Gobbi, M., Salmona, M., Re, F., 2016. Pulmonary administration of functionalized nanoparticles significantly reduces beta-amyloid in the brain of an Alzheimer's disease murine model. Nano Res. 9, 2190–2201. https://doi.org/10.1007/s12274-016-1108-8

Savage, J.C., Carrier, M., Tremblay, M.-È., 2019. Morphology of Microglia Across Contexts of Health and Disease, in: Garaschuk, O., Verkhratsky, A. (Eds.), Microglia, Methods in Molecular Biology. Springer New York, New York, NY, pp. 13–26. https://doi.org/10.1007/978-1-4939-9658-2_2

Schaeffer, S., Iadecola, C., 2021. Revisiting the neurovascular unit. Nat Neurosci 24, 1198–1209. https://doi.org/10.1038/s41593-021-00904-7

Seigneur, C., 2009. Current Understanding of Ultrafine Particulate Matter Emitted from Mobile Sources. Journal of the Air & Waste Management Association 59, 3–17. https://doi.org/10.3155/1047-3289.59.1.3

Shou, Y., Huang, Y., Zhu, X., Liu, C., Hu, Y., Wang, H., 2019. A review of the possible associations between ambient PM2.5 exposures and the development of Alzheimer's disease. Ecotoxicology and Environmental Safety 174, 344–352. https://doi.org/10.1016/j.ecoenv.2019.02.086

Sudre, C.H., Bocchetta, M., Cash, D., Thomas, D.L., Woollacott, I., Dick, K.M., van Swieten, J., Borroni, B., Galimberti, D., Masellis, M., Tartaglia, M.C., Rowe, J.B., Graff, C., Tagliavini, F., Frisoni, G., Laforce, R., Finger, E., de Mendonça, A., Sorbi, S., Ourselin, S., Cardoso, M.J., Rohrer, J.D., Andersson, C., Archetti, S., Arighi, A., Benussi, L., Binetti, G., Black, S., Cosseddu, M., Fallström, M., Ferreira, C., Fenoglio, C., Fox, N.C., Freedman, M., Fumagalli, G., Gazzina, S.,

Ghidoni, R., Grisoli, M., Jelic, V., Jiskoot, L., Keren, R., Lombardi, G., Maruta, C., Mead, S., Meeter, L., van Minkelen, R., Nacmias, B., Öijerstedt, L., Padovani, A., Panman, J., Pievani, M., Polito, C., Premi, E., Prioni, S., Rademakers, R., Redaelli, V., Rogaeva, E., Rossi, G., Rossor, M.N., Scarpini, E., Tang-Wai, D., Thonberg, H., Tiraboschi, P., Verdelho, A., Warren, J.D., 2017. White matter hyperintensities are seen only in GRN mutation carriers in the GENFI cohort. NeuroImage: Clinical 15, 171–180. https://doi.org/10.1016/j.nicl.2017.04.015

Sweeney, M.D., Zhao, Z., Montagne, A., Nelson, A.R., Zlokovic, B.V., 2019. Blood-Brain Barrier: From Physiology to Disease and Back. Physiol Rev 99, 21–78. https://doi.org/10.1152/physrev.00050.2017

Thal, D.R., von Arnim, C.A.F., Griffin, W.S.T., Mrak, R.E., Walker, L., Attems, J., Arzberger, T., 2015. Frontotemporal lobar degeneration FTLD-tau: preclinical lesions, vascular, and Alzheimer-related co-pathologies. J Neural Transm 122, 1007–1018. https://doi.org/10.1007/s00702-014-1360-6

Thurgur, H., Pinteaux, E., 2019. Microglia in the Neurovascular Unit: Blood–Brain Barrier–microglia Interactions After Central Nervous System Disorders. Neuroscience 405, 55–67. https://doi.org/10.1016/j.neuroscience.2018.06.046

Toledo, J.B., Arnold, S.E., Raible, K., Brettschneider, J., Xie, S.X., Grossman, M., Monsell, S.E., Kukull, W.A., Trojanowski, J.Q., 2013. Contribution of cerebrovascular disease in autopsy confirmed neurodegenerative disease cases in the National Alzheimer's Coordinating Centre. Brain 136, 2697–2706. https://doi.org/10.1093/brain/awt188

Uemura, M.T., Maki, T., Ihara, M., Lee, V.M.Y., Trojanowski, J.Q., 2020. Brain Microvascular Pericytes in Vascular Cognitive Impairment and Dementia. Front Aging Neurosci 12, 80. https://doi.org/10.3389/fnagi.2020.00080

Wake, H., Moorhouse, A.J., Nabekura, J., 2011. Functions of microglia in the central nervous system – beyond the immune response. Neuron Glia Biol. 7, 47–53. https://doi.org/10.1017/S1740925X12000063

Weisman, G.A., Ajit, D., Garrad, R., Peterson, T.S., Woods, L.T., Thebeau, C., Camden, J.M., Erb, L., 2012. Neuroprotective roles of the P2Y2 receptor. Purinergic Signalling 8, 559–578. https://doi.org/10.1007/s11302-012-9307-6

Winkler, E.A., Sengillo, J.D., Sullivan, J.S., Henkel, J.S., Appel, S.H., Zlokovic, B.V., 2013. Blood–spinal cord barrier breakdown and pericyte reductions in amyotrophic lateral sclerosis. Acta Neuropathol 125, 111–120. https://doi.org/10.1007/s00401-012-1039-8

Xie, J., Shen, Z., Anraku, Y., Kataoka, K., Chen, X., 2019. Nanomaterial-based blood-brain-barrier (BBB) crossing strategies. Biomaterials 224, 119491. https://doi.org/10.1016/j.biomaterials.2019.119491

Zlokovic, B.V., 2011. Neurovascular pathways to neurodegeneration in Alzheimer's disease and other disorders. Nat Rev Neurosci 12, 723–738. https://doi.org/10.1038/nrn3114

Zlokovic, B.V., 2005. Neurovascular mechanisms of Alzheimer's neurodegeneration. Trends Neurosci 28, 202–208. https://doi.org/10.1016/j.tins.2005.02.001

ACKNOWLEDGMENTS

At the end of my PhD, I would like to say a few words to thank all the people who shared or contributed to this experience.

I would like to express my deepest gratitude to my supervisor, Prof. Giulio Sancini, to whom I virtually give a pen, he will understand why. Thank you for teaching me that in science, as well as in life, there are few but firm principles.

I would also like to thank the PhD program in Neuroscience based at the School of Medicine and Surgery of the University of Milano-Bicocca and in particular the coordinator, Prof. Rosa Maria Moresco, for her availability and Dr. Elisabetta Donzelli, who attentively followed us during these years, promptly answering all our questions.

I would like to express my sincere thanks to Dr. Paolo Spaiardi, for his great competence and his infinite patience in explaining, teaching and sharing.

I am grateful also to Dr. Claudia Verderio, my first tutor during my master thesis. She passed on her passion for research to me. Thanks for helping me years later with precious suggestions.

My thoughts turn to all people who shared this experience with me. Thanks to Sara, my lab mate, for sharing our days in lab, thanks for her help and for our coffee breaks; thanks to Vanessa for her wise advice; a special thanks to Greta, my earlier lab mate, now true friend, our afternoons always will be in my memories.

Thanks to all my friends, a fundamental part of my life.

I am forever grateful for my caring, patient, and supportive family.
My biggest thanks go to my beloved mum and dad, my words cannot express how grateful I am to have them by my side. There is nothing specific to thank them for because I owe them everything.

Thanks to my sister Federica; when I was a child, she gifted me the book *Brilliant women in science* with the wish that my name could be there. I am light years away from being there, but it was an inspiration to me.

Thanks to Evan, my sister's husband, that from July of this year has become part of our lovely family.

A special thanks goes to my grandmother Lucia, with whom I share the determination. Anyone who knows her, knows what it means.

As a part of my family, I want to thank Fabio, my greatest support and supporter, he has a special place in everything I do. Thank for being in my life.